Development of Improved Guidelines and Designs for Thin Whitetopping:
Design, Instrumentation, Construction, and Initial Environmental Response of Full-Scale BCOA Sections

July 2018

Angel Mateos
John T. Harvey
Fabian Paniagua
Julio Cesar Paniagua
Rongzong Wu

Development of Improved Guidelines and Designs for Thin Whitetopping: Design, Instrumentation, Construction and Initial Environmental Response of Full-Scale BCOA Sections

Authors:
A. Mateos, J. Harvey, F. Paniagua, J. Paniagua, and R. Wu

PREPARED FOR:

California Department of Transportation
Division of Research, Innovation, and System Information
Office of Materials and Infrastructure

PREPARED BY:

University of California
Pavement Research Center
UC Davis, UC Berkeley

TECHNICAL REPORT DOCUMENTATION PAGE

1. REPORT NUMBER UCPRC-RR-2017-02	2. GOVERNMENT ASSOCIATION NUMBER	3. RECIPIENT'S CATALOG NUMBER
4. TITLE AND SUBTITLE Development of Improved Guidelines and Designs for Thin Whitetopping: Construction and Initial Environmental Response of Full-Scale BCOA Sections		5. REPORT PUBLICATION DATE July 2018
		6. PERFORMING ORGANIZATION CODE
7. AUTHOR(S) Angel Mateos, John Harvey, Fabian Paniagua, Julio Paniagua, and Rongzong Wu		8. PERFORMING ORGANIZATION REPORT NO. UCPRC-RR-2017-02
9. PERFORMING ORGANIZATION NAME AND ADDRESS University of California Pavement Research Center Department of Civil and Environmental Engineering, UC Davis 1 Shields Avenue Davis, CA 95616		10. WORK UNIT NUMBER
		11. CONTRACT OR GRANT NUMBER 65A0542
12. SPONSORING AGENCY AND ADDRESS California Department of Transportation Division of Research, Innovation, and System Information P.O. Box 942873 Sacramento, CA 94273-0001		13. TYPE OF REPORT AND PERIOD COVERED Research Report January 2015 to December 2016
		14. SPONSORING AGENCY CODE 2878
15. SUPPLEMENTAL NOTES		

16. ABSTRACT

Thin bonded concrete overlay of asphalt (BCOA) is a rehabilitation alternative consisting of a 100 to 175 mm (0.33 to 0.58 ft) thick portland cement concrete (PCC) overlay of an existing flexible or composite pavement. Fifteen BCOA sections were built at the Davis facilities of the University of California Pavement Research Center in February 2016. Eleven of these full-scale sections were tested under accelerated loading, while four of them were used for monitoring the response of BCOA to the ambient environment and cement hydration. This full-scale experiment is part of a research project whose primary goal is to develop recommendations and guidance on the use of thin BCOA as a rehabilitation alternative in California. The design and construction of these sections is presented in this report, together with results from the quality control/quality assurance testing that was conducted. This testing was focused on the four early high-strength mixes that were used in the construction. The concrete mixes included Type II/V and Type III portland cements and calcium sulfoaluminate cement, and they were designed to provide 2.8 MPa (400 psi) flexural strength after either 4 or 10 hours. Concrete overlays were built either on top of old asphalt pavements that had been tested for another research project or on top of a new gap-graded rubberized hot mix asphalt (RHMA-G) layer. Three slab sizes were built: 1.8x1.8 m (6x6 ft), 2.4x2.4 m (8x8 ft), and 3.6x3.6 m (12x12 ft). This report also describes the instrumentation of the sections and evaluates the engineering reasonableness of the initial data collected by the sensors up to August 2016. There are no recommendations presented in this report. Recommendations regarding implementation of BCOA will be included in the final report of this project.

| 17. KEY WORDS
BCOA, rigid pavement, bonded concrete overlay of asphalt, thin whitetopping, rubberized asphalt, PCC-asphalt interface, pavement rehabilitation, early high-strength concrete | 18. DISTRIBUTION STATEMENT
No restrictions. This document is available to the public through the National Technical Information Service, Springfield, VA 22161 | |
| 19. SECURITY CLASSIFICATION (of this report)

Unclassified | 20. NUMBER OF PAGES
183 | 21. PRICE |

Reproduction of completed page authorized

UCPRC ADDITIONAL INFORMATION

1.	DRAFT STAGE Final	2.	VERSION NUMBER 1
3.	PARTNERED PAVEMENT RESEARCH CENTER STRATEGIC PLAN ELEMENT NUMBER 4.58B	4.	DRISI TASK NUMBER 2878
5.	CALTRANS TECHNICAL LEAD AND REVIEWER(S) D. Maskey	6.	FHWA NUMBER CA192878A

7. PROPOSALS FOR IMPLEMENTATION
    This technical report describes the construction of full-scale BCOA sections that were evaluated within the framework of Partnered Pavement Research Center Strategic Plan Element (PPRC SPE) Project 4.58B, "Development of Improved Guidelines and Designs for Thin Whitetopping." Results from this evaluation were used, together with laboratory testing and modeling, to develop recommendations and guidance on the use of thin BCOA as a rehabilitation alternative in California. There are no recommendations presented in this report. Recommendations regarding implementation of BCOA will be included in the final report of this project.

8. RELATED DOCUMENTS
- Mateos, A., J. Harvey, J. Paniagua and F. Paniagua. Development of Improved Guidelines and Designs for Thin Whitetopping: Literature Review. 2015. Technical Memorandum: UCPRC-TM-2015-01.
- Mateos, A., J. Harvey, R. Wu, F. Paniagua, and J. Paniagua. Development of Improved Guidelines and Designs for Thin Whitetopping: Environmental Response of Full-Scale BCOA Sections. Research Report: UCPRC-RR-2017-03 *(in process)*
- Mateos, A., J. Harvey, J. Paniagua, R. Wu, and F. Paniagua. Development of Improved Guidelines and Designs for Thin Whitetopping: Environmental Effects on the Coefficient of Thermal Expansion of the Concrete. Research Report: UCPRC-RR-2017-04 *(in process)*
- Mateos, A., J. Harvey, F. Paniagua, J. Paniagua, and R. Wu. Development of Improved Guidelines and Designs for Thin Whitetopping: Moisture-Related Shrinkage Response of Full-Scale BCOA Sections. Research Report: UCPRC-RR-2017-05 *(in process)*
- Mateos, A., J. Harvey, R. Wu, F. Paniagua, and J. Paniagua. Development of Improved Guidelines and Designs for Thin Whitetopping: HVS Testing of Full-Scale BCOA Sections. Research Report: UCPRC-RR-2017-06 *(in process)*
- Vandenbossche, J., and J. DeSantis. Development of Improved Guidelines and Designs for Thin Whitetopping: Development of an Improved Faulting Model for BCOA. Research Report: UCPRC-RR-2017-07 *(in process)*
- Mateos, A., J. Harvey, R. Wu, F. Paniagua, and J. Paniagua. Development of Improved Guidelines and Designs for Thin Whitetopping: Laboratory Testing of Concrete and Concrete-Asphalt Interface. Research Report: UCPRC-RR-2017-08 *(in process)*
- Mateos, A., J. Harvey, R. Wu, F. Paniagua, and J. Paniagua. Development of Improved Guidelines and Designs for Thin Whitetopping: Summary, Conclusions, and Recommendations. 2018. Research Report: UCPRC-SR-2018-01

9. LABORATORY ACCREDITATION
    The UCPRC laboratory is accredited by AASHTO re:source for the tests listed in this report

10. SIGNATURES

A. Mateos **FIRST AUTHOR**	J.T. Harvey **TECHNICAL REVIEW**	D. Spinner **EDITOR**	J.T. Harvey **PRINCIPAL INVESTIGATOR**	D. Maskey **CALTRANS TECH. LEADS**	T.J. Holland **CALTRANS CONTRACT MANAGER**

Reproduction of completed page authorized

DISCLAIMER

This document is disseminated in the interest of information exchange. The contents of this report reflect the views of the authors who are responsible for the facts and accuracy of the data presented herein. The contents do not necessarily reflect the official views or policies of the State of California or the Federal Highway Administration. This publication does not constitute a standard, specification or regulation. This report does not constitute an endorsement by the Department of any product described herein.

For individuals with sensory disabilities, this document is available in alternate formats. For information, call (916) 654-8899, TTY 711, or write to California Department of Transportation, Division of Research, Innovation and System Information, MS-83, P.O. Box 942873, Sacramento, CA 94273-0001.

PROJECT OBJECTIVES/GOALS

Thin whitetopping, also known as bonded concrete overlay of asphalt (BCOA), is a rehabilitation alternative consisting of a 100 to 175 mm (0.33 to 0.58 ft) thick portland cement concrete overlay on an existing flexible or composite pavement. It has been frequently used in different U.S. states and in other countries in the Americas, Europe, and Asia. This research report describes the construction of 15 full-scale BCOA sections that were evaluated within the framework of Partnered Pavement Research Center Strategic Plan Element (PPRC SPE) Project 4.58B, whose primary goal is to develop recommendations and guidance on the use of thin BCOA as a rehabilitation alternative in California. This project is a continuation of SPE 4.58, "Evaluate Early Age and Premature Cracking for PaveM and LCCA." Project 4.58B was accomplished through nine tasks:

- Task 1: Performance of a literature review
- Task 2: Development of Concrete Mix Designs for Thin BCOA in California
- Task 3: Development of Mix Designs for Rubberized Asphalt for Use as a Base for Thin BCOA
- Task 4: Improved Modeling of Thin BCOA for Cracking and Development of Recommended Designs in California
- Task 5: Modeling of Thin BCOA for Faulting and Development of Recommended Designs
- Task 6: Evaluation and Performance Estimates of Improved Designs Using the Heavy Vehicle Simulator and Mechanistic-Empirical Analysis
- Task 7: Development of Preliminary Maintenance and Rehabilitation Strategies, Cost Estimates, and Life-Cycle Assessment Inventory Framework
- Task 8: Evaluation of Improved Designs on Mainline Highway at MnROAD
- Task 9: Final Recommendations, Report, and Guidelines

This report presents the construction of HVS test sections as part of Task 6, and the evaluation of initial responses to the environment as part of Task 4.

ACKNOWLEDGMENTS

(This page intentionally blank)

EXECUTIVE SUMMARY

The design, construction, and initial monitoring of fifteen full-scale bonded concrete overlay of asphalt (BCOA) pavement sections are described in this report. This full-scale experiment is part of Caltrans/UCPRC Partnered Pavement Research Center Strategic Plan Element (PPRC SPE) 4.58B, whose primary goal is to develop recommendations and guidance on the use of thin BCOA as a rehabilitation alternative in California. Thin BCOA is a rehabilitation technique consisting of a 100 to 175 mm (0.33 to 0.58 ft) thick concrete overlay of an existing flexible or composite pavement.

In addition to funding and time availability, the design of the full-scale experiment was determined by three main factors: 1) the technical issues that were regarded as most important for the goals of Project 4.58B but, at the same time, had not been fully solved to date; 2) the testing capabilities of the Heavy Vehicle Simulator (HVS); and 3) the availability of old, distressed, asphalt pavements at the UCPRC Davis testing facility. Input from national experts on concrete pavements and BCOA was sought out and included in the development of the study plan. This resulted in 11 sections being designed for HVS testing (termed *HVS sections)*. The following are the design factors considered most important for inclusion in the study:

- Concrete types (each type of concrete is preceded by a shortened name by which it is referred to in places in this report):
  - P2: Type II/V portland cement with a 10-hour design opening time (OT)
  - P2-ICC: Internally cured concrete based on the previous mix (Type II/V cement with a 10-hour design OT)
  - P3: Type III portland cement with a 4-hour design OT
  - CSA: Calcium sulfoaluminate cement (CSA) with a 4-hour design OT

  Note: the Caltrans flexural strength requirement for opening time is 2.8 MPa (400 psi).

- Slab dimensions: half-lane width (1.8×1.8 m [approximately 6×6 ft] slabs), widened lane (2.4×2.4 m [approximately 8x8 ft] slabs), and full-lane width (3.6×3.6 m [approximately 12×12 ft] slabs)
- Asphalt base types: conventional hot mix asphalt (old, existing mix) and rubberized asphalt (new placement)
- Asphalt base thicknesses: 50 to 120 mm (2 to 4.7 in.)
- Asphalt surface preparation techniques: sweeping (no texturing), micromilling, and milling
- Concrete curing procedures: curing compound and shrinkage-reducing admixture (topical use)

In addition to the eleven sections to be tested with the HVS, four additional sections were built to monitor the response of the slabs to the ambient environment and cement hydration. These four sections (termed *ENV sections)* are replicates of other HVS sections. Additionally, two of the HVS sections were also instrumented with sensors to monitor response to the ambient environment.

Pre-paving work (which included milling or micromilling of asphalt surfaces), the placement of the paving forms, and the installation of sensors took place in late 2015 and early 2016. Construction of the concrete overlays took place on February 23 and 25, 2016. With the exception of a CSA-based mix, the concrete was produced in a fixed batching plant and transported to the construction site in ready-mix trucks. The CSA-based concrete was produced at the construction site using volumetric batching equipment. In all cases, the concrete was directly placed in the sections using the discharge chute of the truck. A hand-operated roller screed was used for placement and consolidation of the concrete. Because of the high workability of all the mixes, minimum additional vibration was required in most sections. The concrete surface was finished with bull floats and edge trowels, and then longitudinal tining was applied by hand pulling a metal rake. The concrete was cured with standard curing compound that was manually applied on the sections. In one of the sections, a shrinkage-reducing admixture (SRA) solution was applied to the surface before the curing compound. Joints were cut to a depth of one-third of slab thickness. No major incidents occurred during construction.

Weather conditions during construction were relatively mild. Wind speeds were low, with maximum values below 10 km/h (6.2 mph). The sky was mostly clear during the first construction day, February 23, and it was partly cloudy on the second construction day, February 25. Air temperatures ranged from 5 to 20°C (40 to 70°F) during concrete placement, while the asphalt surface temperature right before concrete placement ranged from 8 to 30°C (46 to 86°F).

QC/QA testing was conducted according to Caltrans specifications, except on the beams conditioned for flexural strength testing. This conditioning was conducted following ASTM C78 and ASTM C31, which is different from the curing procedures included in the Caltrans CT 524 standard. A number of additional tests, records, and verifications were also conducted in order to obtain greater knowledge about the mixes being placed. The main conclusions from the QC/QA testing are presented below:

- Previous laboratory testing confirmed that all the mixes fulfilled the Caltrans requirements included in Section 39 of the Standard Specifications and in the Standard Special Provisions 40-5 applicable to jointed plain concrete pavements built with rapid strength concrete.

- The minimum flexural strength requirement of 2.8 MPa (400 psi) was fulfilled by all the mixes at the design opening time during construction, with the exception of the Type III cement concrete placed the second construction day. The actual opening time of this mix was slightly over the design opening time of four hours.

- All the portland cement–based mixes far exceeded the Caltrans 10-day flexural strength requirement of 4.5 MPa (650 psi) during construction. The flexural strength of these mixes increased more than 100 percent from the opening age to 10 days.

- The increase in flexural strength from design opening age to 10 days was much smaller in the CSA-based concrete than in the mixes with portland cement. The 10-day flexural strength of the CSA-based concrete placed the first construction day was slightly below 4.5 MPa (650 psi), the Caltrans minimum requirement.

- The replacement of 50 percent of the sand of the Type II/V cement mix with pre-wetted lightweight aggregates resulted in a decrease in flexural strength of 30 percent after 10 hours (design opening time of the original mix) and of 25 percent after 10 days compared with the original mix. This decrease was much higher than the expected result based on preliminary laboratory testing and results from similar experiments.

- Some section-to-section differences can be expected for the mix with Type II/V cement. The concrete used for construction of two of the sections was very fluid, and it presented some visual indications of segregation in one of these two sections.

A set of beams was cured and tested after the design opening time according to the California Test (CT) 524 specification. The test results were compared to those obtained from the set of beams cured and tested according to ASTM C31 and ASTM C78. The main conclusions of this comparison are:

- Flexural strength differences between both sets of beams were related to the formula used to determine the flexural strength. Differences between both sets of beams were not statistically significant when the same formula was used in the calculations.

- No clear difference was found between both curing approaches based on the temperatures recorded inside the beams.

- The temperatures measured inside the beams for both curing approaches were considerably higher than the temperatures measured in the pavement slabs. Consequently, both curing approaches would have considerably overestimated the maturity of the concrete in the slabs at the design opening time.

It must be emphasized that these outcomes were highly dependent on the specific weather conditions during construction. In extremes of weather, with either lower or higher temperatures, differences between ASTM C78-10 and CT 524 would be expected, since weather conditions are expected to affect the CT 524 beams much more than they are expected to affect the beams cured following the ASTM procedures.

Compressive strength (fc) was used to predict the flexural strength (MR) of the field mixes used in this BCOA construction. A specific equation MR-fc was calibrated for each of the mixes using the results of MR and fc testing conducted on the mixes prepared in the laboratory. Then, the compressive strength of each of the field mixes was used to predict the field flexural strength. The root mean square (RMS) of the prediction error ranged from 0.25 MPa (37 psi) in the mix with CSA cement to 1.33 MPa (193 psi) in the mix with Type III cement. For two of the mixes, prediction error also depended on concrete age. The pooled (four mixes) RMS of the prediction error was 0.97 MPa (140 psi), which seems relatively high for the approach to be used for QC/QA.

A total of 560 sensors were placed in the sections, most of them embedded in the concrete. The instrumentation of the HVS sections included strain gages to measure horizontal strain in the concrete and asphalt under dynamic loading, either from the HVS or the falling weight deflectometer. The environmental response instrumentation included sensors to measure relative humidity and moisture content as well as vibrating wire strain gages to monitor horizontal strain in the slabs due to cement hydration and environmental agents. Both the HVS and environmental instrumentations also included the following sensors: 1) thermocouples placed at several locations and depths; 2) joint displacement measuring device (JDMD) sensors to measure vertical movements at the corners and edges of slabs, and the opening and closing of transverse joints; and 3) interface opening measuring device (IOMD) sensors to measure opening and closing at the concrete-asphalt interface. The 245 sensors placed in the ENV sections began collecting data on the day before the construction of the overlay.

Data from several environmental sensors were discarded based on a review of data collected since the overlay construction up until August 4, 2016. The discarded data corresponded to five thermocouples, one moisture content sensor, and one vibrating wire strain gage. With these exceptions, all of the environmental sensors provided data that were compatible with the thermal, moisture-related, and structural responses that can be expected of the BCOA sections due to environmental actions and cement hydration process.

TABLE OF CONTENTS

LIST OF FIGURES

LIST OF TABLES

LIST OF ABBREVIATIONS

AASHTO	American Association of State Highway and Transportation Officials
ACI	American Concrete Institute
ANOVA	Analysis of Variance
ASTM	American Society for Testing Materials
BCOA	Bonded Concrete Overlays of Asphalt
CEB-FIB	Comité Euro-International du Béton-Fédération Internationale de la Précontrainte
CSA	Calcium Sulfoaluminate
CT	Caltrans
CTE	Coefficient of Thermal Expansion
cwt	Hundredweight (100 pounds)
DAS	Data Acquisition System
ELTD	Equivalent Linear Temperature Difference
FAM	Fine Aggregate Matrix
FWD	Falling Weight Deflectometer
FST	Field Setting Time
HMA	Hot Mix Asphalt
HVS	Heavy Vehicle Simulator
ICC	Internal-Curing concrete
IOMD	Interface Opening Measuring Device
JDMD	Joint Displacement Measuring Device
LCCA	Life-Cycle Cost Analysis
LVDT	Linear Variable Displacement Transducer
LWA	Lightweight Aggregates
MC	Moisture Content
MEPDG	Mechanistic-Empirical Pavement Design Guide
MR	Modulus of Rupture
NMAS	Nominal Maximum Aggregate Size
OT	Opening Time
PCC	Portland cement concrete
PPRC	Partnered Pavement Research Center
QC/QA	Quality Control/Quality Assurance
RH	Relative Humidity
RHC	Relative Humidity Sensor type Campbell Scientific
RHMA-G	Rubberized Hot Mix Asphalt Gap-Graded
RHS	Relative Humidity Sensor, type Sensirion SHT75
RSC	Rapid Strength Concrete
SRA	Shrinkage-Reducing Admixture
SWCPA	Southwest Concrete Pavement Association
UCPRC	University of California Pavement Research Center
VWSG	Vibrating Wire Strain Gage

SI* (MODERN METRIC) CONVERSION FACTORS

APPROXIMATE CONVERSIONS TO SI UNITS

Symbol	When You Know	Multiply By	To Find	Symbol
LENGTH				
In	inches	25.4	Millimeters	mm
Ft	feet	0.305	Meters	m
Yd	yards	0.914	Meters	m
Mi	miles	1.61	Kilometers	Km
AREA				
in^2	square inches	645.2	Square millimeters	mm^2
ft^2	square feet	0.093	Square meters	m^2
yd^2	square yard	0.836	Square meters	m^2
Ac	acres	0.405	Hectares	ha
mi^2	square miles	2.59	Square kilometers	km^2
VOLUME				
fl oz	fluid ounces	29.57	Milliliters	mL
Gal	gallons	3.785	Liters	L
ft^3	cubic feet	0.028	cubic meters	m^3
yd^3	cubic yards	0.765	cubic meters	m^3
NOTE: volumes greater than 1000 L shall be shown in m^3				
MASS				
Oz	ounces	28.35	Grams	g
Lb	pounds	0.454	Kilograms	kg
T	short tons (2000 lb)	0.907	megagrams (or "metric ton")	Mg (or "t")
TEMPERATURE (exact degrees)				
°F	Fahrenheit	5 (F-32)/9 or (F-32)/1.8	Celsius	°C
ILLUMINATION				
Fc	foot-candles	10.76	Lux	lx
Fl	foot-Lamberts	3.426	candela/m^2	cd/m^2
FORCE and PRESSURE or STRESS				
Lbf	poundforce	4.45	Newtons	N
lbf/in^2	poundforce per square inch	6.89	Kilopascals	kPa

APPROXIMATE CONVERSIONS FROM SI UNITS

Symbol	When You Know	Multiply By	To Find	Symbol
LENGTH				
mm	millimeters	0.039	Inches	in
m	meters	3.28	Feet	ft
m	meters	1.09	Yards	yd
Km	kilometers	0.621	Miles	mi
AREA				
mm^2	square millimeters	0.0016	square inches	in^2
m^2	square meters	10.764	square feet	ft^2
m^2	square meters	1.195	square yards	yd^2
Ha	Hectares	2.47	Acres	ac
km^2	square kilometers	0.386	square miles	mi^2
VOLUME				
mL	Milliliters	0.034	fluid ounces	fl oz
L	liters	0.264	Gallons	gal
m^3	cubic meters	35.314	cubic feet	ft^3
m^3	cubic meters	1.307	cubic yards	yd^3
MASS				
g	grams	0.035	Ounces	oz
kg	kilograms	2.202	Pounds	lb
Mg (or "t")	megagrams (or "metric ton")	1.103	short tons (2000 lb)	T
TEMPERATURE (exact degrees)				
°C	Celsius	1.8C+32	Fahrenheit	°F
ILLUMINATION				
lx	lux	0.0929	foot-candles	fc
cd/m^2	candela/m^2	0.2919	foot-Lamberts	fl
FORCE and PRESSURE or STRESS				
N	newtons	0.225	Poundforce	lbf
kPa	kilopascals	0.145	poundforce per square inch	lbf/in^2

*SI is the symbol for the International System of Units. Appropriate rounding should be made to comply with Section 4 of ASTM E380 (Revised March 2003)

1   INTRODUCTION

Thin bonded concrete overlay of asphalt (BCOA), formerly known as *thin whitetopping,* is a pavement rehabilitation technique alternative that consists of placement of a 100 to 175 mm (0.33 to 0.58 ft) thick concrete overlay on an existing flexible or composite pavement. While the technology for BCOA has been used on highways and conventional roads in several US states as well as in other countries *(1)*, use of BCOA to date has been very limited in California. BCOA technology has steadily improved since the mid-1990s *(1,2,3)* and can now be regarded as a mature technology; however, there are still key gaps in knowledge that require further research. Among the gaps in knowledge are the essentially unknown role and performance of the concrete–asphalt interface, the mechanics of the asphalt base—which is systematically oversimplified in current BCOA design approaches— and the lack of a BCOA faulting model *(4)*. Further research is also needed to determine which are the optimal designs for California—a state with a drier climate and has longer periods without rainfall than most other states. Additional research is also needed regarding important design features of thin BCOA, such as slab dimensions, shoulder types, and the need for asphalt milling before placing the overlay *(4)*.

The University of California Pavement Research Center (UCPRC) investigation partly described in this report resulted from interest in the use of this rehabilitation technique that was expressed by the California Department of Transportation (Caltrans). The project, titled Partnered Pavement Research Program Strategic Plan Element (PPRC SPE) 4.58B, "Development of Improved Guidelines and Designs for Thin Whitetopping," aims to address the differences and unresolved issues noted above. A follow on to an earlier UCPRC project for Caltrans, SPE 4.58, the primary goal of SPE 4.58B is to develop recommendations and guidance on the use of thin BCOA as a rehabilitation alternative for California based on the adoption of, and improvements to, the technology developed in other US states.

Project 4.58B builds on current BCOA knowledge by conducting laboratory testing, modeling, and evaluation of full-scale BCOA sections. It is the construction of the full-scale BCOA sections that constitutes the main topic of this research report. This full-scale evaluation is the sixth of nine tasks included in Project 4.58B; the timeline in Figure 1.1 shows when these tasks were accomplished.

For the full-scale experiment, 15 BCOA sections were built at the UCPRC facility in Davis, California. Eleven of these sections were tested with the Heavy Vehicle Simulator (HVS), an accelerated pavement testing machine capable of applying up to 800 repetitions per hour of a single wheel load up to 110 kN (25 kips). This results in a controlled and accelerated process of damage accumulation that is intended to reproduce long-term in-service traffic damage. These 11 sections are referred to in this report as *HVS sections*. As part of the full-scale experiment, the response of the BCOA sections to environmental actions and cement hydration was measured. Four additional

sections, intended to replicate four of the HVS sections, were built and instrumented with this purpose. These four sections are referred to in this report as *ENV sections*. Response to ambient environmental conditions and cement hydration was also measured in two of the *HVS sections*. Consequently, these two sections are regarded as both *HVS* and *ENV* sections, depending on the context, in this report. This set of fifteen sections includes a variety of BCOA solutions of interest for to Caltrans. The range of the different design factors is presented below:

- Concrete types (each type of concrete is preceded by a shortened name by which it is referred to in places in this report):
    - P2: 10 hour design opening time (OT) with Type II/V portland cement
    - P2-ICC: Internally cured concrete based on mix P2
    - P3: 4 hour design OT with Type III portland cement
    - CSA: 4 hour design OT with calcium sulfoaluminate (CSA) cement

    Note: the Caltrans flexural strength requirement for opening time is 2.8 MPa (400 psi).

- Slab dimensions: half-lane width (1.8×1.8 m [approximately 6×6 ft, slabs], widened lane (2.4×2.4 m [approximately 8×8 ft] slabs), and full-lane width (3.6×3.6 m [approximately 12×12 ft] slabs)
- Asphalt base type: conventional hot mix asphalt (HMA, old, existing mix) and gap-graded rubberized hot mix asphalt (RHMA-G, new placement)
- Asphalt base thicknesses: 50 to 120 mm (2 to 4.7 in.)
- Asphalt surface preparation techniques: sweeping (no texturing), micromilling, and milling
- Concrete curing procedures: curing compound and shrinkage-reducing admixture (topical use)
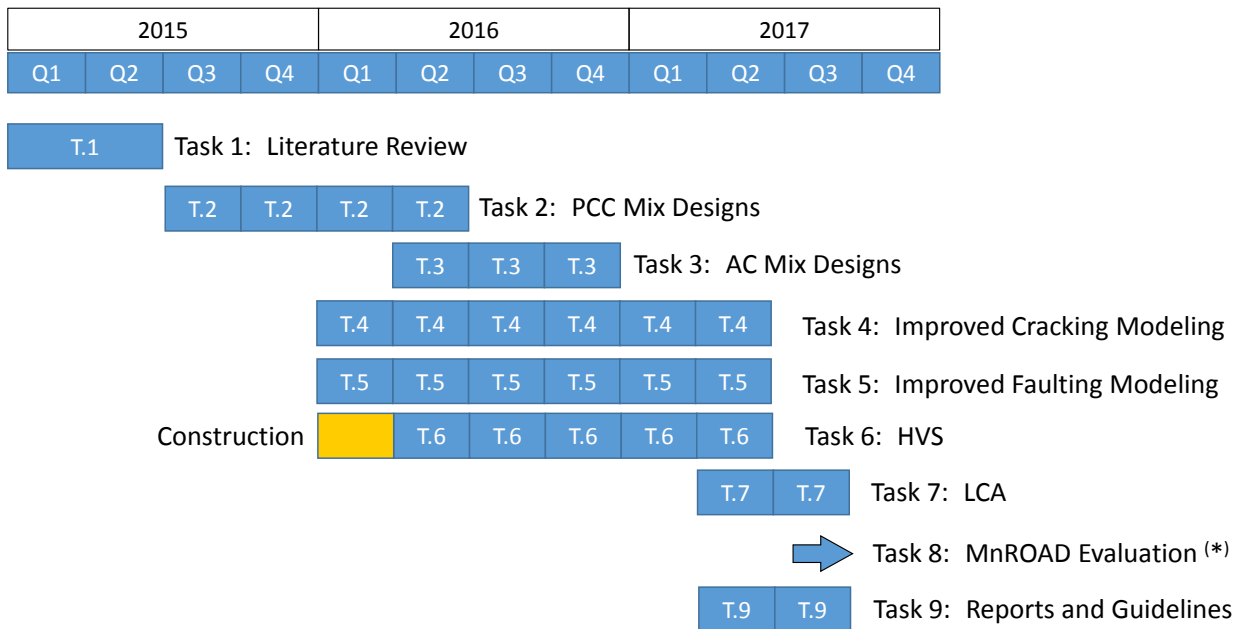
(*) *No BCOA section could be included in 2017 MnROAD construction cycle.*

Figure 1.1: Project timeline.

Construction of the concrete overlay took place on February 23 and 25, 2016. A picture of the test track, taken after construction of the overlay and shoulders, is presented in Figure 1.2, and a plan showing the fifteen sections is presented in Figure 1.3. The Lane 1 overlay (Sections A to H and L) was placed on February 23, while the Lane 2 overlay (Sections I to K and M to O) was placed on February 25. One day was required between the construction of Lane 1 and the construction of Lane 2 for instrumentation of Lane 2. The construction process and other related activities are described in this report. Description of the BCOA sections is included in Chapter 2. This description includes the concrete overlay and the previously existing asphalt pavements. The conceptual design of the sections, i.e., why these fifteen sections were selected, is also included in Chapter 2. A total of 560 sensors were placed in the sections, most of them embedded in the concrete, in order to measure displacement, strain, temperature, moisture, and relative humidity. Three hundred and fifteen of these sensors were dedicated to HVS testing, while the remaining 245 constituted the instrumentation of the *ENV sections*. The instrumentation is described in Chapter 3. The overlay construction itself is described in Chapter 4, and some representative pictures have been included in the appendix. Granular shoulders were placed after the concrete overlay construction. A description of the granular shoulders is also included in Chapter 4. The quality control/quality assurance (QC/QA) activities conducted during concrete overlay construction are described in Chapter 5 along with results of the different QC/QA tests. Chapter 6 presents a representative compendium of the data collected from the environmental sections up until August 4, 2016. An evaluation of the engineering reasonableness of the collected data is also included in Chapter 6.

Figure 1.2: Full-scale test track.
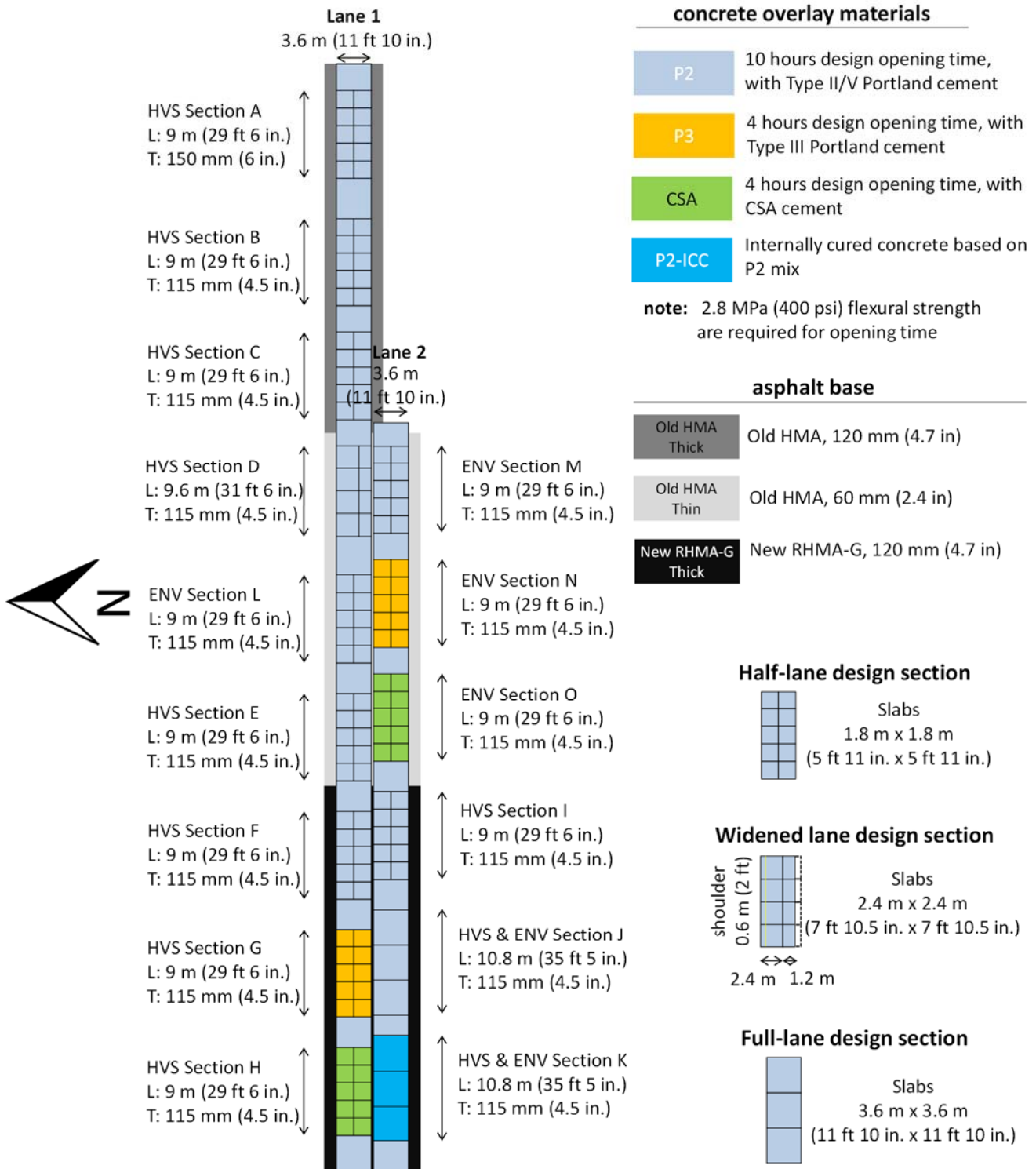
Figure 1.3: Full-scale test track layout.

2 DESCRIPTION OF BCOA SECTIONS IN THE FULL-SCALE EXPERIMENT

2.1 Existing Flexible Pavements

BCOA is a rehabilitation technique in which a concrete overlay is placed on a previously existing distressed pavement. Therefore a suitable portion of the test track for this study was built on a remnant pavement constructed for an earlier UCPRC project *(5)* that studied full-depth reclamation (FDR) and had an existing thin HMA overlay on approximately half of the FDR sections and unsurfaced FDR in the rest.

Figure 2.1 shows the old pavement in cross section and the BCOA project laid out in two lanes. The old FDR layer was 250 mm (10 in.) thick and consisted of material reclaimed from a 120 mm (4.7 in.) asphalt pavement and 130 mm (5.1 in.) of Caltrans Class 2 aggregate base. During its original construction, part of the FDR layer was stabilized with an asphalt emulsion, cement, or foamed asphalt with cement, and one part had no stabilization. All *HVS sections* were located on the unstabilized FDR area, while three of the *ENV sections* were located on the area where the FDR layer was stabilized with asphalt emulsion (Figure 2.1). Both the stabilized and unstabilized FDR layers rest on 320 mm (12.6 in.) of Class 2 aggregate base remaining from a previous study, on top of a prepared clay subgrade. The stiffness values of the subgrade, measured with a dynamic cone penetrometer, ranged from an estimated 100 to 150 MPa (15,000 to 22,000 psi) *(6)*.

The surface layer, that had been placed on the FDR layer in November 2012, consisted of dense-graded hot mix asphalt that included PG 64-16 binder and 15 percent reclaimed asphalt (RAP), with a 19 mm (3/4 in.) nominal maximum aggregate size (NMAS), a mix commonly used in California. In the full-depth reclamation experiment, two different asphalt thicknesses were evaluated: 60 and 120 mm (2.4 and 4.8 in.). For the first case, one asphalt lift was used and in the latter case two lifts were used (in Figure 1.3 these two thicknesses are labeled "Old HMA" and highlighted in light and dark grey, respectively). The condition of these flexible sections was relatively poor to begin with, mainly due to permanent deformation caused by HVS testing in the FDR experiment. Some areas of the pavement also showed localized rutting (approximately 20 to 25 mm) [3/4 to 1 in.]) and/or fatigue cracking. Only one of these damaged areas was in the wheelpath of a BCOA section that was subjected to HVS testing. This area, where the asphalt presented fatigue cracking, was located within Section C. This is one of the reasons why milling rather than micromilling was applied in this area, as described in Section 4.1 of this report.

As noted in the introduction, the use of new asphalt as a base for BCOA is also considered in this research project. If BCOA can be placed on new asphalt surfaces it could be used for rehabilitating pavements in relatively poor condition as well as those that are in fair to good condition as is currently generally recommended *(3)*. Caltrans

was interested in the evaluation of rubberized asphalt mixes for the purpose of bringing damaged asphalt concrete into better condition as part of BCOA.
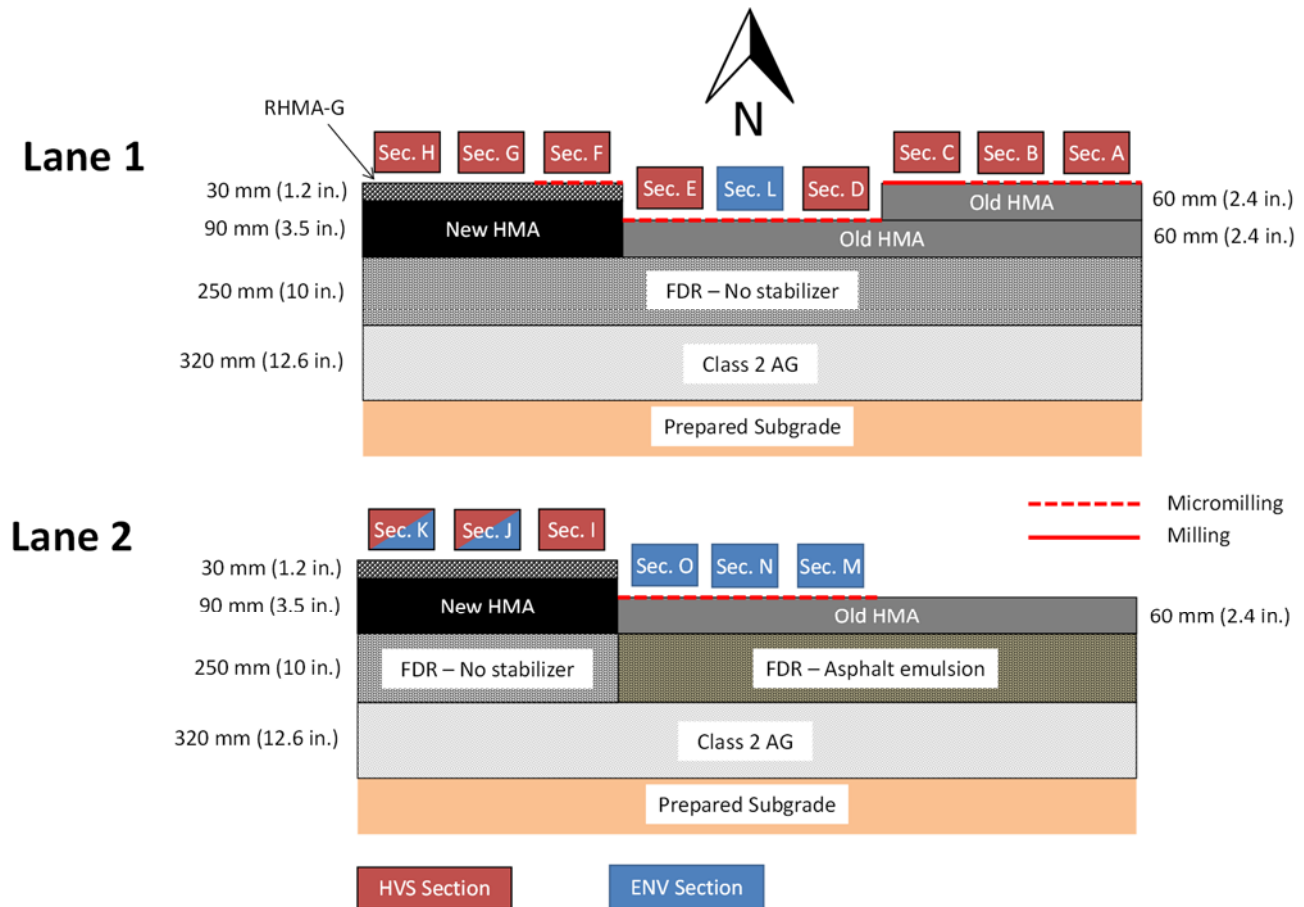
Note: The blue sections are the *environmental sections* (ENV sections), where the effects of temperature and moisture-related shrinkage were monitored. The red sections are the *HVS sections* that were subjected to accelerated pavement testing with the HVS. Sections J and K are both ENV and HVS sections, since they were used to monitor the effects of temperature and moisture-related shrinkage and were also subjected to HVS testing.

Figure 2.1: Cross section of flexible pavements used for BCOA construction.

To evaluate the use of newly placed, unmilled asphalt bases under BCOA, parts of both lanes of the test track were paved with new mixes on October 13, 2015. The new asphalt was placed on an area of the test track where the FDR layer had not been paved over in the earlier experiment (see Figure 1.3). First, a 90 mm (3.5 in.) thick dense-graded, hot mix asphalt (HMA) layer was placed on the FDR layer and then a 30 mm (1.2 in.) thick rubberized mix layer was placed on the dense-graded HMA (see Figure 2.1). The dense-graded HMA was 19 mm (3/4 in.) NMAS, with a PG 64-16 binder and 15 percent RAP (as noted earlier, this dense-graded mix is commonly used in California). The rubberized mix was a gap-graded type (RHMA-G), with a 12.5 mm (1/2 in.) NMAS and 7.5 percent (by total weight of mix) asphalt rubber binder content. The asphalt rubber binder included a PG 70-10 base binder and 19.5 percent crumb rubber modifier. Both asphalt mixes were designed, produced, and placed

according to Section 39 of the 2015 Caltrans Standard Specifications. A low NMAS was selected for the rubber mix so that it could be placed in a thin 30 mm (1.2 in.) lift. It was expected that the high binder content of these gap-graded mixes, together with the improved fatigue resistance provided by the rubber modifier would significantly slow asphalt cracking propagation downward at the joints in the concrete slabs, and upward from any cracking in the underlying existing asphalt layers, even when it was placed as a thin layer. The fact that the rubberized mix was placed on top of a new asphalt layer rather than on an old distressed asphalt was not considered a limitation because the main objective of the study is to obtain insight into the interaction between the rubberized asphalt and the concrete overlay.

2.2   Conceptual Design of BCOA Sections

The design of the BCOA sections to be evaluated in the full-scale HVS experiment was determined considering several different factors:

- *The availability of old, distressed, asphalt pavements at the Davis UCPRC testing facility.* As noted above, a decision was made to use an already existing pavement with four 75 meter long lanes that had been constructed earlier for a research project on full-depth reclamation (FDR). The 11 BCOA sections to be tested with the HVS were constructed on parts of this pavement where no stabilizer had been used in the full-depth reclamation process, as shown in Figure 2.1. This setup was chosen to avoid introducing another variable, the stabilizer, into the full-scale experimental testing design. Due to space considerations, three of the ENV sections had to be placed in an area of the test track where the FDR layer had been stabilized with asphalt emulsion. But this was considered to be a minor limitation since no HVS testing was planned for these sections; their only planned use was for monitoring the response of the pavement to environmental actions, which mainly depends on the concrete and asphalt layers.
- *HVS testing length.* Because the HVS applies a load along an 8 meter-long (26 ft) path, the length chosen for the sections had to exceed this value. Since the weight of the HVS could cause considerable damage to the BCOA sections, it was also necessary to leave space between the sections where the machine's load stands could be set during testing. The load stands of the HVS could not be placed on top of a BCOA section since they would produce considerable damage due to the heavy weight of the machine.
- *The variables regarded as important for the goals of Project 4.58B.* The results of a literature review conducted in Task 1 of this research project, together with input from national experts on BCOA, indicated a number of important issues that warrant additional research that would likely improve thin BCOA technology. These issues, which are summarized in the conclusions chapter of the literature review *(4)*, were grouped into four categories: 1) PCC mix design, 2) slab geometry and configuration, 3) asphalt base, and 4) PCC-asphalt interface. The issues were used to determine the variables to include in the full-scale HVS experiment and the levels of each variable, as reflected in Table 2.1 below. They were also used to determine how the full-scale experiment was conducted, including what instrumentation was used and the way data was analyzed.

The factors described above, together with funding and testing time limitations (the project end was September 2017), determined the construction of 11 sections to be tested with the HVS (the *HVS sections*). As noted, four additional sections intended to replicate three of the HVS sections were also built to measure the response of the

slabs to the ambient environment (the *ENV sections*). The layout of the 15 sections is presented in Figure 2.2, together with interactions and corresponding study variables.

Table 2.1: Variables Included in the Full-Scale Experiment

Category	Issues Requiring Further Research	Variable / Levels
1) PCC mix design	a. Evaluation of the beneficial effects of internal-curing concrete (ICC) for BCOA b. Balancing the short construction windows with the demanding structural requirements of BCOA through materials type selection and mix design	Mix type: ✓ Include internally cured concrete ✓ Several opening times (OT) compatible with Caltrans construction windows ✓ Cement type (portland cement Types II/V or III or calcium sulfoaluminate cement) ✓ Consider advanced curing techniques
2) Slab geometry & configuration	a. Optimization of panel size b. Optimization of length-to-width ratio and maximum dimension-to-thickness ratio c. Evaluation of the beneficial effects of widened slabs	Slab horizontal dimensions: ✓ Half-lane and full-lane width slabs ✓ Include widened slabs section
3) Asphalt base	a. Optimization of the rubberized hot mix asphalt (RHMA) mix design for BCOA bases where new bases will be placed prior to placement of concrete b. Understanding the interaction between asphalt base properties (existing aged HMA and new RHMA) and BCOA distress mechanisms c. Determining the implications of the use of new RHMA bases on BCOA performance	Asphalt base type: ✓ Old HMA ✓ New RHMA-G
4) PCC–Asphalt interface	a. Mechanical characterization of the interface b. Prediction of interface performance c. Evaluation of PCC-asphalt bond in the laboratory d. Optimization of techniques to improve PCC-asphalt bonding	Asphalt surface preparation: ✓ Sweeping (no texturing) ✓ Milling ✓ Micromilling[*]

* The micromilling technique was evaluated in this experiment, in addition to milling. Milling is the classical technique that has been used before placing a concrete overlay. Micromilling is conducted using the same machine employed for milling but with a different drum that has a more teeth with smaller spacing than the one used for milling. The cost of micromilling is similar to that for milling, but it can remove asphalt surfaces as thin as 8 mm (1/3 in.), and with a greater precision than standard milling.
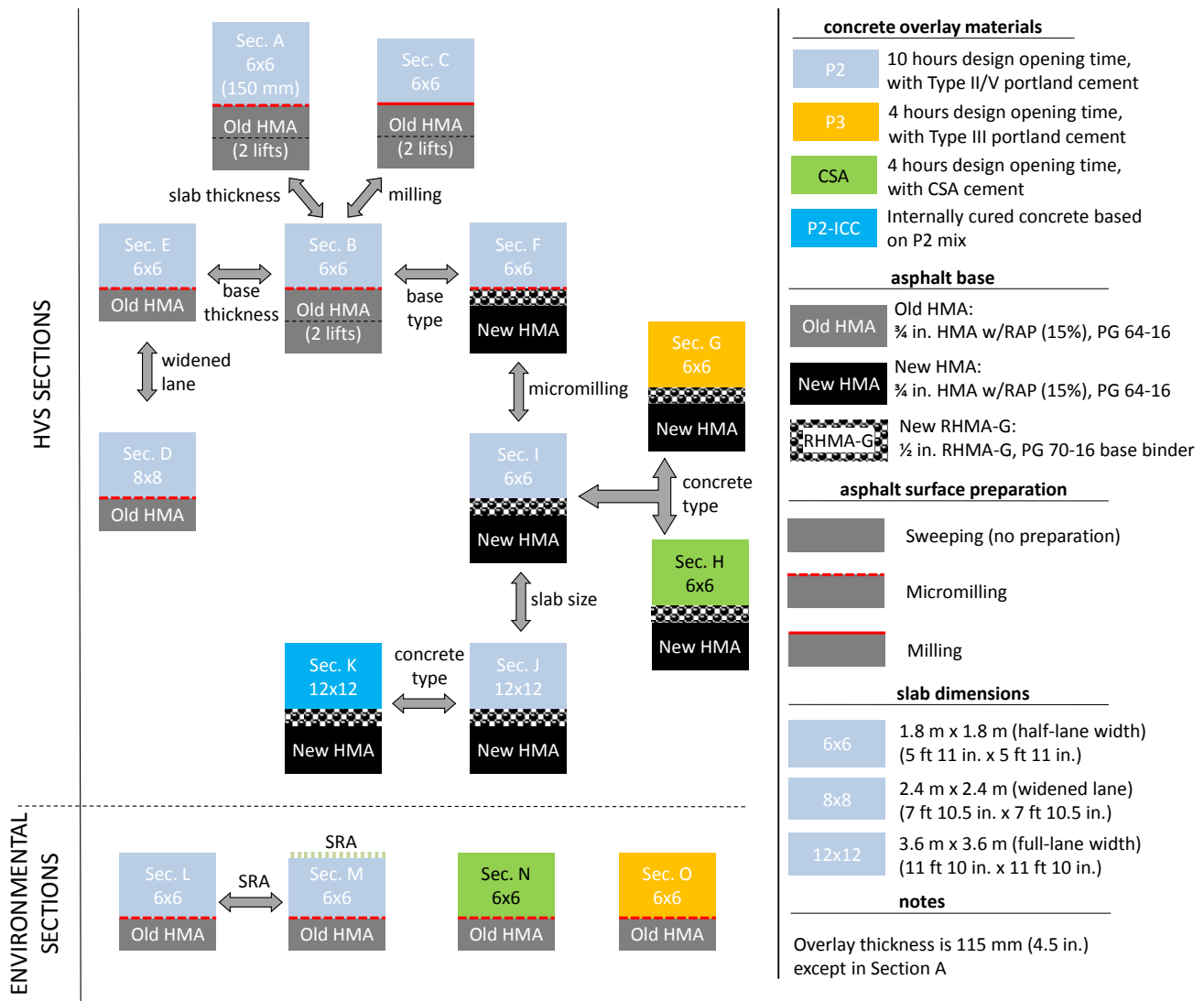
Figure 2.2: Factorial design of BCOA sections to be evaluated in the full-scale experiment.

2.3 Concrete Overlay Mixes

2.3.1 Concrete Mix Designs Supplied by Industry for the BCOA Sections

Mix designs were provided by the concrete industry. In particular, Teichert Materials supplied the portland cement–based designs, CTS Cement supplied the CSA concrete design, and Trinity Aggregates was involved in the design of the internally cured concrete. The mixes are presented below.

- P2 is a 10-hour design opening time mix using Type II portland cement.
- P3 is a 4-hour design opening time mix using Type III portland cement.
- CSA is a 4-hour design opening time mix using CSA cement.
- P2-ICC is an internally cured concrete based on P2 mix.

The design opening times (OT) of the concrete mixes were based on the construction windows, overnight and 24 hr/weekend, established by Caltrans. Specifically, a 4-hour design OT is required for mixes used in overnight road closures and a 10-hour design OT is required for mixes used with 24 hour and weekend-long construction windows. For this project, Caltrans also added a requirement that the 10-hour OT mix be produced with Type II cement. Further, since the cement type might significantly impact the bonding between the concrete and the asphalt, a second cement type, calcium sulfoaluminate (CSA), was included in addition to portland cement. CSA cement was selected because of its moisture-related shrinkage properties. This cement is frequently used for slab replacements in the California road network due to its early high strength.

All the mixes were designed to fulfill the 2015 Caltrans Standard Specifications Section 40,"Concrete Pavement," and 2010 Standard Special Provisions 40-5_A11-15-13, which includes specifications for constructing jointed plain concrete pavements with rapid strength concrete (RSC). These specifications require flexural strengths of 2.8 MPa (400 psi) after 4- and 10-hour opening times and 4.5 MPa (650 psi) after 10 days.

Mix designs were previously validated at the UCPRC, on the basis of flexural strength after design opening time and 24 hours. UCPRC staff had been previously trained by industry experts on laboratory production of specimens using RSC. This training was organized by the Southwest Concrete Pavement Association (SWCPA), with participation of experts from this association, Teichert Materials, CTS Cement, and BASF Corporation. Continuous support was also provided by SWCPA, Teichert Materials, and CTS Cement during the validation process, which resulted in several adjustments to gradations and admixture dosages.

All the mixes used the same aggregate source, which was alluvial sand and gravel from the Teichert Perkins plant in Sacramento. Mix design proportions including cement, aggregates, water, and admixtures are indicated in Table 2.2.

All the mixes used for the construction of the BCOA sections fell within the Caltrans definition of RSC (up to 9 days opening time). A high cement content and a high dose of superplasticizer (high-range water reducer) and accelerator were required for the portland cement–based designs to fulfill these specifications, as reflected in Table 2.2. The cement content of the portland cement–based mixes, 800 pounds per cubic yard, is the maximum amount allowed by Caltrans for structural concrete, except for precast members. The hydration stabilizer was required to prevent the Type III cement from setting before delivery at the construction site. For this same reason, the accelerator was dosed directly into the ready-mix truck at the construction site, immediately before the concrete was placed. Compared to portland cement–based designs, the CSA concrete had a lower cement content and lower dose of superplasticizer. It should be noted that the amount of admixtures of all these RSC designs are

highly dependent on both the concrete and the ambient temperatures, and must be specifically tailored for each concrete placement depending on concrete mixing temperature, ambient temperature, and travel time. The admixture dosages indicated in Table 2.2 correspond to standard laboratory temperature, 23°C (73°F).

2.3.2 Mix Design for the Internal-Curing Concrete

The 10 hour OT mix design supplied by Industry (Table 2.2) was adapted to produce internal-curing concrete (ICC). *Internal curing* is defined by the American Concrete Institute as a "process by which the hydration of cement continues because of the availability of internal water that is not part of the mixing water" *(7)*. This technique is particularly recommended for mixes with low water/cement ratios, where significant internal drying takes place *(8)*. This internal drying happens because of cement hydration water demand and because of the net volume reduction resulting from cement hydration (chemical shrinkage). This drying mechanism is usually referred to as *self-desiccation*. As a result, an increase in capillary pressure takes place in pores partially filled with water, which is the leading mechanism of moisture-related shrinkage. Both Type II/V and Type III mix designs have a low water/cement ratio, so either of the two could have been selected for producing the ICC. The former was preferred since it was the reference mix used in most sections. The full lane–width slab size (3.6×3.6 m² [approximately 12×12 ft²]) was selected for the evaluation of the ICC. A slab of this size, coupled with the reduced thickness of the BCOA, is expected to result in considerably high stresses due to moisture-related shrinkage. That is why this slab size was selected for the ICC evaluation, since the internal curing is expected to significantly reduce the autogenous component of moisture-related shrinkage.

Internal curing can be achieved by using different materials that readily release water as needed for hydration or to replace moisture lost through evaporation or self-desiccation. To date several materials have been used for this purpose: prewetted lightweight aggregates (LWA), prewetted crushed returned concrete fines, superabsorbent polymers, and prewetted wood fibers *(8)*. For this project, fine LWA were selected for several reasons. First is that the use of LWA is the current established practice for ICC within the US *(8)*. Second, an ASTM standard exists for characterizing LWA for internal-curing concrete (ASTM C1761/C1761M-2015). Third, it was believed that the internal-curing effect achieved with fine LWA would not be very different from the effect achieved with superabsorbent polymers or with wood fibers, since these are also uniformly distributed in the cement paste. The use of superabsorbent polymers or wood fibers presents advantages in terms of implementation, especially in geographical areas where fine LWA were unavailable at a reasonable cost.

Table 2.2: Concrete Mix Designs Employed in the Construction of the BCOA Sections

	P2	P2-ICC	P3	CSA
Design OT	10 hours	10+ hours [4]	4 hours	4 hours
Cement Type	Type II/V	Type II/V	Type III	CSA
1 cubic yard				
1" x #4 CA	1,400 lb	1,400 lb	1,400 lb	1,799 lb
3/8" x #8 CA	550 lb	550 lb	550 lb	
Sand	1,143 lb	566 lb	1,188 lb	1,260 lb
LWA (Sand)		396 lb		
Cement (content)	799 lb	799 lb	799 lb	682 lb
Water	267 lb	267 lb	250 lb	287 lb
Water Reducer [1]	96 oz (12 oz/cwt)	96 oz (12 oz/cwt)	100 oz (12.5 oz/cwt)	54.5 oz (8 oz/cwt)
Stabilizer [2]			352 oz (44.1 oz/cwt)	68.2 oz (10 oz/cwt)
Accelerator [3]	599 oz (75 oz/cwt)	599 oz (75 oz/cwt)	599 oz (75 oz/cwt)	
1 cubic meter				
1" x #4 CA	831 kg	831 kg	831 kg	1,068 kg
3/8" x #8 CA	326 kg	326 kg	326 kg	
Sand	678 kg	336 kg	705 kg	748 kg
LWA (Sand)		235 kg		
Cement (content)	474 kg	474 kg	474 kg	404 kg
Water	158 kg	158 kg	148 kg	170 kg
Water Reducer [1]	3,700 ml (780 ml/100 kg)	3,700 ml (780 ml/100 kg)	3,870 ml (820 ml/100 kg)	2,100 ml (520 ml/100 kg)
Stabilizer [2]			13,600 ml (2,870 ml/100 kg)	2,640 ml (650 ml/100 kg)
Accelerator [3]	23,200 ml (4,900 ml/100 kg)	23,200 ml (4,900 ml/100 kg)	23,200 ml (4,900 ml/100 kg)	
Specifications				
water/cement	0.33	0.33	0.31	0.42
Specif. Slump	150 – 225 mm (6 – 9 in.)	150 – 225 mm (6 – 9 in.)	200 mm min. (8 in. min.)	100 – 200 mm (4 – 8 in.)
Air Content	1.5%	1.5%	1.5%	2.0%

[1] The Type II/V and Type II cement designs used MasterGlenium® 7500, and the CSA cement design used MasterGlenium® 3400. Both are BASF products that meet ASTM C494/C494M compliance requirements for Type F, high-range, water-reducing admixtures.

[2] MasterSet® DELVO. A BASF product that meets ASTM C494/C494M compliance requirements for Type B, retarding, and Type D, water-reducing and retarding, admixtures.

[3] MasterSet® AC 534. A BASF product that meets ASTM C494/C494M compliance requirements for Type C, accelerating, admixtures.

[4] The ICC is produced by replacing part of the normal aggregates with lightweight aggregates (LWA). This replacement is expected to result in a decrease of the short-term strength. Consequently, the opening time of the ICC mix was expected to be longer than 10 hours, which is the design opening time of the P2 mix that served as the basis of the ICC design. This is indicated with the "10+ hours" OT in the table. The design OT of the ICC was determined after laboratory testing of this material, but not as part of the construction QC/QA testing presented in this report.

Several LWA sources and materials were explored for this project, but the material selected was an expanded shale/clay produced by Trinity Aggregates at its Frazier Park plant in Southern California. This material was selected due to its high water absorption capacity, which is close to 20 percent, and its fine gradation, with a fineness modulus below 3. Both values are based on characterization results that were supplied by Trinity Aggregates and verified at the UCPRC. A fine gradation, compared to a coarse gradation, entails a more uniform distribution of the internal water supply, i.e., a higher percentage of the cement paste that can be reached by the LWA water for the same travel distance (8).

In order to achieve the internal curing effect, 50.7 percent of the volume of the normal sand of the P2 mix was replaced by fine LWA. This replacement percentage was determined by Trinity Aggregates in cooperation with Teichert on the basis of actual absorption and the unit weight determined for the LWA at the concrete mixing plant. The measured absorption and unit weight were, respectively, 17.0 percent and 1.81, with both in prewetted[1] surface-dry condition. Calculation of the required volume replacement was based on a validated methodology (8). According to this methodology, internal water demand is first determined by assuming a cement chemical shrinkage of 0.07 ml/g (ml water per gram of cement, 9.6 percent on a cement volume basis), and then considering partial cement hydration due to the reduced water/cement ratio (0.33 in this particular mix). Next, the amount of LWA is determined to supply this internal demand, considering LWA absorption, unit weight, and desorption. For this LWA material, desorption was determined to be 89 percent. This indicates that 89 percent of the absorbed water is released at relatively high relative humidity (over 94 percent, according to ASTM C1761-15).
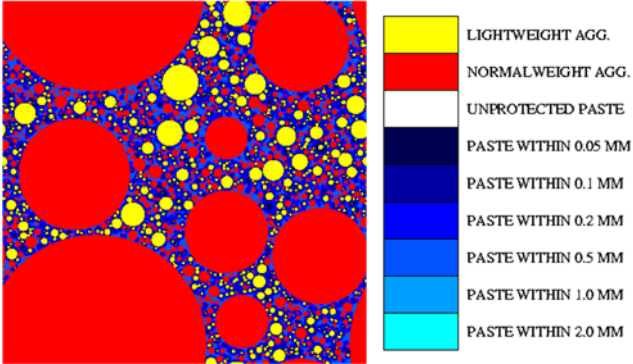
The amount of cement paste that can be reached by the LWA water (protected cement paste) was determined as a function of the travel distance using the software developed by Bentz et al. (9) that is available online. This calculation is based on the gradation of the original mix, the percentage replacement for each sieve size (on a volume basis), and the volume fraction that aggregates represent in the concrete mix. For 50.7 percent sand replacement, which was the value finally adopted for the ICC used for this BCOA construction (Table 2.2), almost 100 percent of the cement paste would be at a distance less than 0.5 mm from an LWA grain. This is much lower than the 2 mm limit indicated by Bentz and Weiss (8). Results of the computations are presented in Table 2.3. It should be noted that the rapid strength gain of the 10 hour OT mix entails a rapid cement hydration process, so not much time would be available for water to travel from the LWA reservoirs to the cement paste. This emphasizes the importance of a fine LWA gradation which, for the same volume replacement and compared to a

---

[1] The term "prewetted" is typically used for LWA rather than "saturated" since it is difficult to achieve complete surface saturation for this type of material. This is because the surface voids may not be fully saturated with water after the immersion period due to the high porosity of the LWA.

coarse gradation, results in higher percentage of cement paste reached for the same travel distance. As explained above, this was one of the reasons why this particular LWA source and material were selected.

Table 2.3: Protected Cement Paste

Distance from LWA surface (mm)	Protected Paste Fraction
0.050	0.21456
0.100	0.45810
0.200	0.81025
0.500	0.99915
1.000	1.00000
2.000	1.00000

LIGHTWEIGHT AGG.
NORMALWEIGHT AGG.
UNPROTECTED PASTE
PASTE WITHIN 0.05 MM
PASTE WITHIN 0.1 MM
PASTE WITHIN 0.2 MM
PASTE WITHIN 0.5 MM
PASTE WITHIN 1.0 MM
PASTE WITHIN 2.0 MM

Software *(9)* available at
concrete.nist.gov/~bentz/intcuring.html

The introduction of this source of LWA in the mix design was also evaluated during the mix validation process that took place before construction of the BCOA. It was verified that the flexural strength of the 10 hour OT mix decreased between 10 and 20 percent after introduction of the LWA. This testing was conducted 10 and 24 hours after mixing. This short-term strength decrease was expected, and has been reported before *(8)*. The strength decrease is due to the lower strength of LWA compared to normal aggregates. The opposite would be expected in the long term, due to the increased degree of hydration of the cement in the internally cured concrete.

2.4 Concrete Overlay Curing Procedure

The Caltrans Standard Specifications for concrete pavements (Section 40) require concrete curing by using either the waterproof membrane method or the curing compound method. The latter was preferred in this experiment since it is the most widely used practice for concrete pavements in California. According to Caltrans specifications, the curing compound must fulfill ASTM C309-11 prescriptions for Type 2 (white pigmented), Class B (resin) compounds, and it must be applied at a nominal rate of 270 ml/m² (150 ft²/gal). The same product, DSC White Resin Cure CA supplied by Dayton Superior Corporation, was used for all the BCOA sections. Only Section M was treated differently: it was cured earlier with a shrinkage-reducing admixture (SRA) before the standard curing compound was applied.

Section M of the full-scale experiment was included to study an advanced curing technique which was of specific interest of Caltrans. The spraying of an SRA onto the surface (referred to as "topical use") as opposed to the conventional practice of mixing SRA into the entire concrete mix was selected for examination after input came

from national experts on concrete curing and consultants in the concrete pavements industry. The technique offers several advantages, including the reduced need for SRA, which is expensive, compared with standard use of SRA (introduced during mixing) and its easy implementation in construction. In their most common use, SRAs are added to the mixing water to reduce the drying shrinkage of concrete *(10)*. The admixture's main effect is to reduce water surface tension and, as a result, to reduce capillary water suction. This reduces moisture-related shrinkage, since capillarity water suction is its driving force.

There are only a few documented studies of topical use of SRA, and all of these have occurred in the laboratory. The goal of this technique is to supply the SRA where it is needed most: on the surface of the slabs, where moisture is lost through evaporation. It is thought that this would make efficient use of the SRA, thus reducing the considerable cost associated with its standard use. In this technique the SRA would be applied in essentially the same way as the standard curing compound. According to Bentz *(11)*, the optimal time at which to apply the SRA is "when the top surface of the concrete first appears dry and free of surface water, much the same as the current criteria for the application of curing compounds." SRA solution concentration and application rates were determined after documented laboratory studies and a pilot project conducted at the UCPRC between November 2015 and January 2016, as explained below.

Laboratory studies focused on the topical use of SRA have applied SRA solutions from 10 to 50 percent concentration, at a rate of 50 to 300 ml SRA/m² (1.4 to 8.5 oz/yd²) *(11,13,14)*. Villani et al. *(12)* found that adding an SRA will proportionally reduce water surface tension up to a 5 percent SRA concentration, and that no further reduction could be expected beyond that concentration. At this concentration the water in concrete pores maximizes the SRA effect. However, this concentration of SRA cannot be determined during its application and it will change with time, depending on the concrete's moisture and the diffusion of SRA in the water in the pores. For this reason, determining the SRA solution concentration and dosage required for the BCOA construction was not a trivial matter.

A practical limit for the amount of SRA to spray can be determined based on the amount of SRA that would be required if it were used in the mixing water (conventional use). This practical limit depends on the overlay thickness and the SRA dosage in its standard use. The recommended dosage of MasterLife® SRA 20, the product selected for this project, is 2.5 to 7.5 l/m³ (0.5 to 1.5 gal/yd³); this results in a dosage of 290 to 860 ml/m² for a 115 mm (4.5 in.) thick overlay (Section M). The lower bound of this interval is similar to the upper limit of the application rates reported in laboratory studies, as indicated above. For this reason 300 ml SRA/m² (8.5 oz/yd²) was regarded as a practical limit for the application rate on Section M.

A dosage of 100 ml SRA/m² was applied to an instrumented slab that was built at the UCPRC in November 2015. A 20 percent SRA solution was used in this occasion. The concrete mix used for this pilot study was very similar to the 10 hour OT mix (P2) used for the BCOA construction described in this report. Another slab was built with the same material at the same time, but it was cured with standard curing compound. Moisture-related shrinkage was monitored in both slabs, using vibrating wire strain gages, between November 2015 and January 2016. Similar moisture-related shrinkage values were measured in both slabs, which means that an SRA dosage of 100 ml/m² (4.8 oz/yd²) did not improve drying shrinkage versus a standard curing compound. Based on this result, a decision was made to apply on Section M an SRA dose of 300 ml/m² (8.5 oz/yd²), the practical limit described above.

As indicated, the SRA was applied in a 20 percent solution on the pilot project built at the UCPRC in November 2015. It should be noted that the amount of SRA solution that can be applied is driven by the amount the concrete surface can absorb. It might not be possible to apply the desired amount of SRA if weather conditions are not dry enough. In the case of the pilot project, the solution was applied three times—with a 20 minute interval between applications—to reach the final SRA dosage of 100 ml/m² (2.8 oz/yd²). A main conclusion learned from this pilot study is that SRA dosage, timing, and concentration, have to be engineered for the specific concrete to be used and for the range of environmental conditions that can be expected during construction. Leaving dosage exclusively to the absorption capacity of concrete may result in little control of the amount of SRA actually applied. For Section M, the SRA solution concentration was increased to 50 percent, since the amount of SRA to apply was significantly higher than the amount applied in the pilot project.

It should be mentioned that the savings associated with topical use of the SRA, compared to the standard use, would not be particularly high with thin BCOA because of the small slab thickness. On the other hand, the savings would be much larger with standard jointed plain concrete pavements (JPCP). Compared to the standard use of SRA at a rate to 5 l/m³ (2 gal/yd³), the topical use of SRA at a rate to 300 ml/m² (8.5 oz/yd²) would produce a savings of 4,420 liters (1,170 gal) of SRA per lane-mile for a 210 mm (8.3 in.) thick JPCP and 10,150 liters (2,680 gal) SRA per lane-mile for a 405 mm thick (16 in.) JPCP. Assuming an SRA cost of $5.3/liter ($20/gal), the savings would be $23,000 and $54,000, respectively, for 210 and 405 mm thick JPCP. It should be noted that 210 and 405 mm are, respectively, the minimum and maximum thicknesses of JPCP in specified in the Caltrans *Highway Design Manual.*

3   INSTRUMENTATION OF THE BCOA SECTIONS

The instrumentation of the sections was conceived with the goal of measuring the slabs' response to HVS loading and environmental actions. This goal requires measuring the structural response and also the thermal and moisture-related response. In the first case, the instrumentation is focused on strains and displacements. In the second case, instrumentation is focused on temperature, moisture content, and relative humidity, which are internal variables linking external environmental actions to slabs' structural response. It should be clarified that these internal variables are not only determined by the environmental actions during the early-age of the concrete, since cement hydration has a strong influence on them. In fact, the term "environmental actions" is used in this report for clarity of the explanation, although the term "moisture and temperature-related actions" would better describe the intended meaning. A summary of measured variables is presented in Table 3.1.

Table 3.1: Summary of Variables Measured in the Full-Scale Experiment

	Structural Response	Thermal and Moisture-Related Response
HVS Loading	• Concrete and asphalt horizontal strains • Corner and edge deflections • Concrete-asphalt interface opening • Transverse joint opening	• Concrete and asphalt temperatures
Environmental Actions	• Concrete horizontal strain • Corner and edge deflections • Concrete-asphalt interface opening • Transverse joint opening	• Concrete and asphalt temperatures • Concrete relative humidity • Concrete moisture

Environmental conditions, in particular air temperature, air relative humidity, rainfall, solar radiation, and wind speed, were recorded by means of a weather station located next to the test track.

Not all variables were measured in all sections. As explained above, the test sections were classified into two main groups: HVS sections and ENV sections. The instrumentation of these two section types differed considerably, as is explained below. However, Sections J and K were exceptions that served as both HVS and ENV sections, so they were provided with both HVS and ENV instrumentation.

The eleven HVS sections (including Sections J and K) were instrumented with resistive strain gages to measure strain under the HVS rolling wheel. Linear Variable Differential Transformer (LVDT) sensors were also installed in each section for HVS testing. These LVDTs measured corner and edge deflections, the concrete-asphalt interface opening, and the opening of transverse joints (horizontal). All sensors were connected to the HVS's data acquisition systems (DAS), which can collect data at the speed required to monitor the slabs' responses to

"dynamic" loading applied by the rolling wheel. The HVS sections were also instrumented with thermocouples that were connected to the HVS's data acquisition systems during HVS testing.

The six ENV sections (including Sections J and K) were instrumented with vibrating wire strain gages (VWSG) to measure strain due to temperature and moisture-related changes. Temperature, concrete moisture, and concrete internal relative humidity were also measured in these sections. Since all these variables change under environmental actions at a very low rate compared to structural response under HVS loading, these data were collected using a static DAS. Unlike the dynamic DAS measurements for the HVS sections, where many measurements per second are taken, environmental responses can be measured on a single point every few minutes. The ENV sections were also instrumented with LVDTs to monitor corner and edge deflections, concrete-asphalt interface opening, and the opening of transverse joints due to environmental actions and the cement hydration process. Environmental sections sensors started to collect data the day before the overlay construction.

3.1   Sensor Types and Characteristics

Each variable and its corresponding sensor type, including the make and model, are presented in Table 3.2. Sensor selection was conducted based on UCPRC experience, the expected range of measured variables, sensor accuracy, DAS requirements, and the ease of installation in the sections.

Table 3.2: Sensor Types and Characteristics

Variable	Record Type	Sensor Make/Model	Sensor Type/Characteristics
Temperature	Static & Dynamic	Omega / 5TC-PVC-T-24-180	Thermocouple
Strain (asphalt)	Dynamic	Tokyo Sokki / PMFLS-60	Resistive gage
Strain (concrete)	Dynamic	Tokyo Sokki / PML-60	Resistive gage
Strain (concrete)	Static	GeoKon / VW Model 4200	Vibrating Wire Strain Gage
Displacement	Static & Dynamic	Several LVDT models were used: - Dytronics / DSD800SE5 - MacroSensor / (GHSD 750-050, GHSD 750-250, GHSDR 750-250, HSD 750-250, HSD 750-500) - Omega / LD620-5 - Solartron / MV00257SEL0AH	DC operated LVDT with varied ranges
Relative humidity	Static	Sensirion / SHT75	Accuracy (25°C): • ±2% (10% – 90% range) • ±4% (0% – 100% range)
Relative humidity	Static	Campbell Scientific / CS215-L	Accuracy (25°C): • ±2% (10% – 90% range) • ±4% (0% – 100% range)
Moisture	Static	SMT Research Ltd. / Embedded Moisture Sensor (EMS)	Wood resistance humidity sensor with built-in thermistor

3.2 Instrumentation Plan

3.2.1 Instrumentation Used in the HVS Sections

The instrumentation of the HVS sections, shown in Figure 3.1, was designed to measure structural response under the HVS load, and in particular to measure the responses related to the typical distress mechanisms observed in BCOA sections. These distresses have been related to slab size *(15,16)*, with longitudinal cracking along the wheelpath typically observed in half-lane width designs (6×6 ft² [approx. 1.8×1.8 m²], slab size) and transverse cracking typically observed in full-lane width designs (12×12 ft² [approx. 3.6×3.6 m²], slab size). For this reason, all the HVS sections were instrumented with two sets of strain gages, one set to measure concrete transverse strain at the center of the wheelpath, and another set to measure concrete longitudinal strain at the midslab exterior edge. The first set of strain gages was particularly useful for studying the longitudinal cracking, while the second one was particularly useful for studying transverse cracking and corner cracking. No slab size distinction was made, which means that all the HVS sections were instrumented with both sets of strain gages, regardless of whether the section design was half-lane, full-lane, or widened lane. This was done because the critical distress mechanism of any particular section might be different depending on whether it was in the field or part of HVS testing. Besides, no matter where the response was measured, it would provide useful information on overall section structural behavior.

The strain gage locations were also determined by the location of the mean wheelpath in the HVS experiment. The mean wheelpath location was set to reproduce a real-traffic transverse distribution. Specifically, the mean wheelpath offset was set to 450 mm (18 in.), following the *Mechanistic-Empirical Pavement Design Guide (17)*. The offset is here defined as the distance between the outer edge of the dual wheel and a hypothetical road marking, which in this case was 100 mm (4 in.) wide, as shown in Figure 3.2. The extreme positions of the wheel in the HVS experiment, corresponding to ±350 mm (14 in.) wander, are also reflected in Figure 3.2. The maximum wander of the wheel, 350 mm (14 in.) in each direction, is a function of the mechanical capabilities of the HVS.

Two strain gages were placed in the concrete slab at each location, one close to the top of the slab (20 mm, 0.8 in., below slab surface) and one close to the bottom (20 mm, 0.8 in., above slab bottom). This configuration was required to evaluate the position of the neutral axis of the slab. The neutral axis was expected to lie below slab half-depth due to the composite action of the concrete overlay and the asphalt base. In fact, the position of the neutral axis is an indicator of the composite action of the two layers, which is the key to good performance by the BCOA sections. Strain was to be measured at three depths in sections built on the new asphalt-surfaced area (Sections F to K). In addition to the top and bottom of the concrete slab, a third depth was selected, at 30 mm below the asphalt surface. This depth corresponded to the interface between the rubberized gap-graded mix

(RHMA-G) and the hot mix asphalt (HMA), as shown in Figure 2.1. These strain gages were placed on top of the HMA layer before the paving of the RHMA-G overlay. A comparison between the strain measured at this depth and the strain measured at the bottom of the concrete slab provides valuable information for evaluating the bonding between these two layers.

Slabs movements were monitored during HVS testing using joint displacement measuring devices (JDMDs), which are LVDT-based sensors that have long been used by the UCPRC *(18)*. The movements monitored include slab deflection and the opening and closing of transverse joints. In all cases, movements are recorded under the moving load of the HVS, including thermal and moisture-related actions. Also, since LVDT sensors can register absolute position, any permanent movements that took place due to slab cracking or settlement were also monitored. In particular, a set of JDMD sensors was installed in each section to measure vertical displacements of the four corners of the section center slab, and joint opening and closing (horizontal) at the outer edges of the two transverse joints of the center slab. JDMDs also measured corner vertical displacements in the slabs adjacent to the center one (see JDMDs in Figure 3.1) because displacements measured on both sides of a transverse joint can be used to estimate load transfer efficiency across the joint. In all these cases, the JDMDs measuring vertical displacements were attached to an arm-rod fixture that was anchored in the subgrade (Figure 3.3). This anchoring system provided a relatively fixed reference (zero displacement) to measure slab deflections.

Finally, two LVDTs called *interface opening measuring devices* (IOMDs) were installed in each section to measure slab–base separation. The LVDT body of these sensors is fixed to the concrete slab, while the tip of the LVDT core rests on top of a metal rod that is anchored in the asphalt base (Figure 3.4). No appreciable opening was expected to be measured by the IOMD sensors unless debonding took place between the concrete slab and the asphalt base.

The data provided by the JDMDs and IOMDs were used to study longitudinal, transverse, and corner cracking. The JDMDs and IOMDs also provided information particularly useful for studying faulting, which is another common distress in BCOA sections *(1)*.
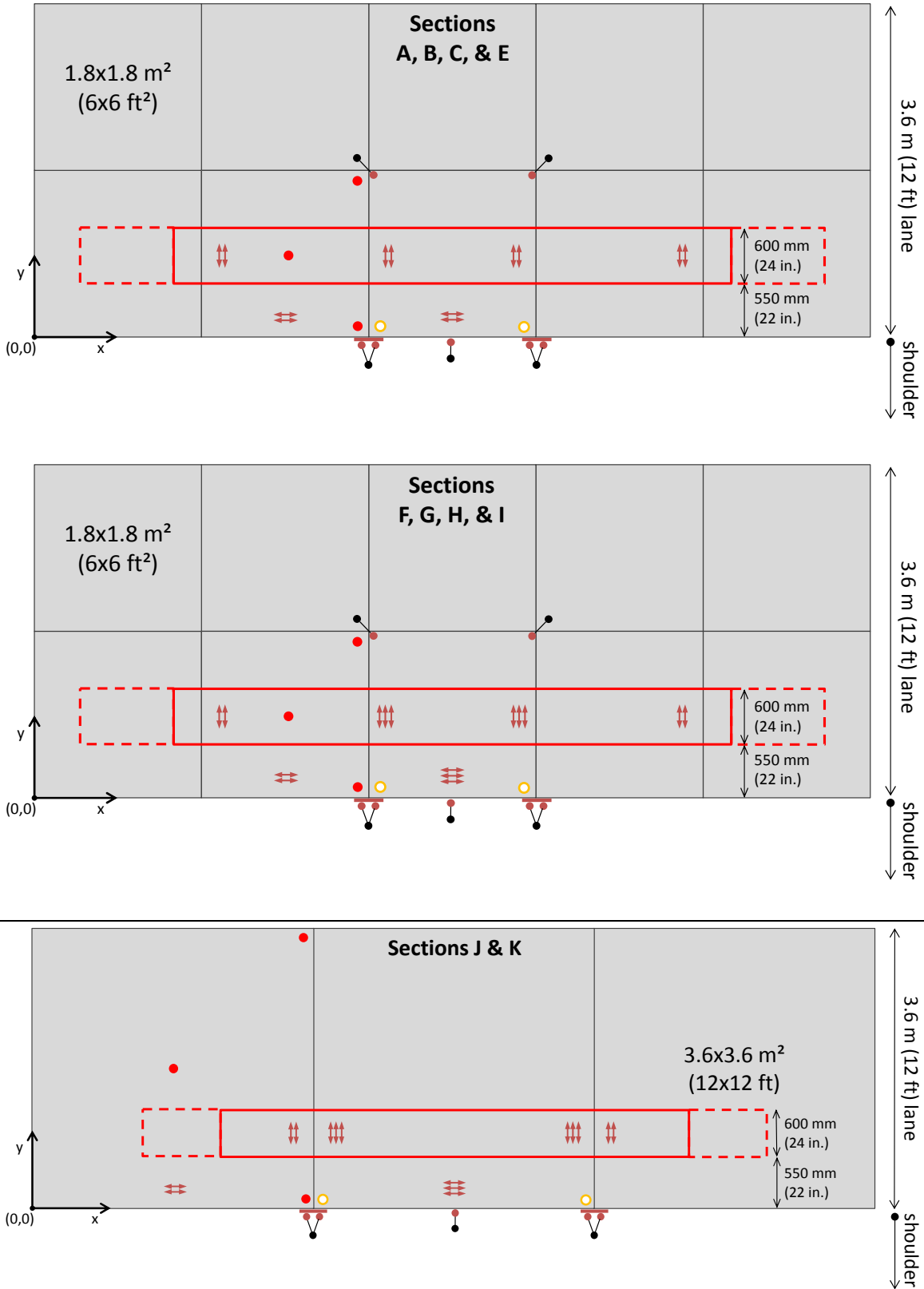
Figure 3.1: Instrumentation of the HVS sections.
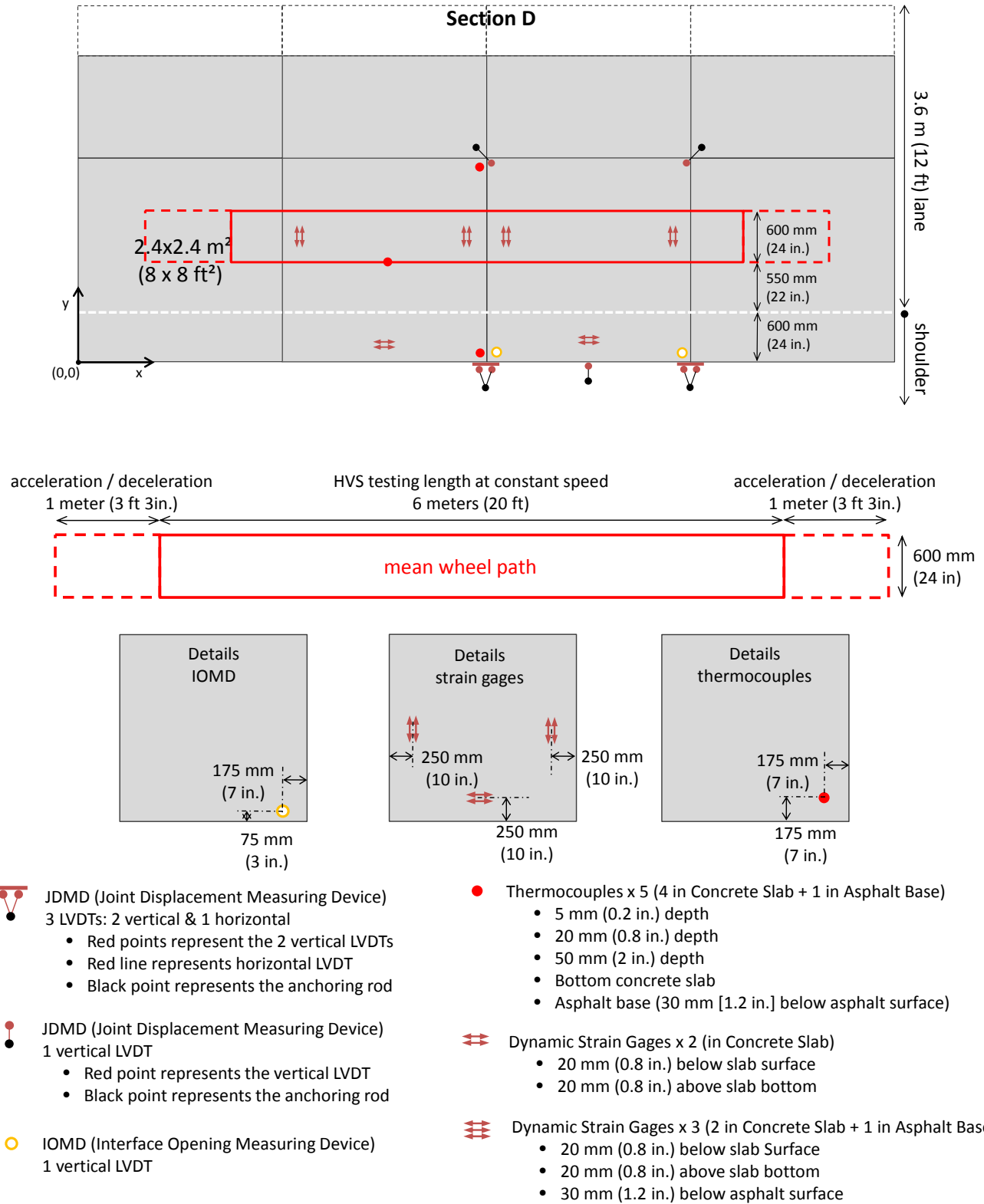
Figure 3.1 *(cont.):* **Instrumentation of the HVS sections.**
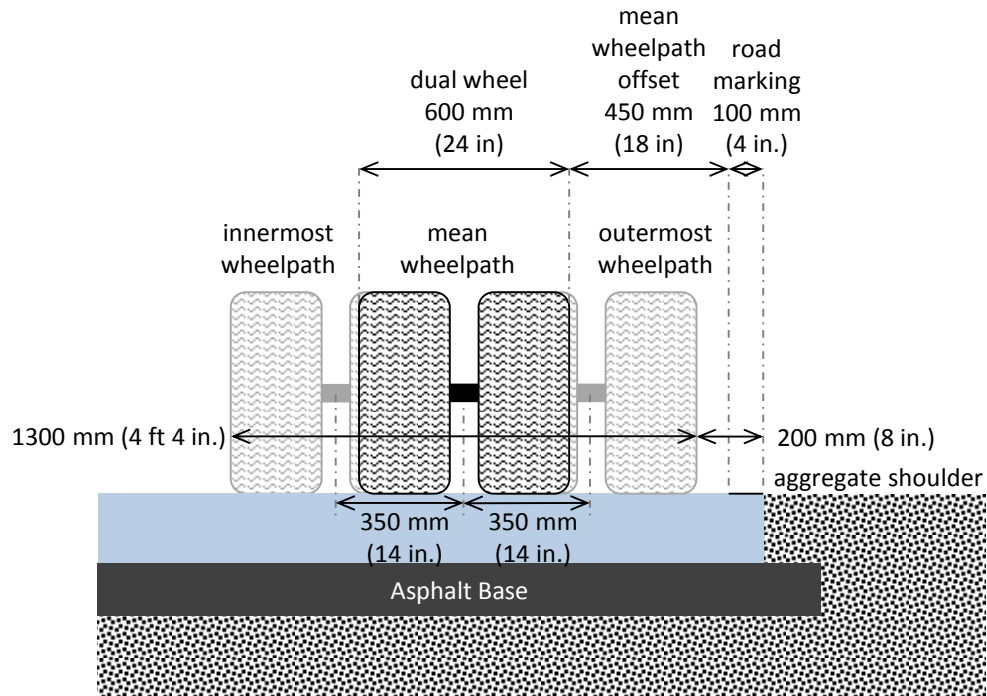
Figure 3.2: Traffic wheelpath in the HVS experiment.
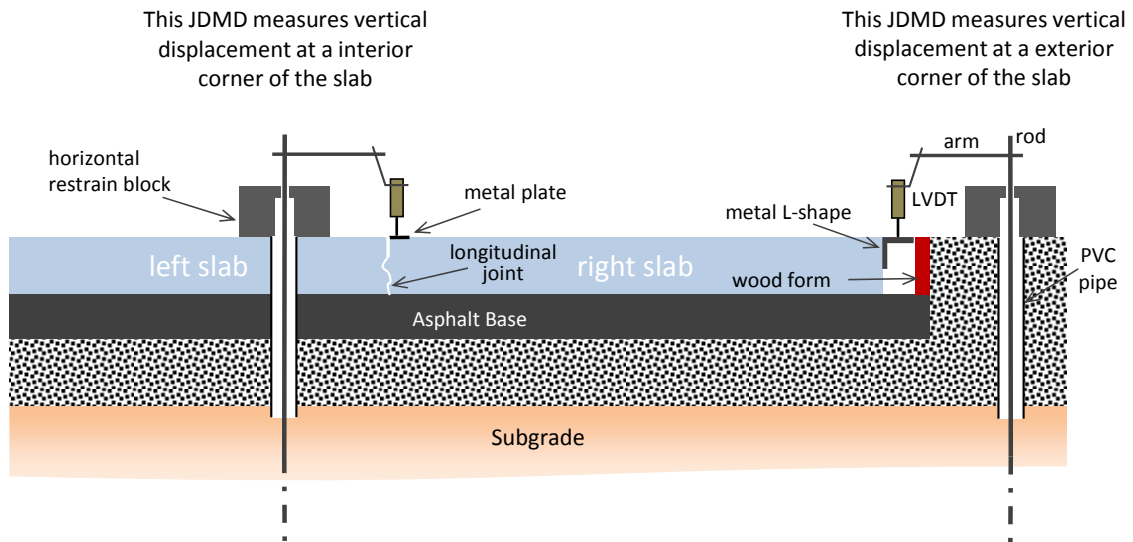
Figure 3.3: Anchoring system for vertical JDMDs.
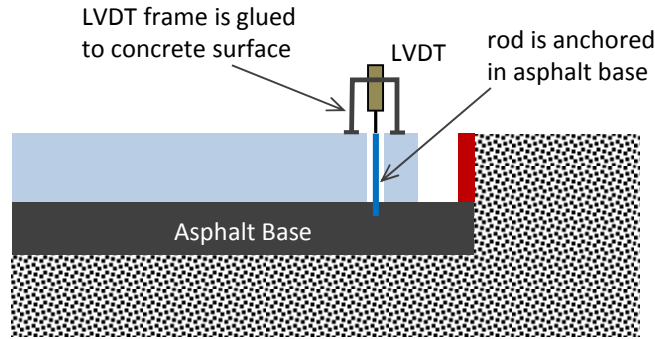
Figure 3.4: Interface opening measuring device (IOMD).

The structural response of any concrete pavement strongly depends on the slab temperature. For this reason, the HVS sections were instrumented with thermocouples to measure concrete temperature at several depths: 5 mm (0.2 in.), 20 mm (0.8 in.), 50 mm (2 in.), and at bottom of the slab (150 mm [5.9 in.] in Section A, 115 mm [4.5 in.] in the rest of the sections). Three locations were instrumented (slab center, slab interior edge, and slab exterior edge) since the UCPRC experience on the Palmdale project *(19)* showed that considerable temperature variation may take place across the lane width. Asphalt base temperature is also expected to strongly influence BCOA response. For this reason, asphalt base temperature was also measured at each of the three locations, at 30 mm below the asphalt surface. A summary of temperature measurement depths is included in Table 3.3.

Table 3.3: Thermocouple Depths (measured from slab surface)

Section A	Rest of the Sections
5 mm (0.2 in.)	5 mm (0.2 in.)
20 mm (0.8 in.)	20 mm (0.8 in.)
50 mm (2 in.)	50 mm (2 in.)
150 mm (5.9 in.) (bottom of concrete slab)	115 mm (4.5 in.) (bottom of concrete slab)
180 mm (7.1 in.) (asphalt base)	145 mm (5.7 in.) (asphalt base)

3.2.2 Instrumentation Used in the Environmental Sections

Instrumentation of the environmental sections, reflected in Figure 3.5, was designed with the goal of measuring the structural response of the slabs due to environmental agents and cement hydration. Sensors to measure concrete temperature, moisture, and internal relative humidity were installed because these internal variables link the effects of environmental agents and cement hydration to the slabs' structural response. Three types of sensors were installed to measure expansion/contraction and bending (which includes curling, and warping) of the slabs due to

temperature and moisture-related changes: vibrating wire strain gages (VWSGs), JDMDs, and IOMDs (see Table 3.2).

The VWSG sensors measure concrete strain and they were placed at three locations in the center slab of each environmental section: at the slab center, at an interior corner, and at a corner at the shoulder. The gages were placed at two depths at each location: 20 mm (0.8 in.) below the slab surface and 20 mm (0.8 in.) above the slab bottom. They were configured this way to enable determination of slab expansion/contraction as well as bending (curling and warping). The strains measured at the corners can be used to determine when the transverse joints deployed. After the joints are deployed, the measured strains at the corners can be considered to represent free concrete expansion/contraction, since the gages are close to the joints. A comparison of the strains measured at the corners to the values measured at the slab center can be used to estimate the strain that is restricted due to the slab's own weight and the slab's interaction with the asphalt base. This "locked" strain is the one that creates stress in the concrete.

The structural response of the slabs was also measured with JDMD sensors in all the environmental sections except Section J. The same JDMD configuration was used in both the ENV and HVS sections. Specifically, a total of nine JDMDs were installed, seven of them to measure vertical deflections and two of them to measure the opening of transverse joints. Corner vertical displacements reflect the slab's curling and warping due to temperature and moisture gradients through the thickness of the slab. Transverse joints opening reflect the slab's average temperature and moisture-related shrinkage.

Two interface opening measuring devices (IOMD) were also installed in the ENV sections. As with the HVS sections, no significant interface opening was expected to be recorded by the IOMD sensors unless concrete–asphalt debonding took place.

The ENV sections were also instrumented with thermocouples to monitor concrete and asphalt temperature. The location and depth of these sensors matched those in the HVS sections. Specifically, they were installed in one slab of each section: at the slab center, at one of the slab's interior corners, and at one of the slab's exterior (shoulder) corners. As with the HVS sections, the thermocouples were installed at five depths: 5 mm (0.2 in.), 20 mm (0.8 in.), 50 mm (2.0 in.), at the slab bottom, and at the asphalt base (30 mm [1.2 in.] below the asphalt surface). It should be noted that other sensors that monitor environmental response (VWSG, relative humidity sensors, and moisture sensors) also include temperature sensors.
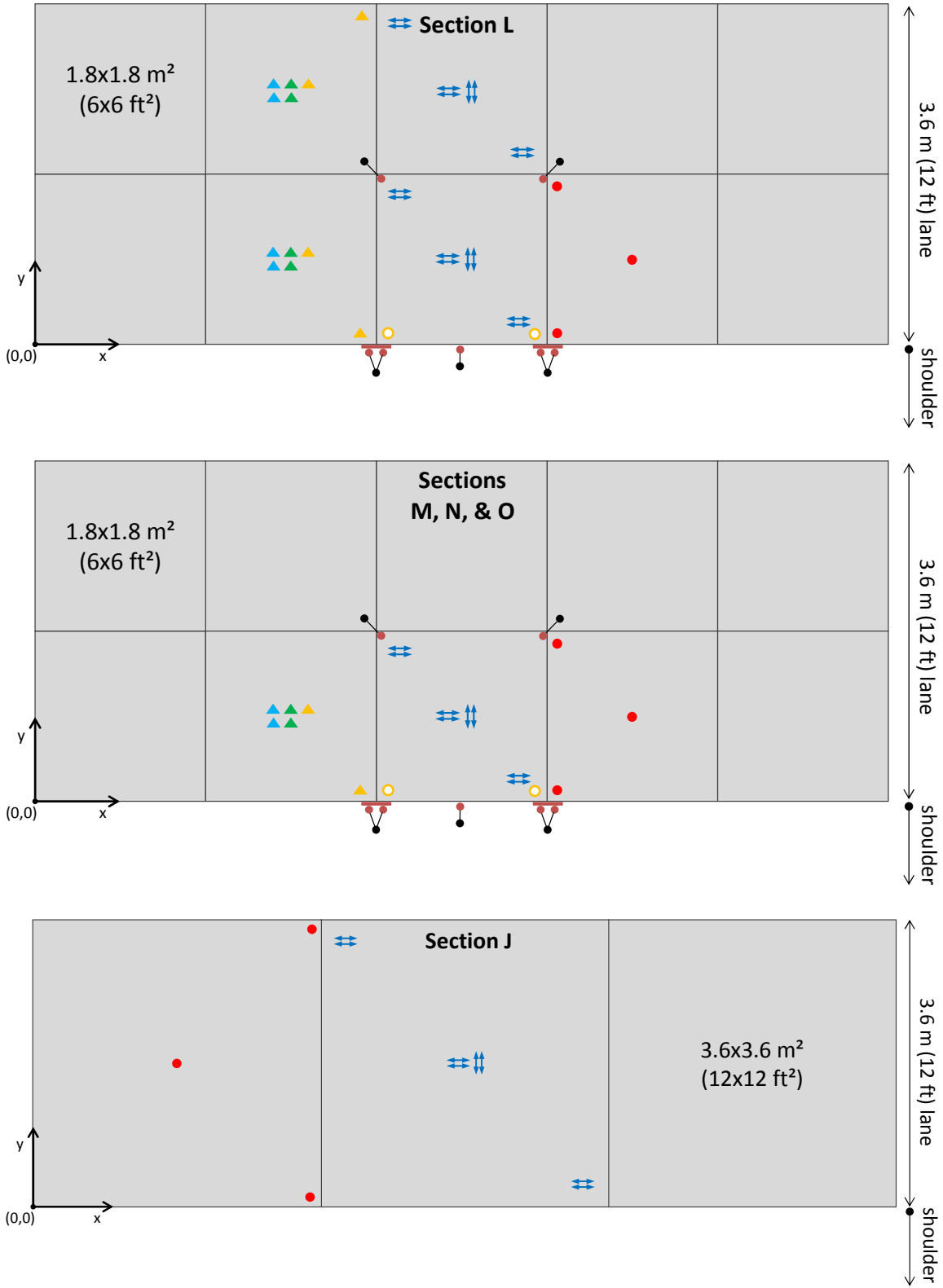
Figure 3.5: Instrumentation of the environmental sections.
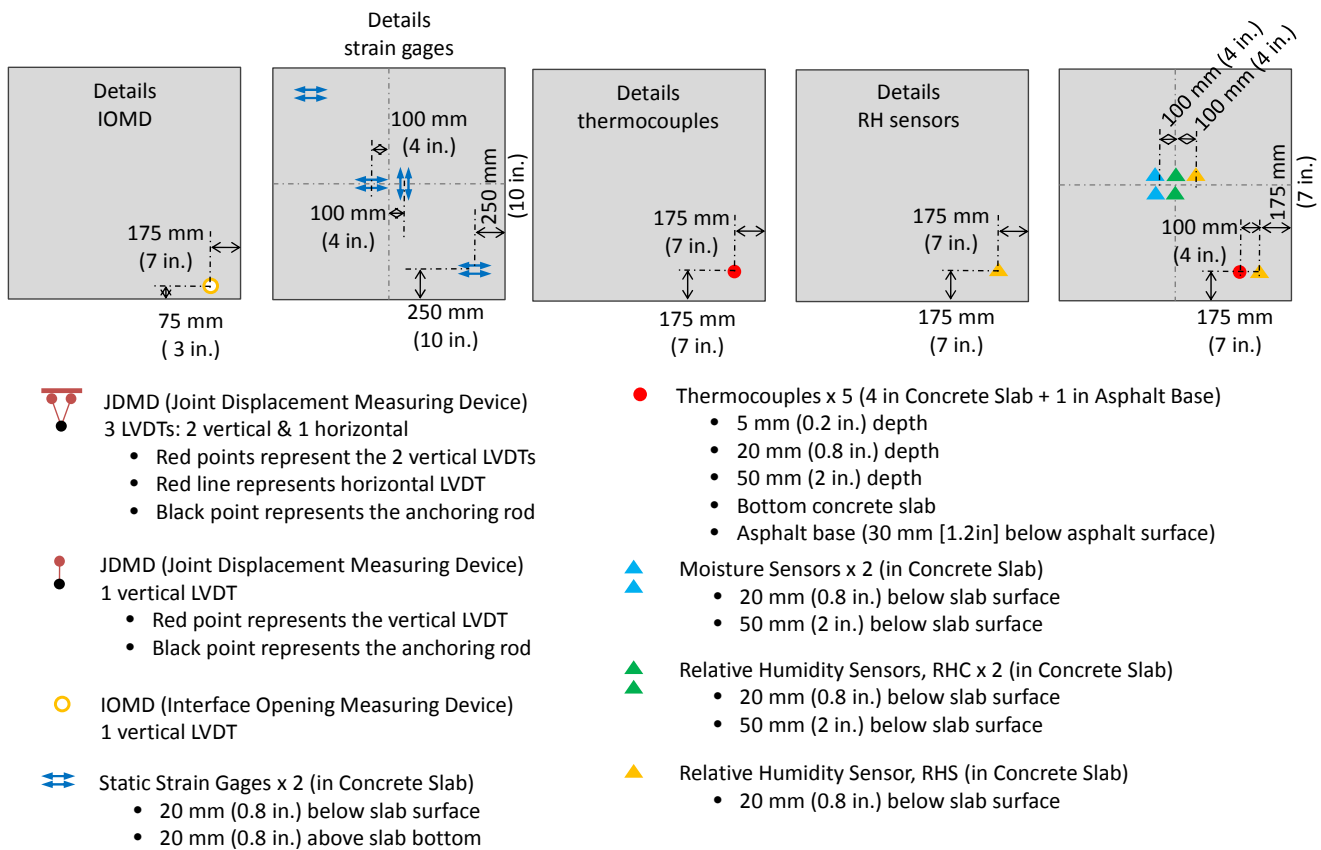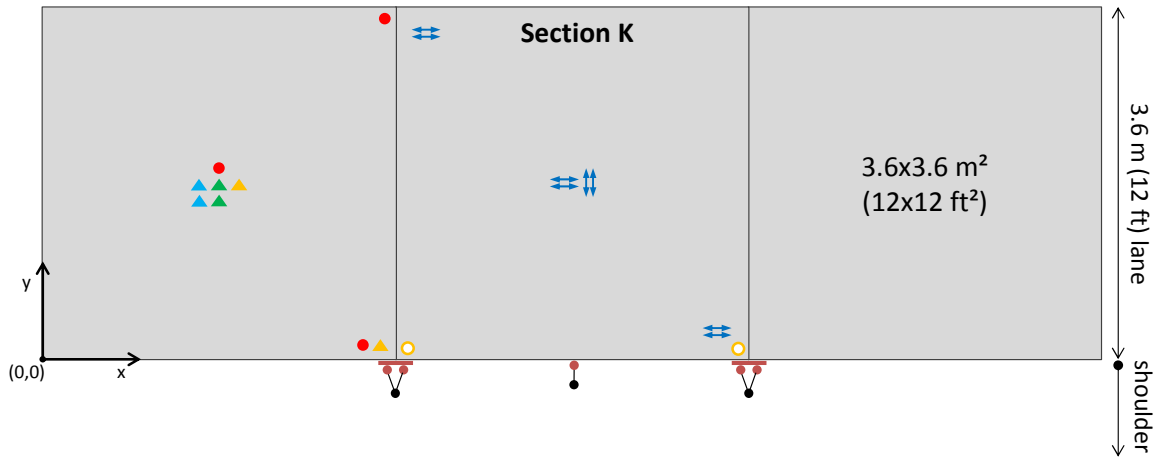
Figure 3.5 *(cont.):* Instrumentation of the environmental sections.

The relative humidity (RH) of the air in the concrete pores was measured in the environmental sections because this relative humidity is related to the suction in the water pores (Kelvin equation), which is the leading mechanism of moisture-related shrinkage *(8)*. In this experiment two types of sensors were used to measure this variable: the Campbell Scientific CS215-L sensor and the Sensirion SHT75. In Figure 3.5, these sensors are referred to as RHC and RHS, respectively. The actual sensor built into the former is also an SHT75 sensor. The main difference

between these sensors is that the CS215-L incorporates signal conditioning, which significantly simplifies data acquisition. The RH sensors were installed at two locations in a slab of each section: at the center of the slab and at an exterior corner, where more drying is expected due to moisture loss through the slab edge. Two depths were instrumented: 20 mm and 50 mm (0.8 in. and 2.0 in.). A 20 mm depth was selected because of the diameter of the RH sensors; this was the shallowest depth at which the RH instruments could provide measurements considered reliable. Specifically, the diameters of the RH sensors were 12.5 mm (0.5 in.) for the CS215-L and 10 mm (0.4 in.) for the encapsulated of SHT75 sensors. Relative humidity at 20 mm (0.8 in.) depth is an indication of autogenous and drying shrinkage, while RH at 50 mm depth is expected to be mainly related to autogenous shrinkage.

Moisture content sensors were installed as well. These sensors include a wooden part whose moisture content is measured and reported by the sensor. This moisture content can be regarded as an indirect indication of the moisture content of the concrete, but it is not the moisture content of the concrete. These sensors were installed at the center of a slab, at 20 mm and 50 mm (0.8 and 2.0 in.) depths.

It should be noted that Section L was instrumented with double the number of VWSGs, RH sensors, and MC sensors. This was done to increase the reliability of the estimation of the different variables in this section. This is so because the concrete type and slab size of Section L are representative of most of the HVS sections.

3.3   Sensor Naming Convention

A coding system has been used to assign each sensor a unique identifier. Each identifier is composed of four parts, separated by dots (for example, "Therm.A.S12+R.180.") How this identifier was arrived at is indicated below:

1. The first part of the name indicates the sensor type and direction (where applicable). The short names used for the different types of sensors are shown in Table 3.4. The direction code is applicable for strain gages and JDMDs.

Table 3.4: Short Names of the Sensor Types

Short Names	Sensor Type	Direction
Therm	Thermocouple	Not applicable
DySG	Dynamic strain gage	Transverse (T)
StSG	Static (vibrating wire type) strain gage	Longitudinal (L)
JDMD	LVDT	Vertical (V) Horizontal (H)
IOMD	LVDT	Not indicated, since they are always vertical
RHC	Relative humidity, CS215-L	Not applicable
RHS	Relative humidity, SHT75 with Univ. of Pittsburgh set up	Not applicable
MC	Moisture content	Not applicable

2. The second part indicates the letter of the section where the sensor was installed. For example, "C" is used for Section C.

3. The third item in the identifier indicates the sensor location, as indicated by the slab or joint number, preceded by the letter "S" for slab or "J" for joint, and by the location within the slab or joint. For example, "J3R" is used for the right edge of Joint 3.

    a. Slab and joint numbers have been assigned as indicated below. Each section has a hypothetical traffic direction (that is, the direction traffic would flow if this was an in-service pavement in the US).

half-lane design

widened lane design

full-lane design
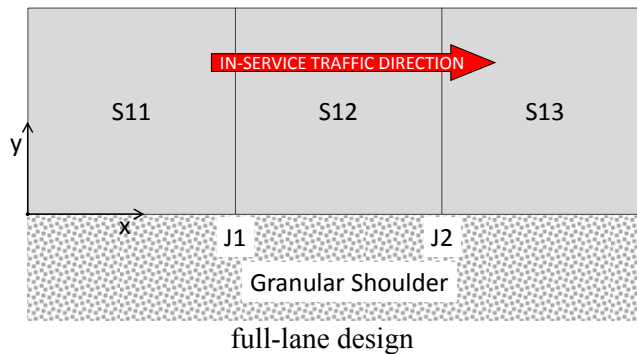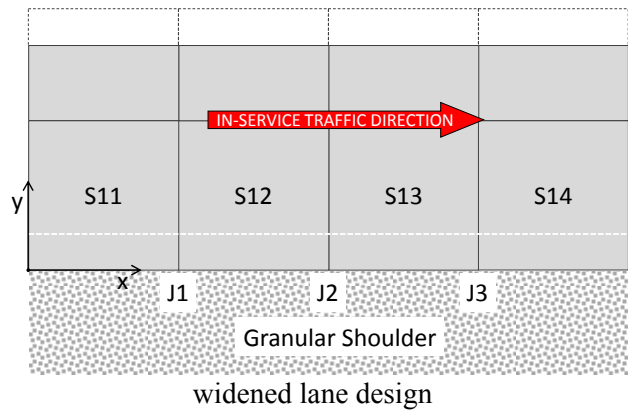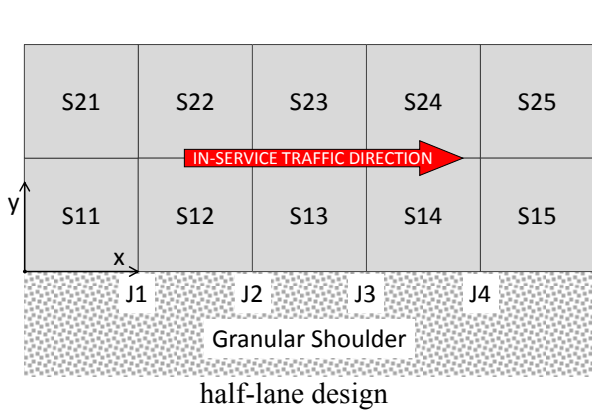
    b. The sensor's location within the slab is indicated with a symbol and a letter, as indicated below. Its location within a joint is indicated with either an "L" for left or an "R" for right. A minus sign (-), an equal sign (=), or a plus sign (+) refers to the approaching, middle, or leave part of a slab, respectively.

IN-SERVICE TRAFFIC DIRECTION

-L	=L	+L
-C	=C	+C
-R	=R	+R

L / C / R
stands for
left / center / right
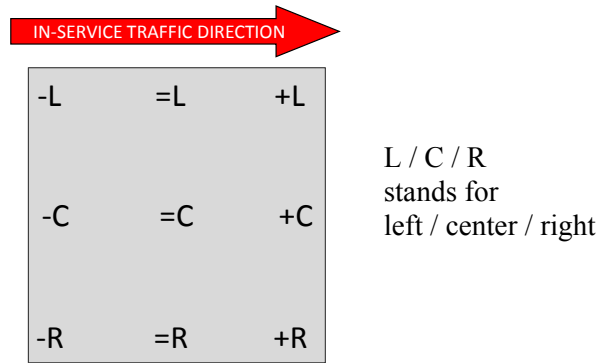
4. The fourth part of the identifier indicates the theoretical depth of the sensor, in millimeters.

Figure 3.6 includes examples of several sensor code identifiers for Sections A and K. Both the HVS and environmental instrumentation for Section K are shown in this figure.

3.4   Sensor Installation

The fifteen full-scale sections have been instrumented with a total of 560 sensors that can be can be classified in three categories, depending on whether they are located in asphalt, in concrete, or on the surface.

- The sensors installed in asphalt include the thermocouples located 30 mm (1.2 in.) below the asphalt surface and the strain gages located at the same depth in the newly surfaced asphalt area (Figure 2.1).
- The second group, all the sensors embedded in concrete, includes the rest of the thermocouples and strain gages, and all the relative humidity and moisture content sensors.
- The third group, all the devices installed on the surface of the concrete, includes both the joint displacement measurement devices (JDMDs) and the interface opening measuring devices (IOMDs), all of which are LVDT sensors that were installed after placement of the concrete overlay.

Asphalt strain gages were installed at the interface between the rubberized gap-graded mix (RHMA-G) and the hot mix asphalt (HMA) layer, both of which were placed on October 13, 2015. The strain gages were placed on top of the HMA layer, then the sensors were protected with fine aggregate mix (FAM) to prevent them from being damaged during the placement of the RHMA-G overlay (Figure 3.7). The sensor cables were protected with asphalt tape so that they would not be moved during the extension of the RHMA-G overlay.

Section A

Therm.A.S12=C.005
Therm.A.S12=C.020
Therm.A.S12=C.050
Therm.A.S12=C.150
Therm.A.S12=C.180

Therm.A.S12+L.005
Therm.A.S12+L.020
Therm.A.S12+L.050
Therm.A.S12+L.150
Therm.A.S12+L.180

1.8x1.8 m

3.6 m lane

DySGT.A.S13-C.020
DySGT.A.S13-C.130

DySGT.A.S14+C.020 (top of slab)
DySGT.A.S14+C.130 (bottom of slab)

y

(0,0)   x

shoulder

Therm.A.S12+R.005
Therm.A.S12+R.020
Therm.A.S12+R.050
Therm.A.S12+R.150
Therm.A.S12+R.180

JDMDV.A.S13=R

IN-SERVICE TRAFFIC DIRECTION

JDMDV.K.S12-L   JDMDV.K.S12+L

Section K

RHC.K.S11=C.020
RHC.K.S11=C.050

MC.K.S11=C.020
MC.K.S11=C.050

StSGL.K.S12=C.020
StSGL.K.S12=C.095

DySGT.K.S12-C.020
DySGT.K.S12-C.095
DySGT.K.S12-C.145

StSGT.K.S12=C.020
StSGT.K.S12=C.095

RHS.K.S11=C.020

3.6x3.6 m

3.6 m lane

y

(0,0)   x

IOMD.K.S12-R

JDMDH.K.J2R

RHS.K.S11+R.020

JDMDV.K.S12+R   JDMDV.K.S13-R

shoulder

DySGL.K.S11=R.020 (top of slab)
DySGL.K.S11=R.095 (bottom of slab)

Figure 3.6: Example sensor codes (Sections A and K).

| **Strain gage on top of HMA, before FAM protection** | **Three strain gages, after FAM protection, before extension of the RHMA-G overlay** |

Figure 3.7: Asphalt strain gages on top of the HMA layer.

The asphalt thermocouples were inserted into a 30 mm (1.2 in.) long hole drilled into the asphalt before placement of the concrete overlay. The thermocouples located at the bottom of the concrete overlay were placed directly on top of the asphalt base. The rest of the thermocouples were attached to a fiberglass rod at the desired heights, as shown in Figure 3.8. The fiberglass rod was then mounted on a chair consisting of a metal disc with a metal tube welded to it, and a horizontal screw was used to fix the rod's position. The tip of the fiberglass rod, where the shallowest thermocouple was installed, was set at a depth of 5 mm (0.2 in.) using the tube-screw system to ensure that the rod tip would be the correct distance from the surface of the concrete after placement of the overlay. The height of the concrete overlay surface was determined by a straightedge resting on top of the paving forms. The same procedure was used for installing the relative humidity and moisture content sensors. This procedure ensured a relatively good match between the theoretical and actual depths of the sensors, which was particularly important for the sensors measuring temperature, moisture content, and relative humidity, because these variables are especially sensitive to how deep they are in the concrete slab.

Moisture content and relative humidity sensors were installed using the same chair used for the installation of the thermocouples. Figure 3.9 contains a diagram of the fiberglass installation frames and photographs of the sensors after installation. As shown in this figure, the sensors were moisture-conditioned before concrete paving because it was important to have them in a moisture/relative humidity condition close to that expected when they were immersed in fresh concrete. The conditioning was accomplished by wrapping the sensors with wet paper towels, and then placing both the sensors and wet paper in a plastic bag, following recommendations of the University of Pittsburgh team.
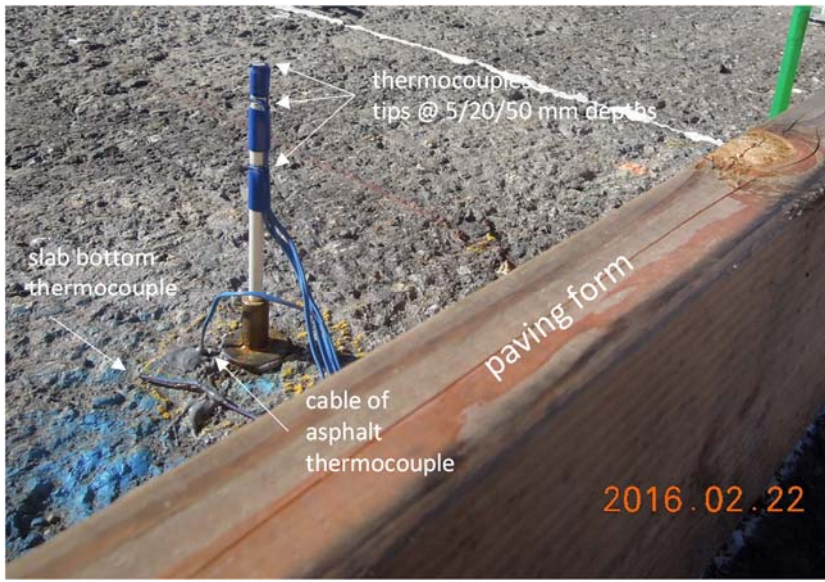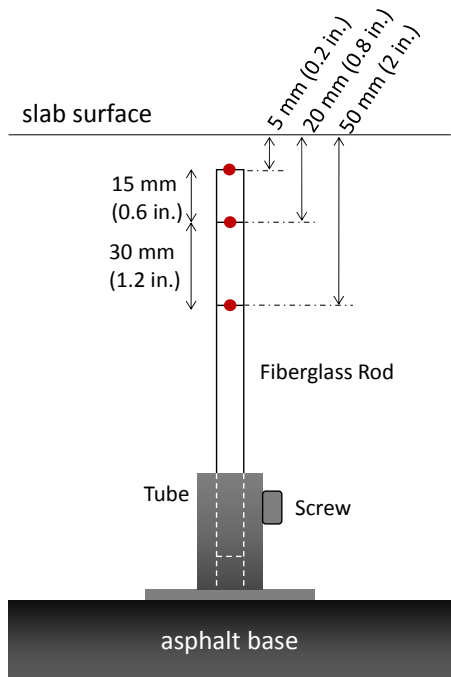
Figure 3.8: Installation of thermocouples embedded in the concrete.

The dynamic and static strain gages were both installed by using fiberglass frames to set them in place, but without the tube-screw system used earlier, even though this meant that the distance between the upper strain gage and the top of the slab might vary from the 20 mm (0.8 in.) target value (because the actual slab thickness might differ from the theoretical one) (Figure 3.10). On the other hand, this allowed the lower strain gage to be located at the correct distance (20 mm [0.8 in.]) from the bottom of the slab and ensured that the distance between both strain gages would match the theoretical distance.
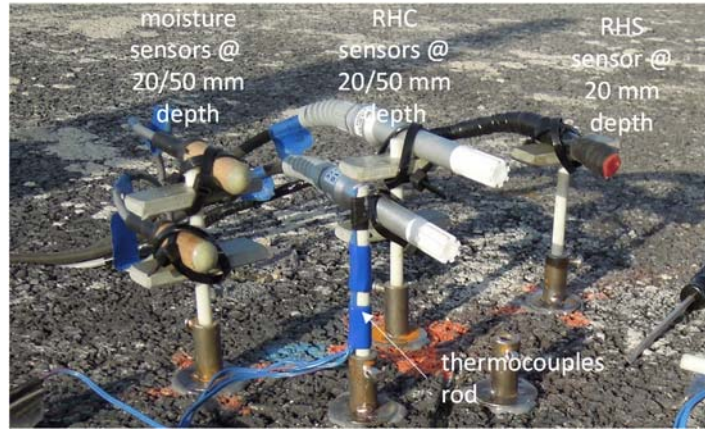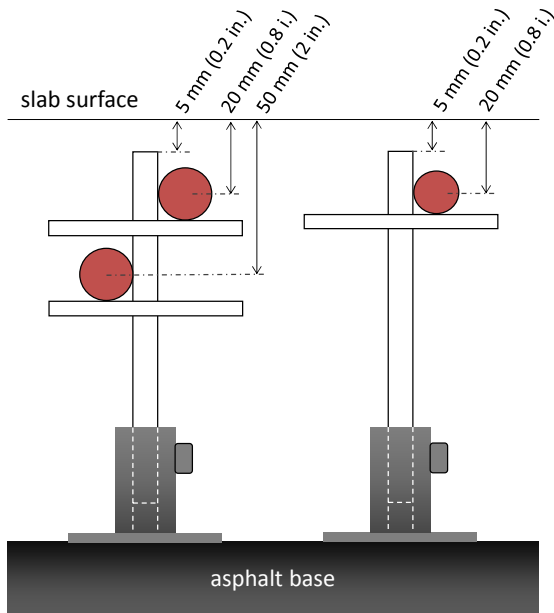
| Moisture conditioning of RH and moisture content sensors | From left to right: two moisture content sensors (the bottom one is under the wet paper towel), two RHC sensors, and one RHS sensor |

Figure 3.9: Installation of relative humidity and moisture content sensors.

The third category of sensors, those installed on the surface of the concrete overlay, includes JDMDs and IOMDs. These LVDT sensors were installed after the concrete saw-cutting operation. The anchoring frames for the vertical JDMDs and IOMDs are depicted, respectively, in Figure 3.3 and Figure 3.4. As explained in Section 3.2.1, the LVDT sensors of the vertical JDMDs were attached to an arm-rod fixture anchored in the subgrade. A PVC pipe that was installed from the surface extended past the bottom of the granular subbase to ensure that the rod was actually anchored in the subgrade and not in the subbase. The rods have two parts, a lower segment that has one end anchored in the subgrade and the other end flush with the overlay surface, and an upper segment that screws into the top part of the lower segment. For the environmental sections, the lower segment of the rods was installed before overlay construction so that vertical JDMDs could be rapidly installed after saw-cutting. Note that in Figure 3.11 three of the rods are located at the shoulder and two of them are located in the lane. For these interior

locations, a short PVC tube was placed on top of each PVC pipe to prevent concrete from adhering to the lower segment of the rod during overlay construction. One of these short PVC tubes can be seen in the upper left of the photograph showing the dynamic strain gages in Figure 3.10. After installing the top part of the rods, a concrete block was placed to prevent the rod from moving horizontally. The aim of this was to minimize rod vibrations caused, for example, by wind. An example showing the vertical JDMDs of Section L appears in Figure 3.11.

Installation frame for dynamic strain gages

Dynamic strain gages
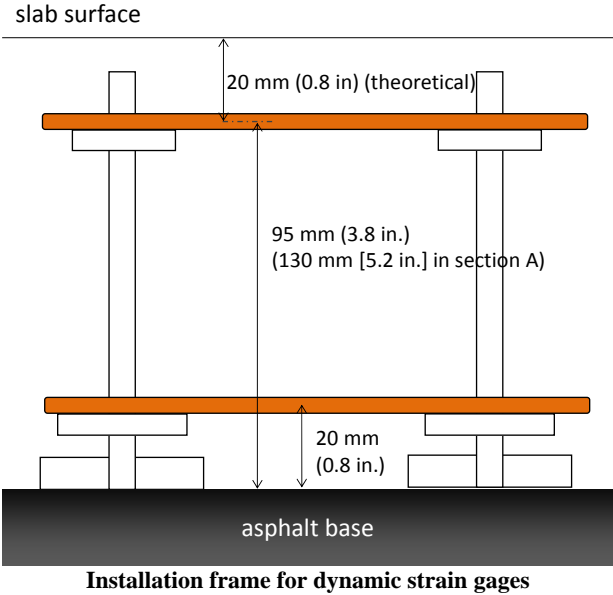
Installation frame for static strain gages
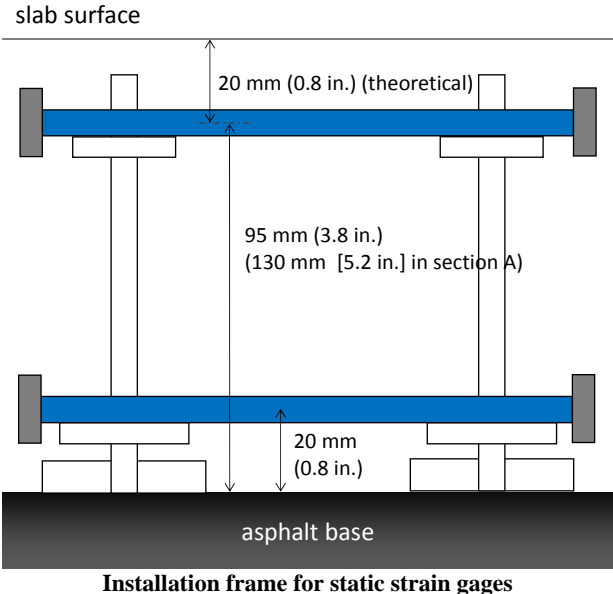
Static strain gages (two longitudinal, two transverse)
Note: **the pink threads will mark the exact location of the VWSGs after overlay paving. The exact location of the gages was required for forensic coring.**

Figure 3.10: Installation of strain gages.
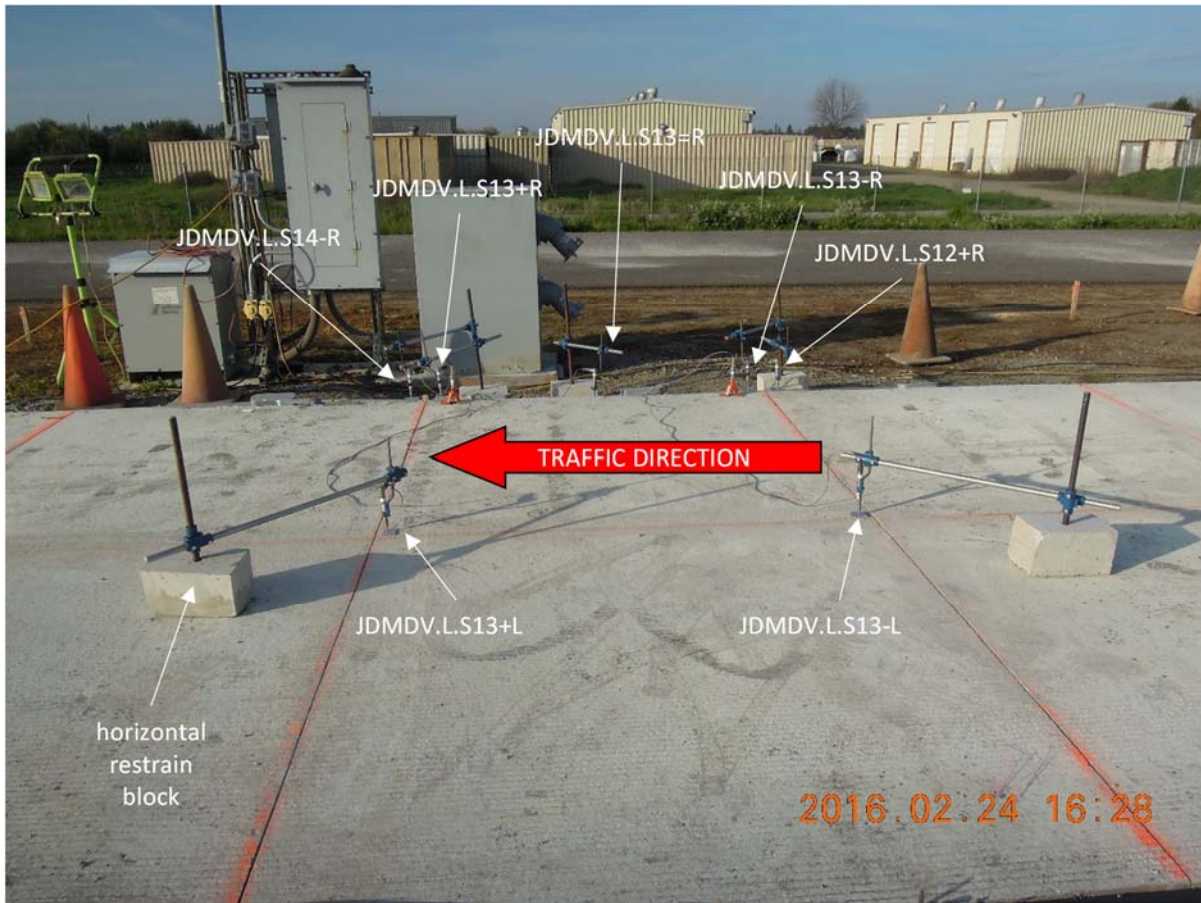
Figure 3.11: Vertical JDMDs (Section L).

Horizontal JDMDs expand across transverse joints, as shown in Figure 3.12. In this part of the experiment set up the LVDTs were fixed with a holder that was glued and screwed to the slab edge. A threaded rod was cast in place for this purpose, using a special paving form (see Figure 3.13). As this figure shows, other threaded rods were also installed to place the targets for the LVDTs.

Figure 3.12: A horizontal JDMD.
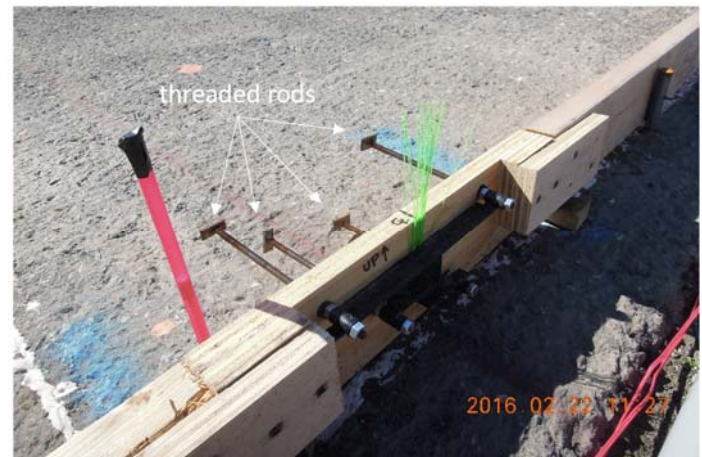
Figure 3.13: JDMD targets and horizontal JDMD holder.

Interface opening measuring devices were installed in five of the environmental sections. As explained above, IOMDs consist of an LVDT that is fixed to the slab surface and whose tip rests on a rod anchored in the asphalt base (see the diagram in Figure 3.4 and the photographs in Figure 3.14). As the figure on the right in Figure 3.13 shows, the rod was sheathed with a plastic straw to prevent it from adhering to the concrete. Using this configuration, the LVDTs capture any separation between the concrete slab and asphalt base. Two vertical rods were also placed in each of the HVS sections so that IOMDs could be installed when the accelerated load testing was conducted.

Figure 3.14: Interface opening measuring device (IOMD).

3.5 Automatic Data Collection

As noted above, the BCOA sections were instrumented with a total of 560 sensors, 315 of which were considered to be "HVS instrumentation" and the rest were considered to be "ENV instrumentation". The HVS instrumentation was focused on the structural response of the sections under the moving HVS wheel. These data were collected by the National Instruments data acquisition systems (DAS) on the two HVS units. The environmental instrumentation was focused on the response of the sections to environmental agents and cement hydration. These static data were collected using three Campbell Scientific data acquisition systems.

The data acquisition systems of the two HVS machines were used for collecting HVS instrumentation data. The HVS machines, including DAS, were moved from one section to another in order to conduct the accelerated load testing. Two sets of eleven LVDTs used as JDMDs and IOMDs were also moved from one section to another for accelerated load testing.

HVS testing started in June 2016, so the two HVS DASs were available since the overlay construction until then. These two DASs were used to monitor the slab movements of two of the environmental sections, M and O. These DAS units collected static LVDT data on these two sections until May 9, 2016, as shown in Figure 3.15.

The two HVS DAS are exactly the same and were designed and built in-house by the UCPRC *(20)*. The modular design of the DAS allows one to accommodate different sensors by simply inserting the corresponding signal conditioning modules. The software allows simultaneous collection of transient dynamic data induced by load and slow-moving static data related to the environment. The DAS has software and hardware components designed to record the operating status of the HVS (traffic count, carriage load, carriage speed, carriage lateral and longitudinal

position, etc.). Data collection can be triggered either manually or automatically following a predefined schedule based on time or traffic count.
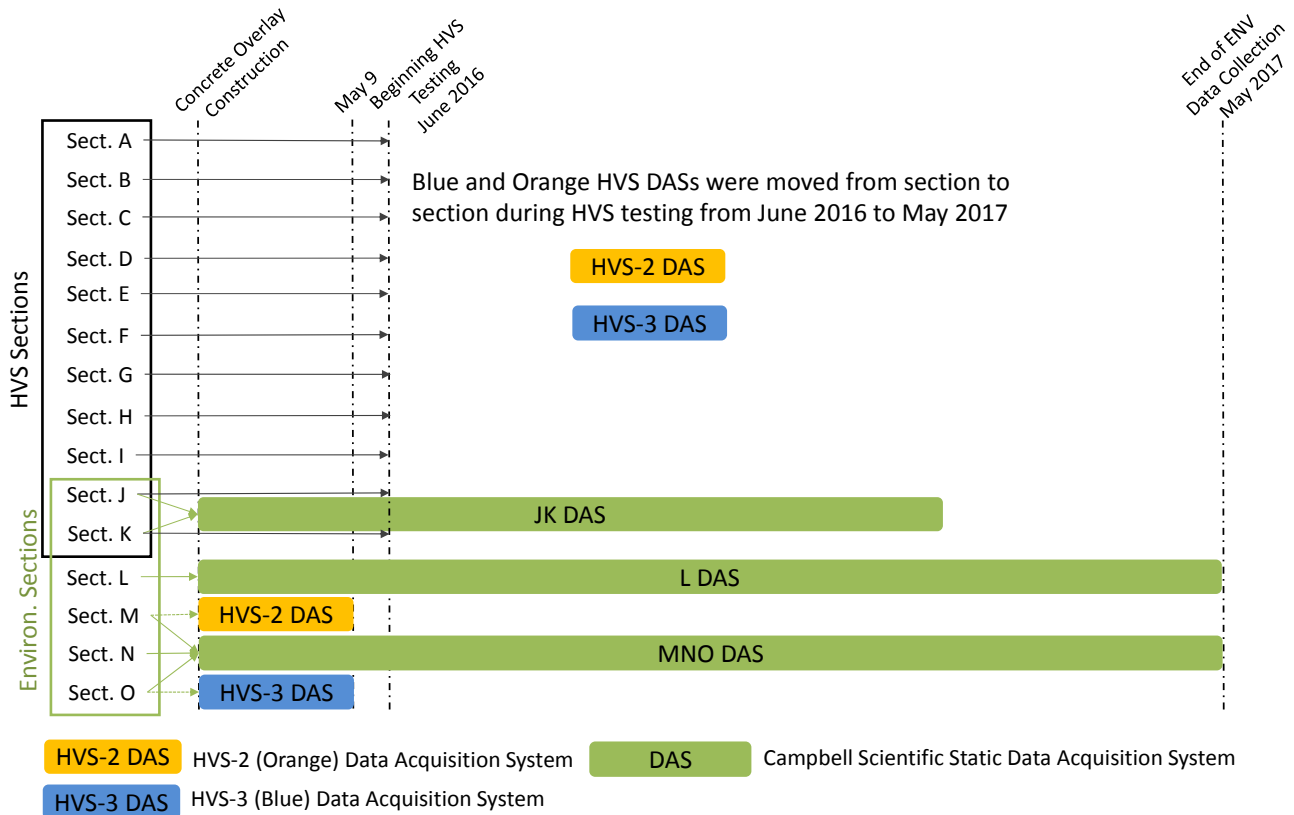
Note: The two HVS units are usually referred to as "Orange" and "Blue," reflecting the colors they are painted.

Figure 3.15: Experiment data collection systems.

The "static data" collected on the environmental sections were collected using three Campbell Scientific data acquisition systems (see Figure 3.15). Data collection started the night before overlay construction, which was February 23, 2016, for the Lane 1 sections and February 25, 2016, for the Lane 2 sections. In the initial phase of data collection, the sampling interval was two minutes. After March 3, 2016, the sampling interval was set to five minutes, and it was set to 20 minutes after November 2016.

A total of three Campbell Scientific DAS units were built by UCPRC for collecting the environmental data (see Figure 3.16). Each of them has a CR1000 data logger connected to various multiplexers to increase the channel count capacity. Each of them can record temperature from thermocouples, static strains from vibrating wire strain gages along with the temperature from the built-in thermistors, and relative humidity and temperature from both

directly connected Sensirion SHT75 humidity sensors and from the Campbell Scientific CS215 sensors. In addition, each DAS can record the voltage signal from DC-operated LVDTs.

Figure 3.16: Pictures of one of the Campbell Scientific data acquisition systems.

Each Campbell Scientific DAS was fitted with a DL121 adaptor to allow an Ethernet connection. A PC was set up to download data via Ethernet from each of the three DAS units at midnight every day using the *LoggerNet* software from Campbell Scientific.

Two A3 NEMA data loggers made by SMT Research (see Figure 3.17) were used to record the moisture content and temperature readings from the embedded moisture sensors (EMS) from SMT. Each EMS provides a moisture reading from the wood sensor and a temperature reading from a built-in thermistor. Each of the A3 boxes has eight channels that can be used to record either moisture content or temperature. A decision was made to use each A3 box to connect six EMS's. Three of the six sensors were installed at 20 mm (0.8 in.) depth in the concrete layer, while the other three were installed at 50 mm (2.0 in.) depth. All six moisture content signals were

connected. The remaining two channels were used to connect the temperature signals with one channel for each depth. The temperature data were needed for correcting the moisture content readings.

Figure 3.17: Photos of the A3 NEMA data logger from SMT Research.

(This page intentionally blank)

4 CONSTRUCTION OF THE CONCRETE OVERLAYS

4.1 Pre-Paving

As explained above, BOCA sections were built along two lanes of the UCPRC full-scale testing site (Figure 2.1). Some of the sections were built on top of existing asphalt pavements that had been tested with the HVS within the framework of another research project. The rest of the sections were built on a new asphalt surface that was paved in October 2015 on top a full-depth reclaimed layer. Several preparatory works were required prior to the construction of the concrete overlay. These are described below.

The area of the testing site corresponding to old pavements was textured to remove surface distresses and to create a uniform surface for overlay construction. Micromilling was used as the reference texturing technique even though standard milling is the technique typically used for BCOA sections in other states. In order to study the effect of the two types of surface texturing, standard milling was applied in a small area corresponding to Section C so that its response could be compared with the results measured on Section B, which was micromilled. The same machine (shown in Figure 4.1) can apply both micromilling and milling but in applying the former a smaller tooth spacing is used (1/4 in. for micromilling versus 5/8 in for milling), which results in smaller ridge-to-valley depths and a more precise asphalt depth than standard milling can provide.

Micromilling was also applied to an area of the new asphalt surface, corresponding to Section F, which was also introduced to study surface texture effect. In this case, results collected on Section F would be compared to those from Section I, where no texturing was used. Figure 4.2 shows the how the surface texturing was laid out.

Figure 4.1: Milling machine with micromilling teeth spacing.
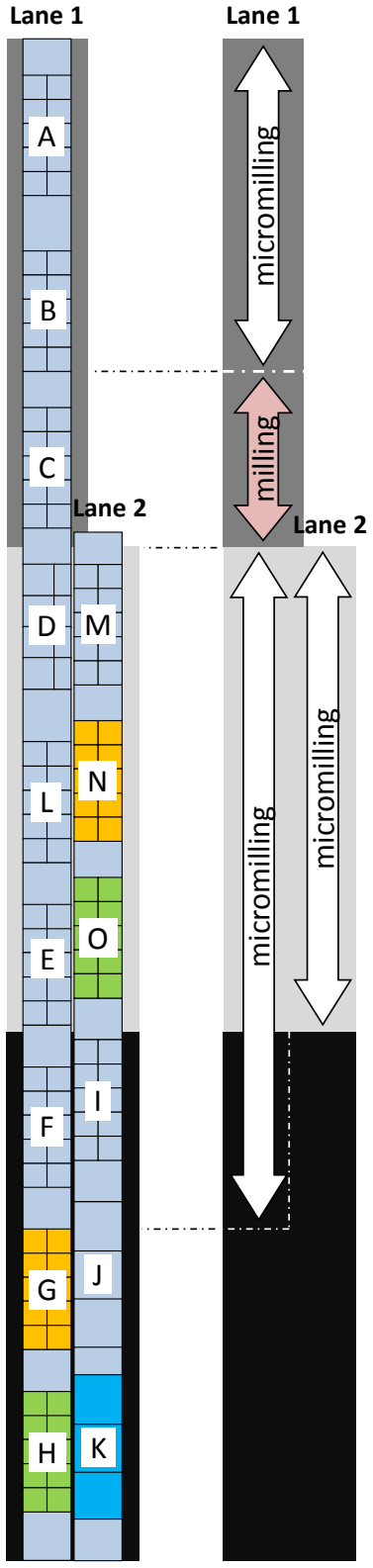
Figure 4.2: Layout of the asphalt surface texturing.

The approximate depths removed by the micromilling and milling operations were, respectively, 15 mm (0.6 in.). and 30 mm (1.2 in.). Where milling was to be applied the asphalt thickness was approximately 120 mm (4.7 in.), which corresponds to two lifts of approximately equal thickness, roughly 60 mm (2.5 in.). This meant that 30 mm (1.2 in.) of the top lift would remain after milling. This was considered a thickness sufficient to avoid affecting the bond between the top and bottom asphalt lifts during milling operation. Nonetheless, debonding took place in a significant area of the section, close to the edge, as shown in Figure 4.3.

After texturing operations, several passes of a sweeper vacuum truck cleared the milled and micromilled surfaces. Two days before construction of the overlay, the asphalt surfaces of all the sections (milled, micromilled, and unmilled asphalt) were swept manually.

Figure 4.3: The appearance of the surface after milling shows debonding of the two older asphalt lifts.

Paving forms were placed the last week of January 2016 so that more than three weeks were available to install embedded sensors in the concrete. All the longitudinal forms and transverse forms of Lane 1 were placed at that time, as were the longitudinal forms for Lane 2. However, the transverse forms of Lane 2 could not be placed since ready-mix trucks were using the lane to access the Lane 1 sections. Transverse forms were necessary not only at the ends of each lane, but also wherever there was a transition in the concrete material being placed or a change in surface elevation, as shown in Figure 4.4. Longitudinal forms were placed in a way that the top edge followed a straight line along each section. This line ensured the theoretical overlay thickness at the two ends of the section, although the thickness at intermediate points of the section might differ from the theoretical one. It

should be noted that all the forms were checked before concrete paving since several weeks had passed since they were installed and some might have come loose.
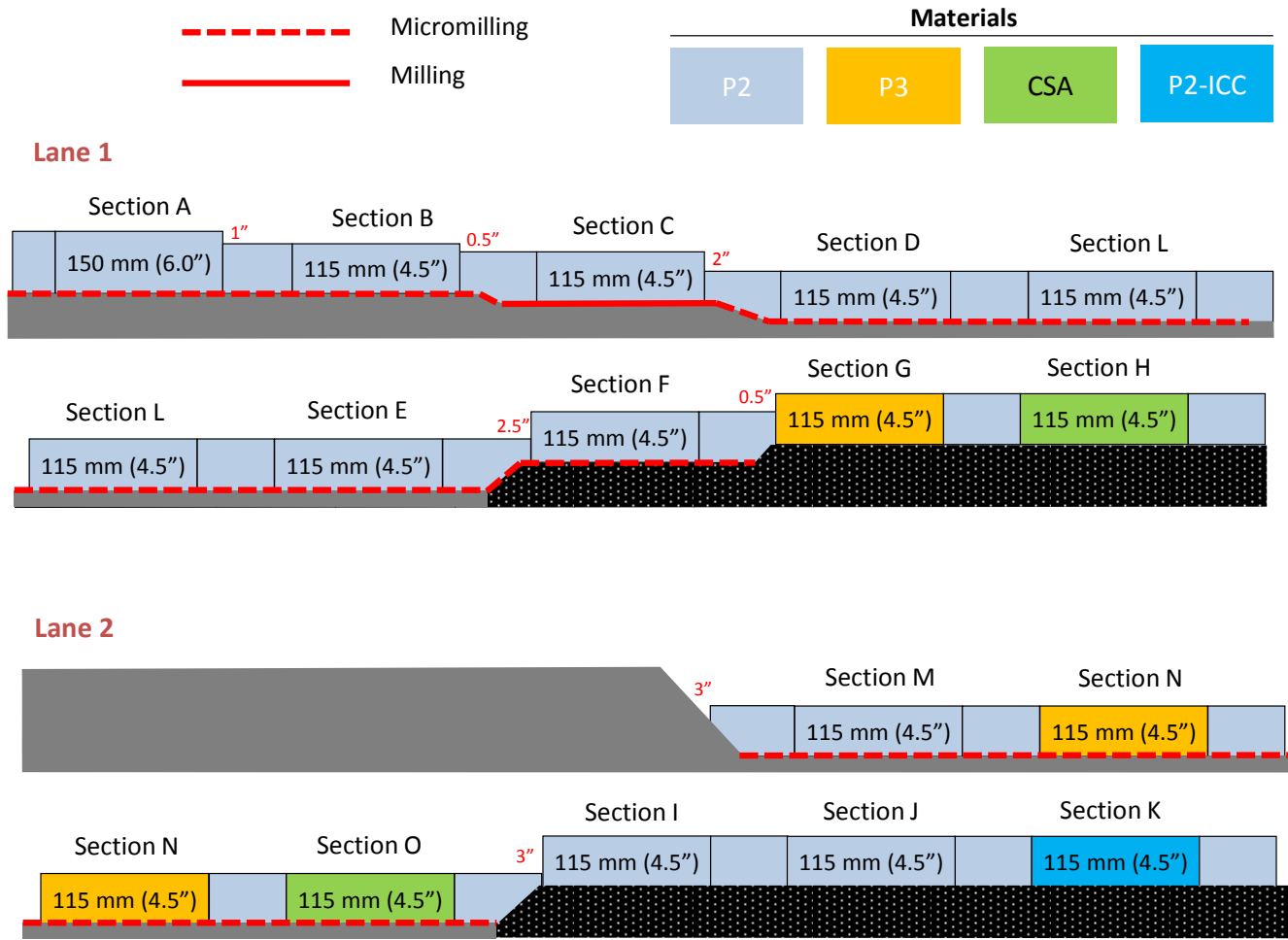
Figure 4.4: Longitudinal profile of the two lanes.
(Note: figure not to scale.)

The installation of sensors in Lane 1 took place during the first three weeks of February 2016, following the techniques presented in Section 3.4 of this report. The Lane 1 environmental sensors were connected to the corresponding DAS, and a first verification that the sensors were functioning correctly was conducted. The environmental sensors in Lane 2 were also connected to the corresponding DAS, but only sensors along the exterior edge were initially installed. These sensors were protected with cones during Lane 1 paving operations on February 23, 2016, as shown in Figure 4.5. As noted above, ready-mix trucks moved along Lane 2 during Lane 1 paving operations. The rest of Lane 2 sensors were installed on February 24, 2016, and the Lane 2 transverse forms were also installed that day. Figure 4.5 shows Lanes 1 and 2 before concrete overlay construction.
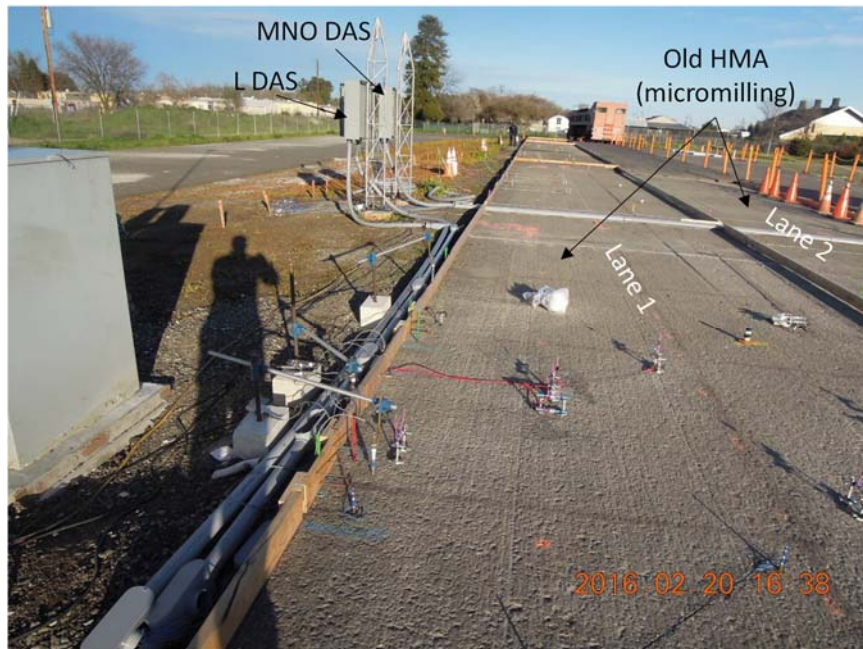
Figure 4.5: Asphalt base before overlay paving.

In the early morning of each paving day the asphalt surface was wetted before concrete placement. This was done to ensure that asphalt surface was wet but without standing water, creating a saturated surface-dry condition.

4.2 Construction of the Overlay

The overlay construction period spanned three days, from February 23 to 25, 2016, with Lane 1 construction on February 23 followed by that of Lane 2 on February 25. The portland cement–based concrete mixes were produced at the Teichert Perkins plant in Sacramento, a thirty minute drive from the UCPRC facility at UC Davis. The accelerator admixture for these mixes was dosed into the ready-mix trucks at the construction site immediately prior to placement of the concrete (Figure 4.6). CSA cement–based concrete was produced using volumetric batching, a method that uses volume rather than weight. This method is commonly used in California with this type of very fast-setting concrete and the specialized equipment to perform it eliminates the risk that the CSA cement concrete will set up in the drum of the ready-mix truck during transportation. The Cement Tech volumetric mixer used for construction of the CSA sections on both construction days is shown in Figure 4.7. Prior to production, the volumetric mixer gate and auger settings were calibrated to produce the specified mix design using the cement, sand, and coarse aggregate held in bins on the equipment. The equipment feeds these raw materials to a mixing chamber where the water and admixtures are metered in. Next, the ingredients are moved through a mixing auger to produce a homogeneous concrete mixture.

Figure 4.6: Accelerator dosed into the ready-mix truck.

Figure 4.7: Volumetric mixer.

With the exception of the lightweight aggregates (LWA), the same aggregates were used for the all mixes, including the CSA-based concrete (Table 2.2). These aggregates came from the Teichert Perkins plant's alluvial deposits in east Sacramento. The LWA for the internally cured concrete were supplied by Trinity Aggregates. These aggregates were supplied to the Teichert plant in pre-wetted, surface-dry condition. In addition, an expert from Trinity Aggregates came to the Teichert plant to ensure that the aggregates were adequately stored and handled, following a specific procedure to keep the moisture condition of the LWA close to pre-wetted surface-

dry, as recommended by the Expanded Shale, Clay, and Slate Institute. The actual absorption and unit weight of the supplied aggregates were determined at the batch plant. These values were used to determine sand replacement for the internal-curing concrete (ICC).

A hand-operated roller screed was used for placement and consolidation of the concrete. This selection was made because of the relatively small configurations of the concrete placements and high workability of the mixes, as reflected in the high specified slump values (see Table 2.2). Minimal additional vibration was required for most sections and a hand vibrator was used where it was required. Both the ready-mix trucks and the volumetric mixer placed the concrete directly onto the sections by using the truck's discharge chute. Due to its high slump value, the concrete could be easily placed over the width of the paved lane. During Lane 1 construction, the trucks moved along the adjacent Lane 2 and during Lane 2 construction they moved along Lane 3.

Apart from the two CSA sections (Section H in Lane 1 and Section O in Lane 2), eight ready-mix trucks were required for the Lane 1 overlay construction and six were required for Lane 2. This includes paving the sections themselves, the intermediate areas between sections, and the ramps to access both lanes. The trucks were assigned consecutive numbers, according to the order in which they were used. For reporting and quality control purposes, the CSA volumetric mixing of each section was also assigned a truck number. Correspondence between truck number and overlay area is shown in Figure 4.8. It should be noted that the intermediate areas between sections were all paved with the P2 mix (10-hour OT, Type II/V cement). These intermediate slabs were required to provide a place for the feet of the Heavy Vehicles Simulators during accelerated loading testing.
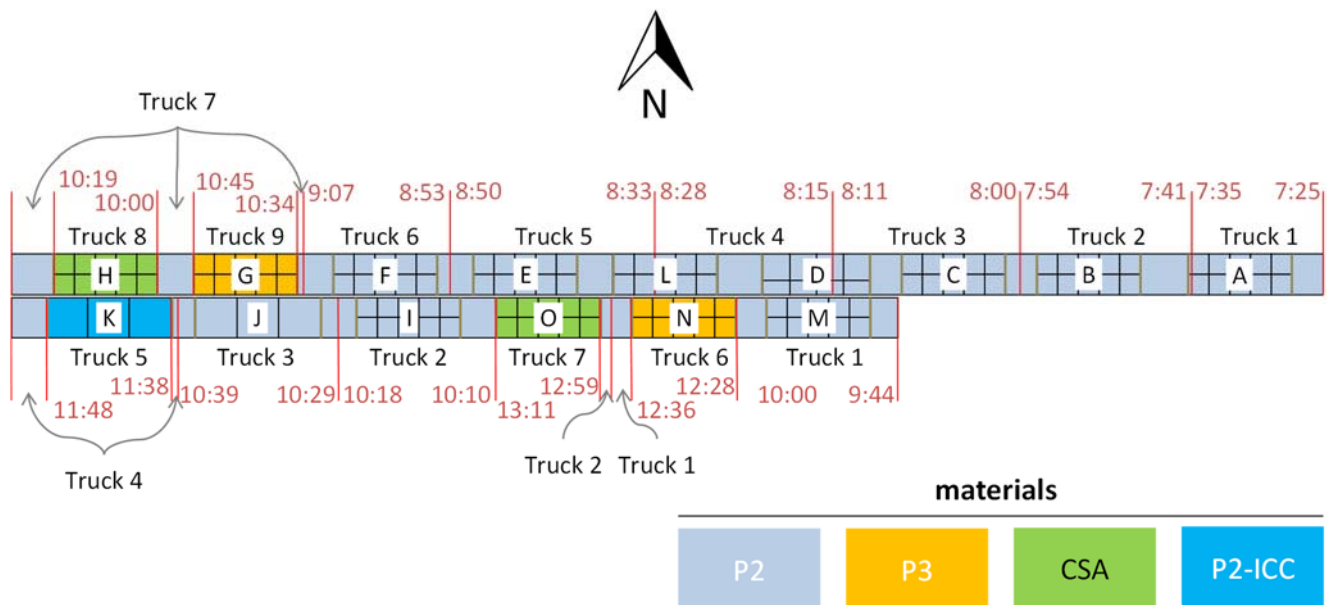
Figure 4.8: Overlay area paved with each truck.
(*Note:* **The start and end placement time for each truck is shown in red.**)

A crew of seven people protected the sensors during the placement and consolidation of the concrete. Each person first shoveled concrete carefully around the sensors, then used the shovel to keep them from receiving the direct impact of concrete poured from a truck's discharge chute, as reflected in Figure 4.9. The shovel also prevented the sensors from being swept away by concrete flow. Once the concrete was discharged onto the section, it was consolidated by hand around the sensors using a manual vibrator with a diameter of one inch. As a result of this protective approach, only one (static) vibrating wire strain gage and one (dynamic) resistive strain gage were lost among all installed sensors.

Figure 4.9: Protecting the sensors during overlay paving.

The concrete surface was finished with bull floats and edge trowels, and then longitudinal tining was applied by hand pulling a metal rake along the surface to create grooves in the pavement with a depth of approximately 5 mm (3/16 in.). Both operations were conducted immediately after screeding, while the concrete was still workable (Figure 4.10).

Application of curing compound—according to Caltrans specifications for concrete pavements—was the curing approach taken for all sections, except for Section M. For this section an advanced curing approach was followed instead, as explained in Section 2.4. This approach was based on the topical use of a shrinkage-reducing admixture (SRA) that was sprayed on the overlay surface (as shown in Figure 4.11) before the curing compound was applied. In fact, three applications of SRA were required to supply the target dosage of 300 ml SRA/m² (8.5 oz SRA/yd²) without having the SRA flow unevenly across the surface or off the surface. The timing for the first application was the same as that for standard curing compound; this can be seen in the photograph on the left side of

Figure 4.11, where the shine on the concrete surface had disappeared, leaving a dry appearance. Subsequent applications were conducted after the concrete had adsorbed the previously sprayed SRA solution. The timing and dosage of the three applications are presented in Table 4.1. As noted earlier, the timing and concentration of the SRA solution (50 percent in this case) depends on weather conditions and target dosage. Final applied dosage was 276 ml SRA/m² (7.8 oz SRA/yd²). Both the curing compound and the SRA were applied manually, as shown in Figure 4.11 and Figure 4.12.

| Bull float finishing | Metal rake tining |

Figure 4.10: Surface finishing and tining of concrete overlay.

| Surface appearance before SRA application | Manual application of the diluted SRA |

Figure 4.11: Application of the shrinkage-reducing admixture (SRA).

Manual spraying of curing compound	Appearance of the final surface

Note: **pads were used to measure the curing compound application rate.**

Figure 4.12: Curing compound application.

Table 4.1: SRA Application on Section M

	Start	**End**	**Amount of SRA Solution**
Section M paving	9:44	9:58	
1st SRA application	10:45	10:55	9.88 kg
2nd SRA application	11:10	11:20	9.10 kg
3rd SRA application	11:30	11:40	8.44 kg
Total solution (50% SRA)			27.4 kg
Total SRA			13.7 kg
Actual SRA dosage (49.7 m²)			276 g SRA/m² (7.8 oz SRA/yd²)
Curing compound application*	12:00	12:02	

Note: * Standard curing compound was sprayed on Section M after SRA application.

Joins were cut to a depth of one-third of slab thickness, which resulted in 50 mm (2 in.) saw cut for Section A and a 38 mm (1.5 in.) saw cut for the rest of the sections (Figure 4.13). Full-depth cuts were conducted at the beginning and end of each section where transverse paving forms had not been previously placed. The objective of this full-depth cutting was to ensure that the performance of each section did not interfere with the performance of the adjacent sections. In addition, the feet of the HVS were expected to significantly damage the intermediate slabs between sections and that damage might affect an adjacent section's slabs without a full-depth cut to prevent it.

Figure 4.13: Saw-cutting operation.

Eight beams, 500×150×40 mm (18×6×1.6 in.), were also fabricated during the second day of overlay construction (Figure 4.14). These beams were used to measure the unrestrained expansion-contraction of the different concrete mixes attributable to changes in temperature and moisture since they were not bonded to any support. A vibrating wire strain gage (VWSG) was placed inside the mold of each beam so that concrete strain could be continuously monitored since setting time. Mix to prepare these beams was taken from one truck of each mix type. A 19 mm (3/4 in.) sieve was used with each sample to remove aggregates that were too large for the desired beam thickness. It should be noted that 14 percent of the coarse aggregate (1 in. × #4) was retained by the 19 mm (3/4 in.) sieve. All the beams were cured in the same form as the corresponding section. For example, the curing compound was applied on the ICC beams at the same time it was applied on Section K where this mix was used. For two of the beams, the SRA spray was applied prior to the application of curing compound. Note that only one beam was prepared for each of the two 4-h OT mixes since no more channels were available in the static DAS to connect the VWSGs.

Figure 4.15 and Figure 4.16 present the timing for the different overlay construction operations for Lanes 1 and 2, respectively. Figure 4.17 shows the test track after the completion of overlay construction.

VWSG inside the mold

- Beams 1 & 2: P2 (Truck 2)
- Beams 3 & 4: P2+SRA (Truck 2)
- Beams 5 & 6: P2-ICC (Truck 5)
- Beam 7: P3 (Truck 6)
- Beam 8: CSA (Truck 7)

Beams after demolding

Note: curing compound application was applied on the beams, as in the sections. SRA was also applied on top of two beams before curing compound spay.

Figure 4.14: Unrestrained shrinkage beams cast on February 25, 2016.
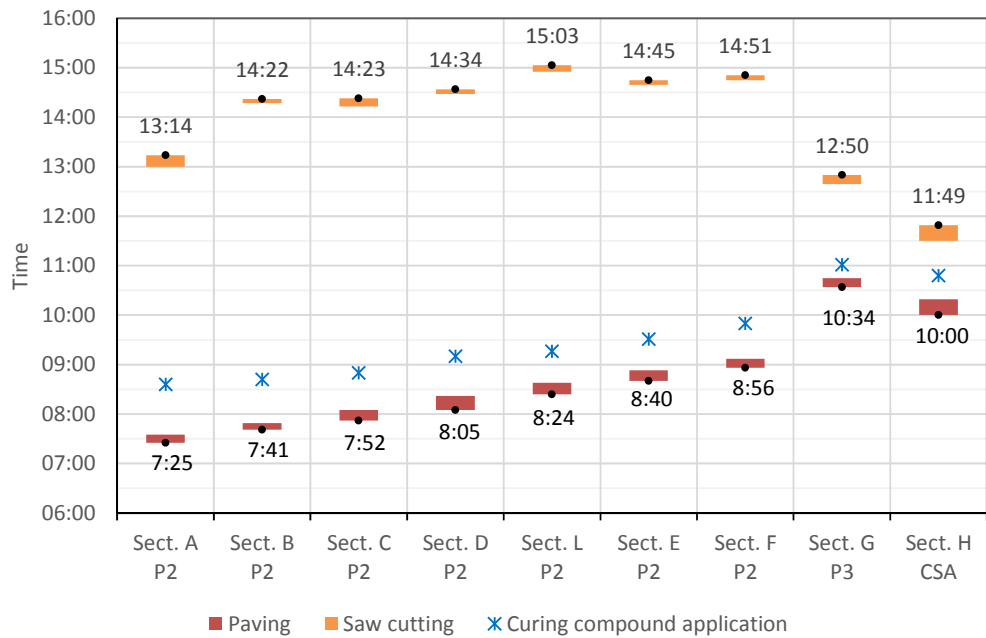
Figure 4.15: Timing of overlay construction operations, Lane 1, Feb. 23, 2016.
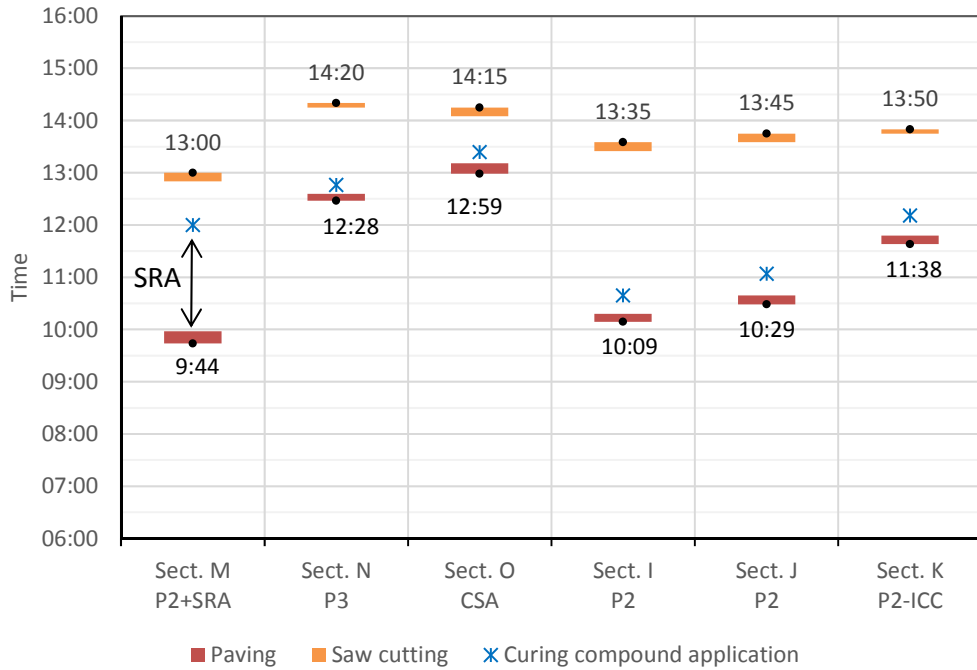
Figure 4.16: Timing of overlay construction operations, Lane 2, February 25, 2016.

Figure 4.17: Full-scale test-track after overlay construction.

4.3   Construction Weather Conditions

Weather conditions during BCOA construction are presented in Figure 4.18 and in Figure 4.19 for air temperature and relative humidity (RH), and for wind speed and solar radiation, respectively. Air temperature ranged from 5 to 15°C (40 to 60°F) during the first construction day (Lane 1), and between 15 and 20°C (60 to 70°F) during the second day (Lane 2). Weather conditions on the two days were similar but on the first day paving was conducted between 7:25 AM and 10:45 AM and between 9:45 AM and 1:10 PM on the second day, which is the reason why the air temperatures were higher during construction of Lane 2 than of Lane 1. Wind speed was relatively low during construction, with maximum values below 10 km/h (6.2 mph). The sky was mostly clear during Lane 1 paving, with some scattered or passing clouds, and it was partly cloudy during construction of Lane 2, as indicated by the solar radiation values in Figure 4.19.

Asphalt temperature was also monitored during overlay construction. This monitoring was conducted by two different means: using a temperature gun and thermocouples in the asphalt. The temperature gun was used to measure the asphalt surface temperature of each section right before concrete placement and unfortunately, it yielded values that were unrealistically low. However, a check of the temperature gun and a review of the operator measuring procedure did not reveal any measuring error. Thermocouples were available in the environmental (ENV) sections, as shown in Figure 3.5, and included asphalt thermocouples installed on the asphalt surface and at 30 mm (1.2 in.) depth at three different locations in each section. These environmental sensors began collecting data the day before construction of the overlay. Measured asphalt temperatures are presented in Figure 4.20 through Figure 4.22. The timeframe when each section was paved is also reflected in these figures.

Section L of Lane 1 is an environmental section. Its asphalt temperature, which is shown in Figure 4.20, can be considered representative of the asphalt temperature of Sections A to D when concrete placement took place because these sections were paved before Section L and they have the same asphalt type as Section L. After concrete is placed, the asphalt temperature is mainly determined by concrete temperature which, at the same time, is mainly determined by weather conditions and heat released due to cement hydration. The asphalt surface temperature significantly increased during Section L concrete placement, as shown in Figure 4.20 because the temperature of the poured concrete, which was roughly 20°C (68°F), was higher than the temperature of the asphalt surface. The minimum asphalt surface temperature when the concrete was placed in Lane 1 was 8°C (46°F) (this occurred in Section A). Low asphalt temperatures negatively impact concrete temperature and, consequently, concrete strength gain. However, this will not make a difference to the HVS evaluation since accelerated loading tests take place months after construction.
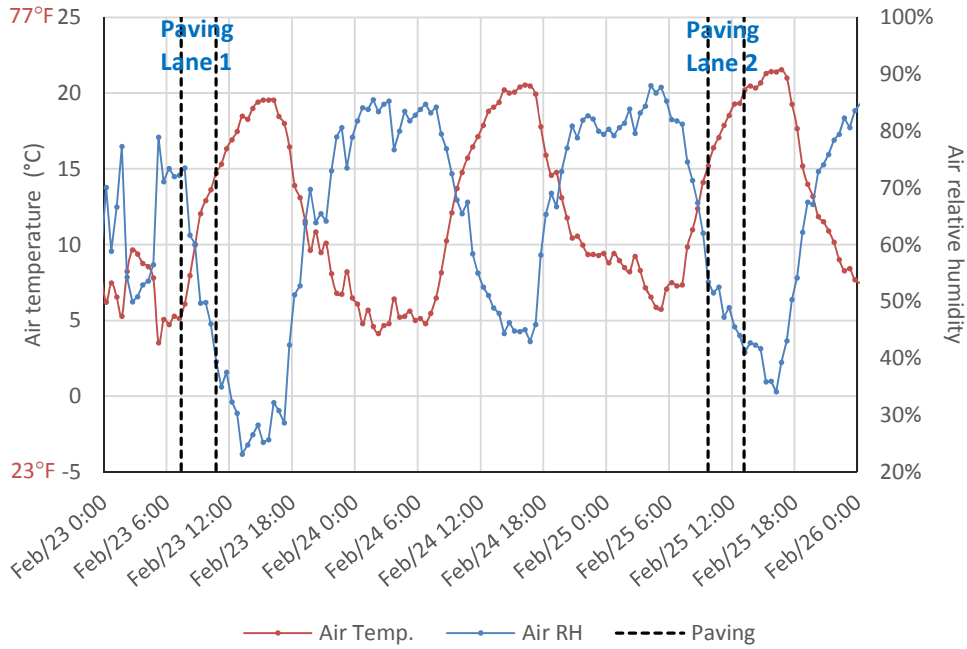
Note: the dashed vertical lines delimit, for each lane, the beginning and end of the paving operation.

Figure 4.18: Air temperature and relative humidity during BCOA construction.
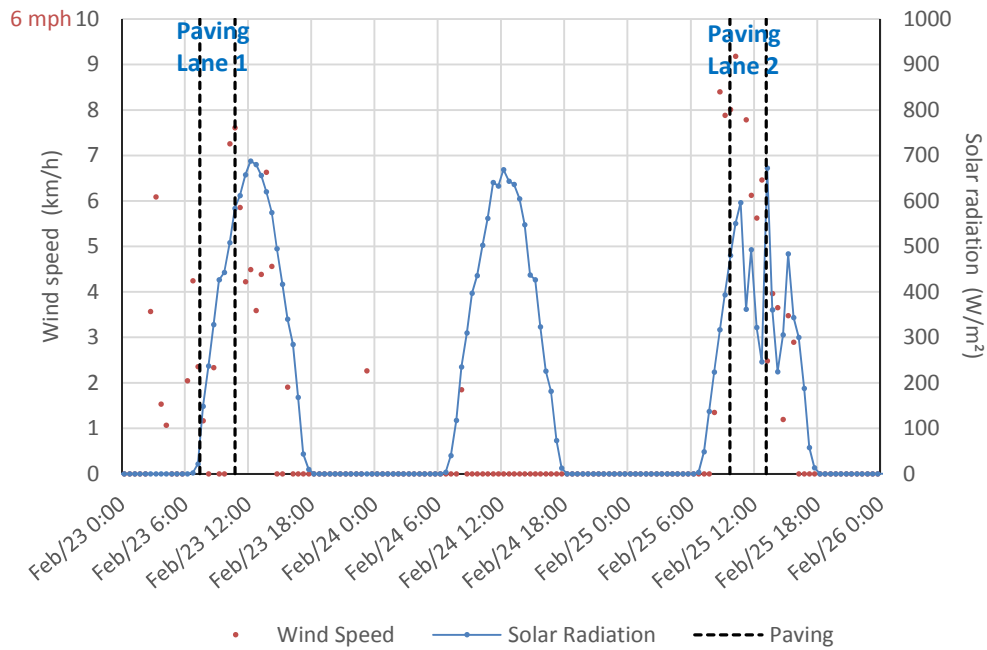
Note: the dashed vertical lines delimit, for each lane, the beginning and end of the paving operation.

Figure 4.19: Wind speed and solar radiation during BCOA construction.

There are five environmental sections in Lane 2, which allowed detailed monitoring of asphalt temperature evolution during overlay construction (Figure 4.21 and Figure 4.22). Again, the asphalt temperature measured on each section could be considered representative of an open-air asphalt surface until the concrete was placed on the section. The asphalt surface temperature right before concrete placement ranged from 19°C (66°F) in Section M to 30°C (86°F) in Sections K and N. Asphalt temperatures at 30 mm (1.2 in.) depth were slightly lower. The Section O temperature decreased before concrete was placed because the section was watered to provide the saturated surface-dry conditions that would improve concrete-asphalt bonding. The rapid increase of the asphalt temperature in this section after concrete was placed was due to the heat released by CSA cement hydration.
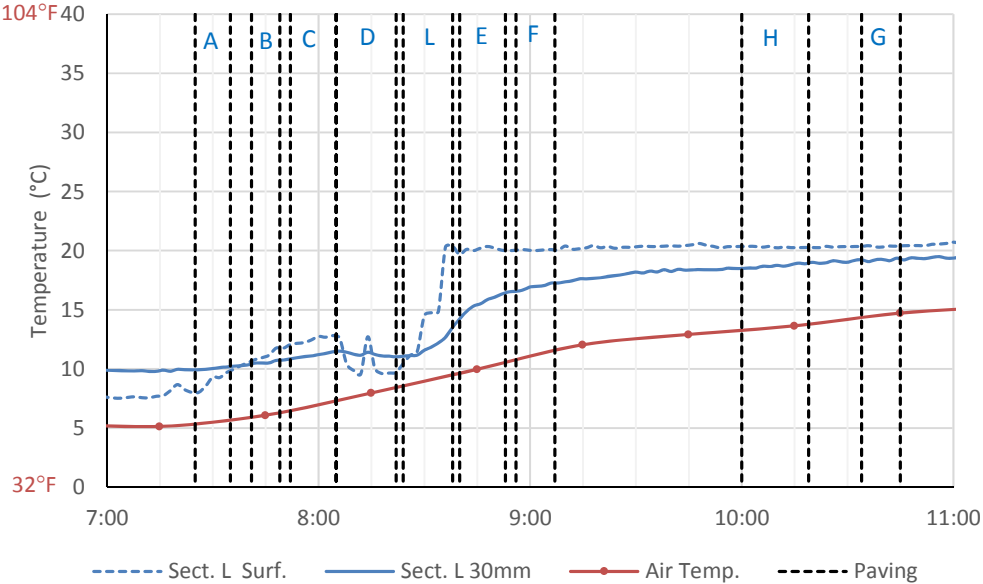
Notes: -The dashed vertical lines delimit, for each section, the beginning and end of the paving operation.
-Temperature was measured on the asphalt surface and at 30 mm below the asphalt surface, at three locations. The average of the three locations is presented for each depth.

Figure 4.20: Asphalt and air temperatures during BCOA construction, Lane 1.
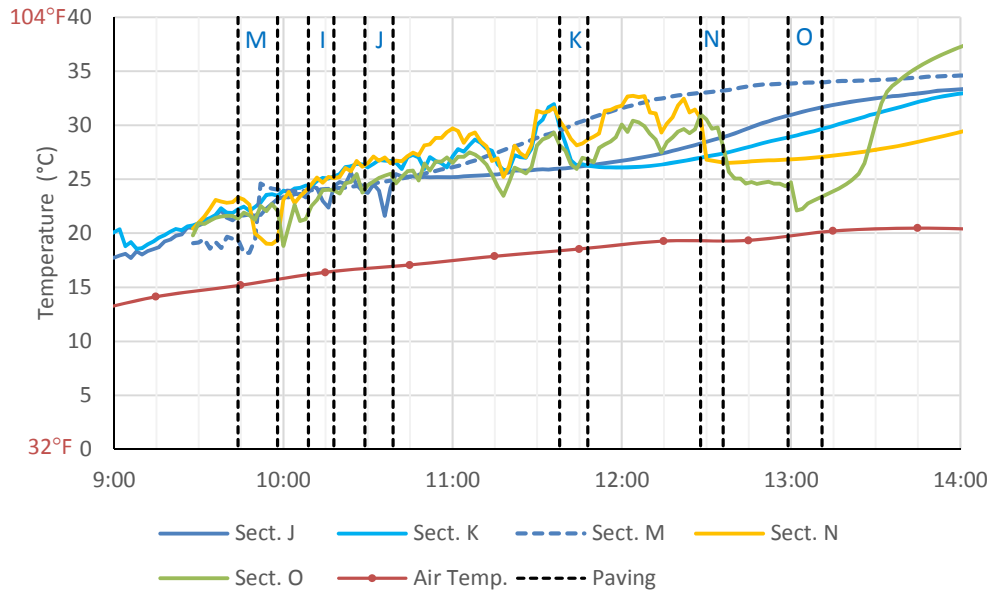
Notes: -The dashed vertical lines delimit, for each section, the beginning and end of the paving operation.
-Asphalt surface temperature was measured at three locations per section. The average of the three
locations is presented for each section.

Figure 4.21: Asphalt surface and air temperatures during BCOA construction, Lane 2.
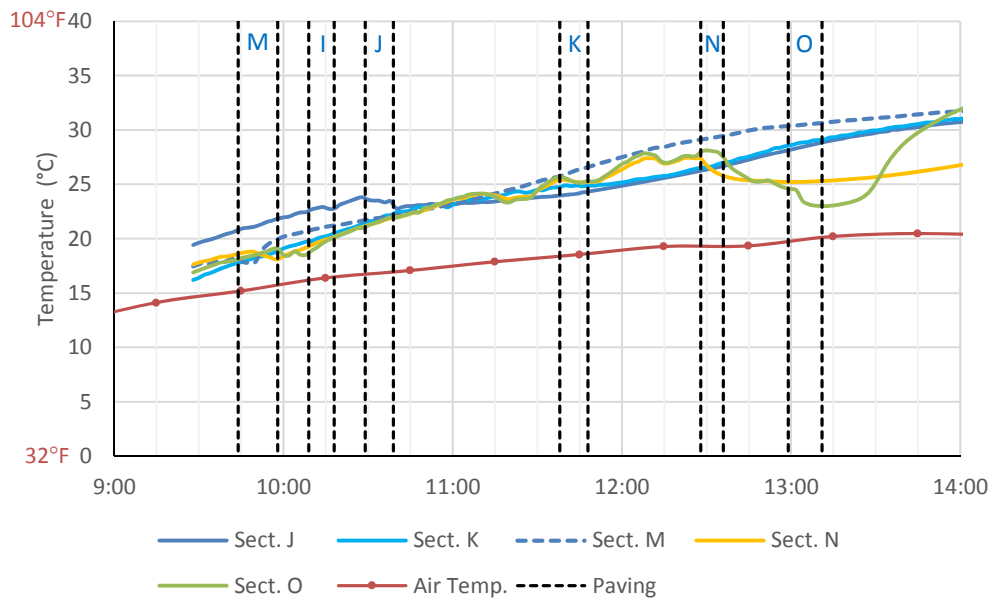
Notes: -The dashed vertical lines delimit, for each section, the beginning and end of the paving operation. Paving
series vertical bars delimit timeframe when each section was paved.
- Asphalt temperature is measured 30 mm below asphalt surface, at three locations per section. The average
of the three locations is presented for each section.

Figure 4.22: Asphalt temperatures at 30 mm (1.2 in.) depth and air temperature during BCOA construction, Lane 2.

4.4   Construction of the Shoulders

No shoulder was built during the overlay construction, as can be seen in Figure 4.17. This would have created practical problems since HVS feet need to rest partially on the shoulder during the accelerated loading, and this requires that the shoulder and slabs surfaces be at approximately the same level. A situation similar occurs with FWD testing. The width of the FWD cart is around two meters (6.6 ft), so it requires a one-meter shoulder (at the same level of slabs surface) in order to test the exterior edges of the slabs. A third reason for building the shoulder was to protect the south edge of the Lane 2 slabs from the direct impact of solar radiation. Since this edge is exposed to the sun, its temperature and rate of drying are higher than that of the north edge. The differential drying (higher on the south edge than on the north edge) was clearly reflected by the joints first deploying on the south edge then on the north edge.

Caltrans Class 2 aggregate base material was used for construction of the shoulders since a minimal amount of traffic is expected on them. Construction took place in late April to early May of 2016. The finished shoulders are shown in Figure 4.23. The feet of the HVS resting partly on the shoulder are shown in Figure 4.24. It should be noted that a metal plate had to be placed under the feet of the HVS because the granular shoulder had insufficient bearing capacity to support weight of the HVS.

Figure 4.23: Granular shoulders of the test track.

Figure 4.24: HVS during loading test.

(This page intentionally blank)

5   QC/QA FOR CONCRETE OVERLAY CONSTRUCTION

Standard concrete quality control and assurance (QC/QA) procedures were followed according to Caltrans specifications for constructing jointed plain concrete pavements with rapid strength concrete. This was because the primary goal of the QC/QA process was to verify that the mixes complied with Caltrans specifications. In addition to this standard QC/QA, other tests, records, and verifications were conducted. The goals pursued with the QC/QA process are presented below.

1. Verify the mixes' compliance with Caltrans specifications for rapid strength concrete (RSC).

2. Compare the results obtained for laboratory mixes. A comprehensive mechanical characterization of the concrete was conducted based on mixes prepared in the laboratory. This characterization focused on the same four mixes used for the construction of the overlays, whose designs are presented in Table 2.2. Results of this characterization are not included in this report.

3. Evaluate the differences among the sections built with the same type of concrete. The experimental design presented in Figure 2.2 assumes that the overlay material is the same in all the sections built with the same type of concrete. The analysis of the results of the full-scale experiment, for both the HVS and environmental sections, needs to account for potential section-to-section differences for the same mix type.

4. Compare the different types of concrete to one another based on their short-term mechanical properties. All the mixes have been designed to provide 2.8 MPa (400 psi) after either 4 or 10 hours. The evolution of this strength after the opening time (OT) may significantly differ from mix to mix. Other mechanical properties are also relevant to concrete pavement performance. Therefore, compressive strength, modulus of elasticity, and coefficient of thermal expansion (CTE) were evaluated for the field (BCOA construction) mixes.

5. Evaluate QC/QA testing methodologies. Two tasks were included in this category. The first is a comparison of ASTM C78-10 and California Test (CT) 524 (2013) to determine the flexural strength of the concrete. The second seeks to relate concrete flexural to compressive strength. The outcomes of these tasks may have applications in QC/QA.

Twining, Inc., a commercial firm with experience in concrete quality control, conducted truck sampling, fresh concrete testing, and specimen preparation, which included curing during the first 24 hours. The firm's inspectors were certified by both the American Concrete Institute (ACI) and Caltrans to conduct the ASTM and CT tests, respectively. UCPRC personnel with the appropriate ACI certification demolded and tested the specimens. The following testing was conducted to achieve the five goals indicated above.

- Fresh concrete testing. Mix from all the trucks were sampled to measure slump. Additionally, each construction day concrete air content, temperature, and unit weight were measured for one truck with each mix type, as reflected in Table 5.1.

- The first construction day a truck with each mix type was sampled to prepare beams to be cured and tested according to ASTM C78-10. The second construction day, a truck with each mix type was sampled to prepare two sets beams to be cured and tested according to, respectively, ASTM C78-10 and CT 524.
- Determination of concrete compressive strength, modulus of elasticity, and coefficient of thermal expansion. Samples taken from one truck for each mix type were made into cylindrical specimens (Table 5.1). Except for the internally cured concrete, all cylinders were prepared the first construction day.

In addition to the specimens to be tested, a beam dedicated to tracking temperature was also cast for each mix. This beam had a thermocouple embedded in it. This approach was necessary because having a thermocouple inside a test specimen would invalidate the test results. The temperature-measuring beams were prepared and cured like the regular testing specimens, and they were also stored in the same location, either in a curing box (ASTM) or on top of the BCOA slabs (CT 524). Temperature tracking continued for the first 24 hours after specimen preparation. After that time, the specimens that had not been tested were stored at a constant temperature in a water bath so temperature tracking was unnecessary.

Table 5.1: Summary of Quality Control Tests

Truck	Mix Short Name: Mix Name	Slump (in.)	Air Content	Temp. °F / °C	Unit Weight pcf / T/m³	ASTM MR	fc	E	CTE	CT MR
1st Construction Day (Lane 1)										
1	**P2:** 10-h OT (Type II/V)	9.50								
2	**P2:** 10-h OT (Type II/V)	9.50								
3	**P2:** 10-h OT (Type II/V)	9.75								
4	**P2:** 10-h OT (Type II/V)	10.25	1.2%	71 / 21.7	153.5 / 2.46	X	X	X	X	
5	**P2:** 10-h OT (Type II/V)	10.00								
6	**P2:** 10-h OT (Type II/V)	7.50								
7	**P2:** 10-h OT (Type II/V)	8.25								
8	**CSA:** 4-h OT (CSA)	9.50	1.6%	67 / 19.4	151.7 / 2.43	X	X	X	X	
9	**P3:** 4-h OT (Type III)	3.50	2.4%	75 / 23.9	151.7 / 2.43	X	X	X	X	
2nd Construction Day (Lane 2)										
1	**P2:** 10-h OT (Type II/V)	9.25								
2	**P2:** 10-h OT (Type II/V)	2.50								
3	**P2:** 10-h OT (Type II/V)	11.50	0.4%	73 / 22.8	155.9 / 2.50	X				X
4	**P2:** 10-h OT (Type II/V)	9.25								
5	**P2-ICC:** 10⁺-h OT ICC (Type II/V)	8.25	1.4%	70 / 21.1	144.5 / 2.31	X	X	X	X	X
6	**P3:** 4-h OT (Type III)	6.75	1.7%	72 / 22.2	152.0 / 2.43	X				X
7	**CSA:** 4-h OT (CSA)	7.50	2.1%	76 / 24.4	150.8 / 2.42	X				X

Notes: MR is modulus of rupture (flexural strength).
fc is compressive strength.
E is modulus of elasticity.
CTE is coefficient of thermal expansion.
CT stands for Caltrans.

5.1 Compliance of the Mixes with Caltrans Specifications for Rapid Strength Concrete

When the opening age of the concrete is less than three days, Caltrans Standard Special Provisions 40-5 require the concrete to have a flexural strength—that is, modulus of rupture (MR)—of 2.8 MPa (400 psi[2]) at opening and 4.5 MPa (650 psi) after 10 days. In both cases, the strength must be determined as the average result acquired from testing three beams according to CT 524. The results of flexural strength testing conducted during BCOA construction are shown in Figure 5.1. ASTM C78-10 testing was conducted both construction days, while CT 524 was followed only on the second day.

P2 (10-h OT with Type II/V cement)

P3 (4-h OT with Type III cement)

CSA (4-h OT with CSA cement)

P2-ICC (ICC based on P2 mix)

Const. Day 1 (ASTM)　Const. Day 2 (ASTM)　Const. Day 2 (CT)　- -●- - CT Requirements
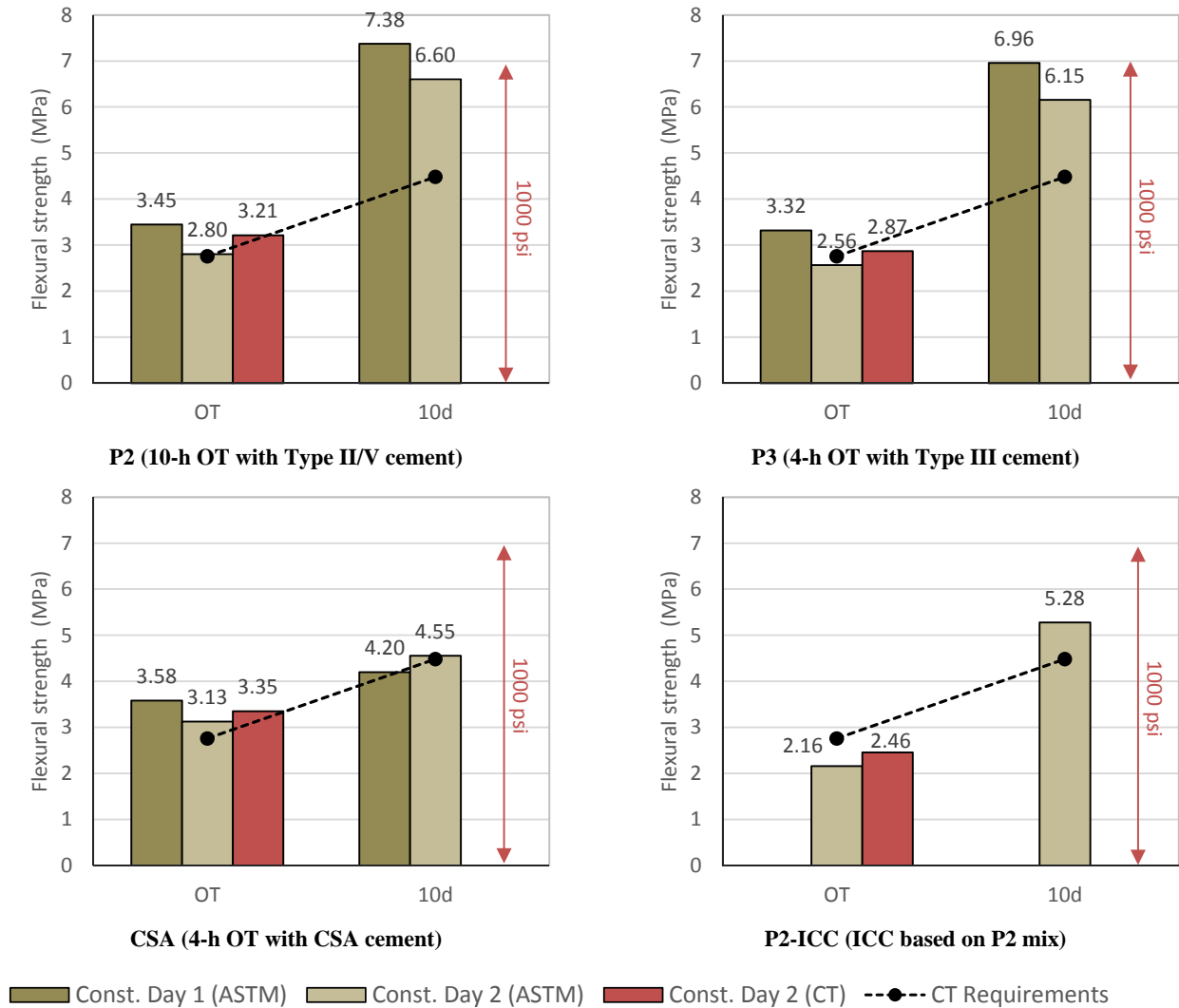
Figure 5.1: Flexural strength testing results.
(Note: each value in the graphs is the mean of three specimens.)

---

[2] Caltrans flexural strength requirements are given in psi units.

For two of the four mixes, P2 and CSA, the flexural strength at the design opening time was above 2.8 MPa (400 psi) both construction days (see Figure 5.1). The strength of the P3 mix was above the Caltrans specification the first construction day but that strength declined slightly below the Caltrans specification the second construction day. The flexural strength of the P2-ICC mix was clearly below 2.8 MPa (400 psi) after 10 hours, i.e., the opening time of this mix was clearly greater than 10 hours. All the portland cement mixes, including the internally cured concrete mix, clearly met the Caltrans strength requirement after 10 days, 4.5 MPa (650 psi). The flexural strength of these PCC mixes increased more than 100 percent between the opening age to 10 days. Depending on the mix, this increase was between 110 percent and 145 percent. The 10 day flexural strength of the CSA mix sampled the first construction day was 4.2 MPa, slightly below the 4.5 MPa (650 psi) Caltrans requirement. This result might have been related to the 9.5 in. slump measured for this mix the first day of construction (Table 5.1). The specified slump for this mix is 4 to 8 inches (Table 2.2). It should be noted that the slump of the P2 mix was over 9 inches (maximum specified value) for most trucks on both construction days, including the trucks that were sampled for the preparation of beams. Similarly, the slump of the P3 mix was below the 8 inch specified minimum slump on both construction days. The discrepancy was particularly high the first day of construction, when a slump of 3.5 inches slump was measured (Table 5.1).

As indicated above, the flexural strength of the P2-ICC mix was clearly below 2.8 MPa (400 psi) after 10 hours. Compared to the P2 mix, upon whose design it is based, the flexural strength of the ICC after 10 hours decreased in 31 percent, based on ASTM C78-10 (2.16 MPa versus 3.13 MPa for P2, the mean of both construction days). This drop was larger than expected, since preliminary laboratory testing resulted in a 10 to 20 percent flexural strength reduction with the same materials and a similar sand volume replacement. The reduction also exceeded values up to 25 percent that were reported in similar cases (8). The QC/QA testing did not reveal a reason for this large decrease in strength. In particular, the 8.5 inch slump measured for the P2-ICC truck was within the specified range of 6 to 9 inches. The large flexural strength decrease seems to be unrelated to temperature. As Figure 5.2 shows, the temperature of the P2-ICC beams was higher than that of the P2 beams during the first 24 hours. The only difference between the P2 and P2-ICC mixes is that some of the sand in the P2 was replaced by LWA in the P2-ICC mix (50.7 percent on a volume basis, see Table 2.2). As explained above, it was expected that the replacement of part of the normal weight aggregates by LWA would result in a decrease in the short-term flexural strength of the concrete because of the lower strength of the LWA compared to standard aggregates. In the long term, some experimental studies have shown an increase in the flexural strength of the ICC compared to the standard concrete because of the higher degree of cement hydration (8). Still, the 10 day flexural strength of the P2-ICC was only 75 percent of the P2 strength.
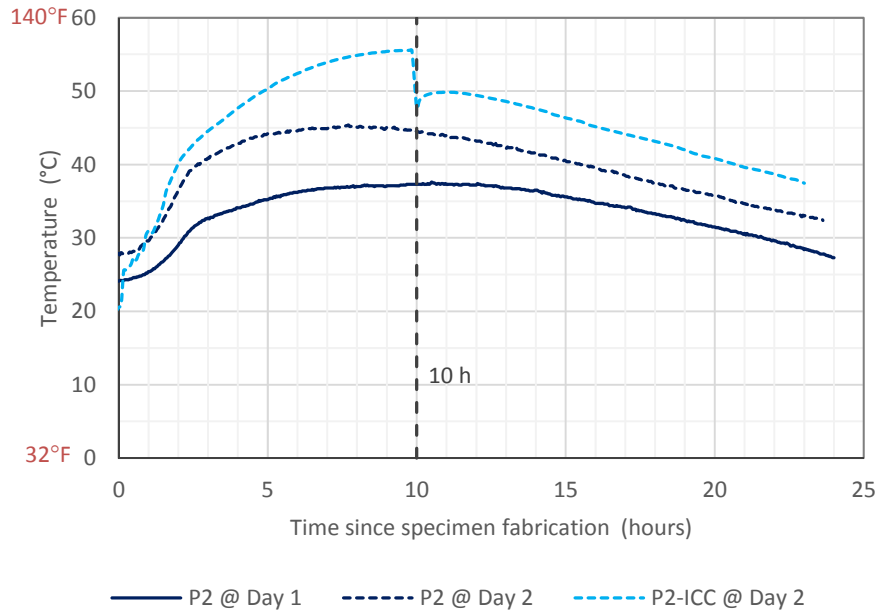
Figure 5.2: Comparison of P2 versus P2-ICC mixes—Internal temperature of beams in the curing boxes (ASTM C31).

The air content of the concrete was, in all cases, within specifications. According to Caltrans Standard Specifications, the tolerance interval is ±1.5 percent of the specified value. The specified air content was 1.5 percent for the portland cement mixes and 2 percent for the CSA mix (Table 2.2). These values are relatively low because the mixes were not designed to be air-entrained. A relatively low air content, but still within specifications, was measured for Truck 3 on the second construction day. This low value was likely due to the higher water content of the mix in this truck, which also resulted in an 11.5 inch slump.

Finally, the curing compound application rate was measured for every section. According to Caltrans Sec. 90, the curing compound dosage should be 150±50 ft²/gal, which is 200 to 400 ml/m². Actual dosage was measured according to California Test 535 (CT 535), using a different number of pads of a different pad size than is in the specification; this exception was made because the specifications, which were conceived for automatic spraying of curing compound on real pavements, were incompatible with the shorter length of the BCOA sections. Instead, three pads measuring 200×225 mm² (8×9 sq. in.) each were used to receive the applied curing compound. The application rate was determined by comparing the weights of the pads before and after curing application. The resulting rates, presented as an average for the three pads of each section, are listed in Table 5.2. As the table shows, Sections K and O did not receive the minimum amount of curing compound.

Table 5.2: Curing Compound Application Rates

Sections Lane 1	Rate ml/m²	Rate ft²/gal		Sections Lane 2	Rate ml/m²	Rate ft²/gal
A	622.9	65.4				
B	360.7	113.0				
C	336.9	120.9				
D	334.9	121.7		M	338.1	120.5
L	417.0	97.7		N	229.5	177.5
E	479.5	85.0		O	**157.0**	**259.6**
F	475.3	85.7		I	426.3	95.6
G	234.3	173.9		J	234.7	173.6
H	409.0	99.6		K	**189.5**	**215.0**

Notes:
The Caltrans specification is 150±50 ft²/gal (200 to 400 ml/m²).

Numbers in bold indicate sections that did not receive the minimum amount of curing compound.

5.2 Differences among Sections Built with the Same Type of Concrete

Flexural strength differences for the same mix between construction days one and two can be seen in Figure 5.1. As shown, the flexural strengths of both portland cement–based mixes, P2 (10-h OT with Type II/V cement) and P3 (4-h OT with Type III cement), were higher on the first construction day than the second day. This was the case for both testing ages, opening time and 10 days. For the CSA mix (4-h OT), the difference between first and second days was smaller than for the mixes mentioned above. An analysis of variance (ANOVA) indicated that the differences between Days 1 and 2 for the CSA mix are not statistically significant at 5% level (p-value=0.069 at OT and p-value=0.091 at 10-d). On the other hand, the difference between Days 1 and 2 for the P2 and P3 mixes are statistically significant (p-value=0.01 for both mixes). Further, the interaction between construction day and testing age was not statistically significant for P2 or for P3. This means, in practice, that the differences between Day 1 and Day 2 are the same at the opening time and after 10 days, which seems to indicate that the reason behind the differences in flexural strength between Days 1 and 2 were not related to the maturity of the concrete.

As noted, a beam was prepared for each mix specifically to track concrete temperature. The temperatures recorded both construction days are shown in Figure 5.3 for the P2 and P3 mixes. The figure shows that the beam temperatures were higher the second construction day than the first day. This is the opposite of the measured flexural strengths for both mixes, which were higher the first day than the second day. This means that temperature was not the reason behind these differences, which agrees with previous ANOVA results. One of the reasons for the higher Day 2 than Day 1 temperatures of the beams is that paving on Day 2 took place later in the day than it did on Day 1 (Figure 4.15 and Figure 4.16). For the P2 mix, the differences (Day 1 versus Day 2 flexural strength)

may have been related to the water content. Truck 3 of the second construction day, from which the P2 mix was sampled to prepare the beams, presented an 11.5 inch slump, which is clearly above the maximum specified value of 9 inches. This would also explain why differences in flexural strength occurred at both testing times. It is still unclear though whether the differences for the P3 mix were related to water content. The slump of the P3 mix was 6.75 inches the second construction day, which is higher than the 3.5 inches measured the first day. This higher slump, whether it was due to higher water content or to the admixture dosage, is still below the minimum of 8 inches specified for this mix (Table 2.2).
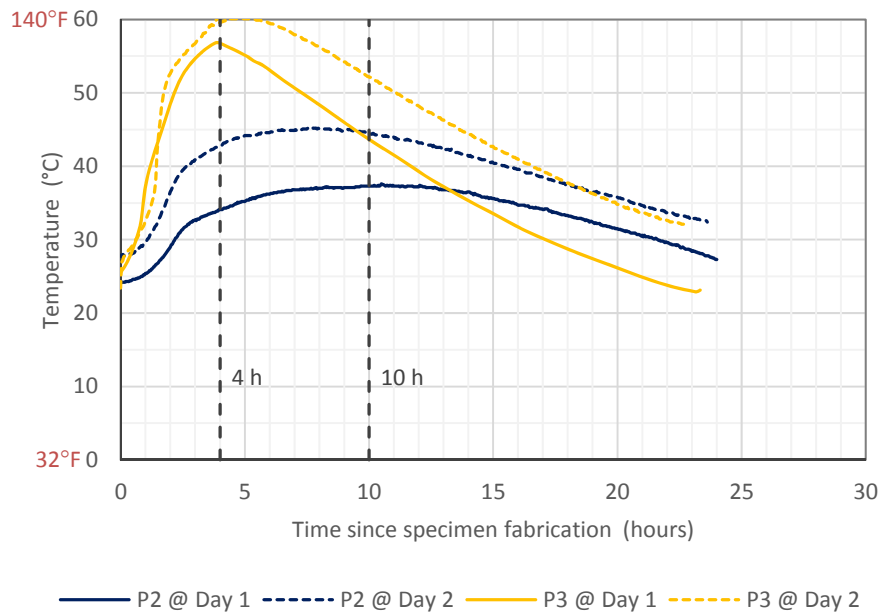
Figure 5.3: Comparison of P2 versus P3 mixes—Internal temperature of beams in the curing boxes (ASTM C31).

Slump was the only variable that was measured for all trucks. The results are presented in Figure 5.4 for Lane 1 and in Figure 5.5 for Lane 2. It must be noted that slump is not the best mix property upon which to assess these types of mixes since it is highly influenced by the use of high-range water reducers and hydration stabilizers. As reflected in these figures, the slump of the P2 mix tended to be above the specified maximum. The concrete of Truck 2 was particularly fluid on Day 1, and some indications of segregation were visible. This truck was used to build Section B. Slump measured for this truck was not higher than the values measured for other trucks, which indicates that, as expected, slump is not the best test to evaluate the consistency of these high-workability mixes. The concrete of Truck 3 on Day 2 that was used to build Section J was also very fluid. The two P3 trucks resulted in slump values below the specified minimum. For the CSA mix, the slump measured for Truck 9 of Day 1— which had concrete used to build Section H—was slightly over the specified maximum, while the slump measured for Truck 7 of Day 2—which had concrete used to build Section O—was within the specified range.

In summary:

- Some section-to-section differences can be expected for the P2 mix, and Sections B and J require particular attention. The concrete used for construction of Section B presented some visual indications of segregation. The mix sampled from the truck used for construction of Section J resulted in a very high slump, and flexural strength testing revealed that this material was weaker than the material sampled and tested the first construction day.
- The P3 mix used the first construction day to build Section G had a lower slump and a higher flexural strength than the material used the second construction day to build Section N.
- No significant differences are expected between the CSA mixes used for the construction of Sections H and O on Days 1 and 2.
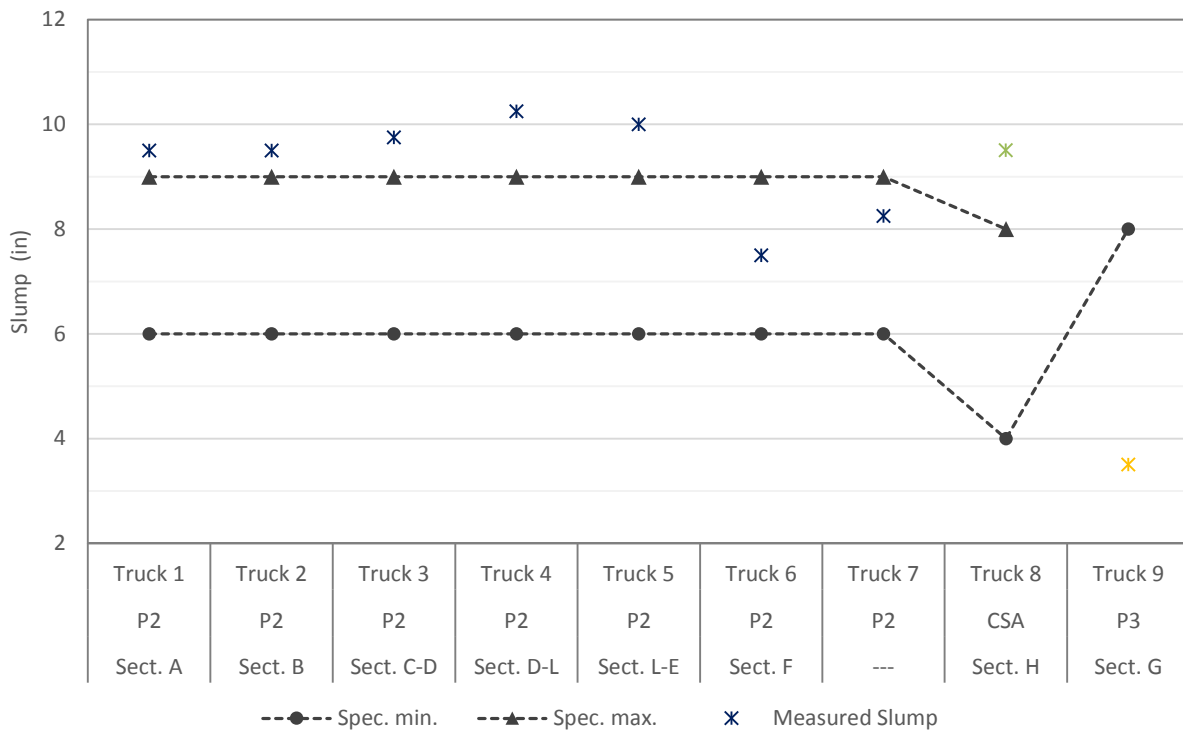
Figure 5.4: Slump test results, Day 1 (Lane 1).
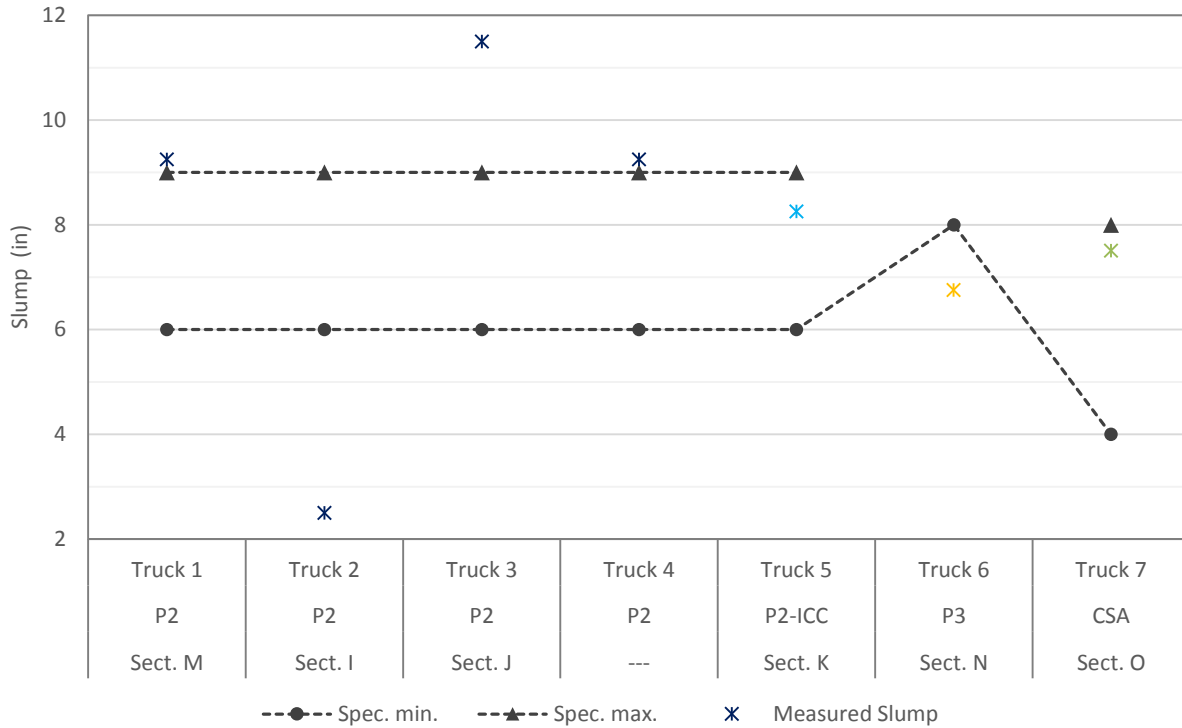
Figure 5.5: Slump tests results, Day 2 (Lane 2).

5.3 Short-Term Mechanical Properties of the Different Types of Concrete

The mechanical properties of the mixes are presented in Figure 5.6 to Figure 5.9, respectively, in terms of modulus of rupture (MR), compressive strength (fc), modulus of elasticity (E), and coefficient of thermal expansion (CTE). The results of the Duncan test, a post hoc test for comparing multiple groups, are also shown in the figures (Duncan test results are explained below). Both flexural and compressive strengths were measured at two ages, at the design opening time and at 10 days. The modulus of rupture was measured by following ASTM C78-10 on both construction days (Table 5.1), with the average value being presented in Figure 5.6. The compressive strength was measured for specimens prepared on just one of the two construction days: Day 1 for mixes P2, P3, and CSA, and Day 2 for the P2-ICC. Three specimens, 150 mm (6 in.) diameter, were tested according to ASTM C39-15 for each mix, with the average compressive strength being presented in Figure 5.7. Two cylinders per mix, 150 mm (6 in.) diameter, were tested according to ASTM C469-14 to determine the modulus of elasticity at the age of 10 days. The average value of E for each mix is shown in Figure 5.8. The coefficient of thermal expansion of each mix, averaged over three specimens, is shown in Figure 5.9. CTE tests were conducted on 100 mm (4 in.) diameter cylinders according to AASHTO T 336-11, for a concrete age of 21 days.
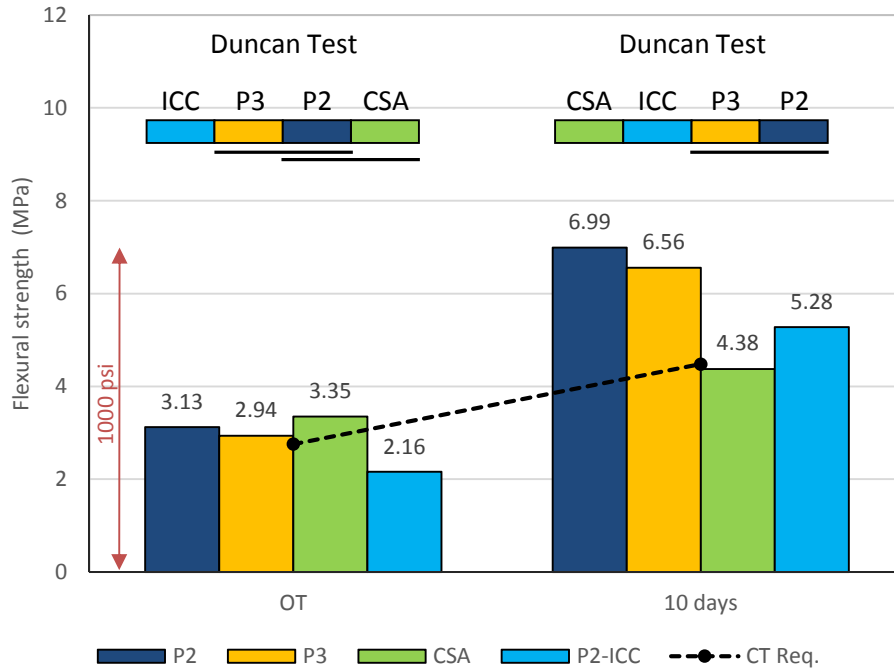
Note: each value in the graph is the mean of the two construction days, with three specimens per mix tested each day.

Figure 5.6: Flexural strengths of the four mixes (ASTM C78-10).
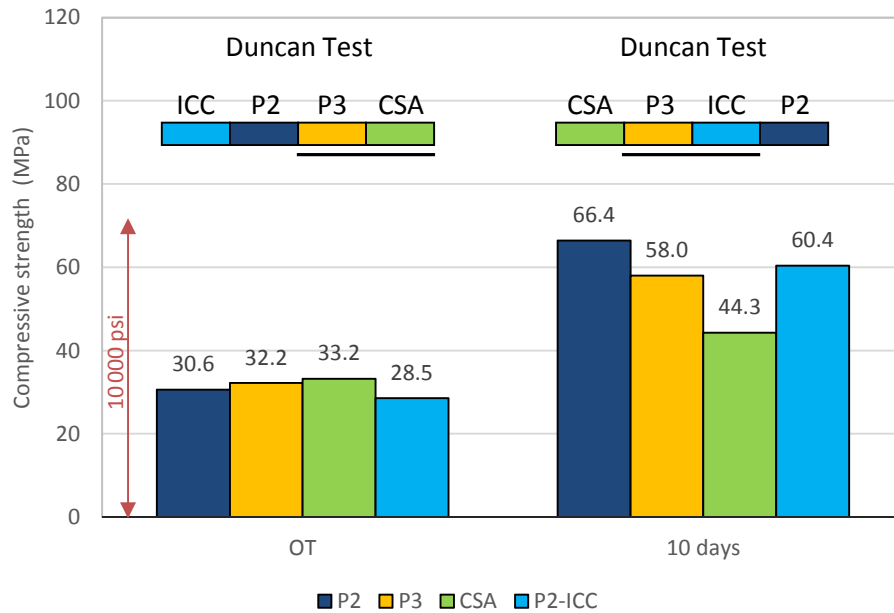
Note: each value in the graph is the mean of three specimens.

Figure 5.7: Compressive strengths of the four mixes (ASTM C39-15).
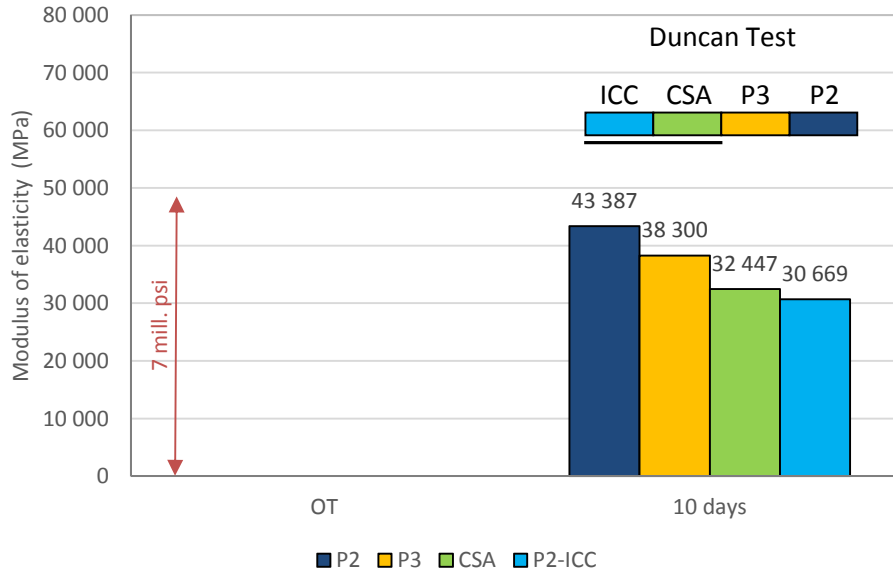
Note: each value in the graph is the mean of two specimens.

Figure 5.8: Modulus of elasticity of the four mixes (ASTM C469-14).
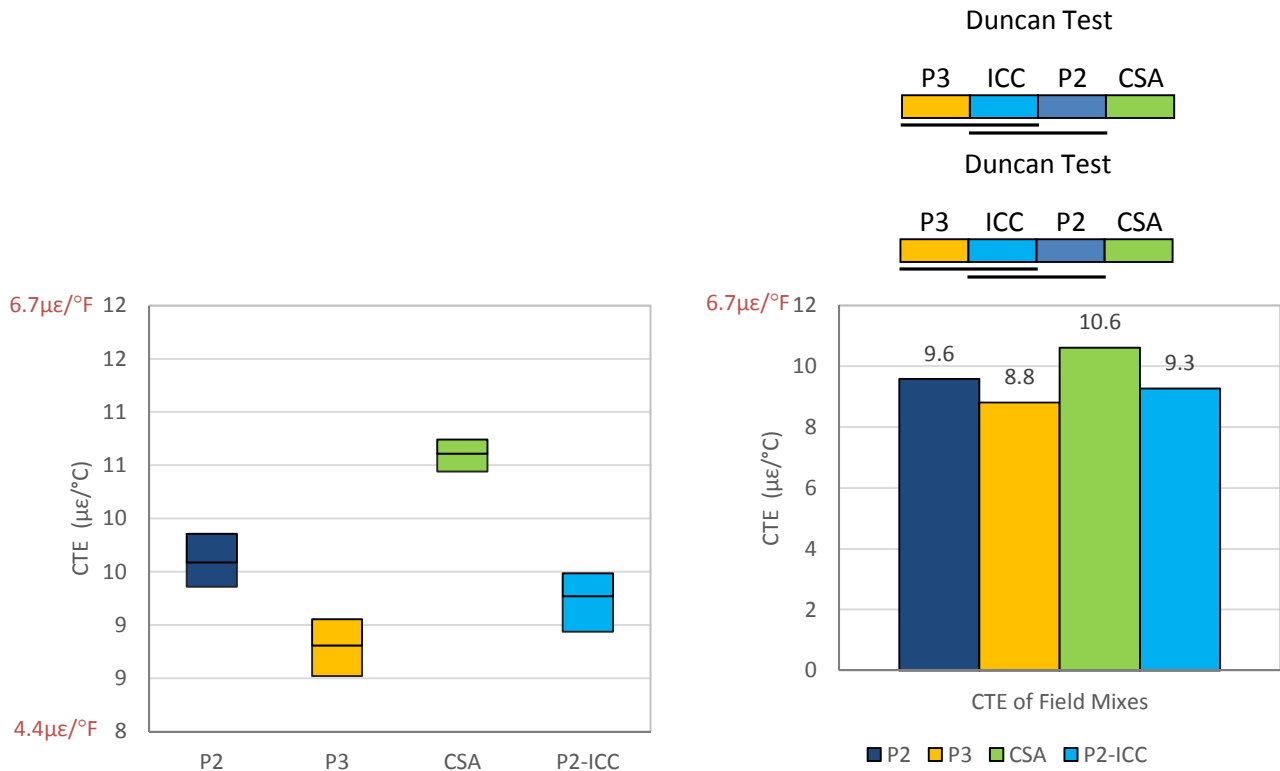
Boxes correspond to min., average, and max. of three specimens.

Each value in the graph is the mean of three specimens.

Figure 5.9: Coefficient of thermal expansion of the four mixes (AASHTO T 336-11).

A series of ANOVA analyses were conducted to determine if the concrete mechanical properties significantly differ from one mix to another. In all cases, the differences were statistically significant. The Duncan test, a post-hoc test for multiple groups comparison, was used to sort the mixes within groups with similar mechanical properties. The results of the Duncan tests are presented in Figure 5.6 to Figure 5.9, respectively, for MR, fc, E, and CTE. When interpreting Duncan test results, a black bar below two mixes means these two mixes do not significantly differ from each other for the corresponding mechanical property. For example, as can be seen in Figure 5.9, mixes P3 and P2-ICC do not significant differ in terms of CTE and the same applies to ICC and P2 mixes. On the contrary, P3 CTE is significantly lower (statistically) than P2 CTE. This difference is very likely caused by the cement type since the two mixes use the same aggregate type and almost identical gradations. The CTE of the CSA mix was higher than the CTE of the other three mixes, which is likely related to the CSA cement.

The ranking of the mixes after the Duncan test is almost identical for flexural and compressive strength, as expected. The relationship between these two variables is analyzed in Section 5.4.2 of this report. The strength rankings, according to Duncan test, changed between the two testing ages, since the CSA mix provided the highest strength at opening time but the lowest after 10 days.

The ranking of the mixes in terms of modulus of elasticity after 10 days is similar to the corresponding ranking in flexural strength. The main difference is with the internally cured concrete and the CSA mix sweep positions. It should be noted that lower stiffness results in lower stresses under traffic and environmental loads, especially under environmental loads. For this reason, the ratio of flexural strength to modulus of elasticity is as important as the flexural strength itself. In this sense, the three portland cement mixes resulted in MR/E ratios around 0.17 percent, while the CSA mix resulted in 0.13 percent.

5.4   Evaluation of Testing Methodologies

5.4.1   Comparison of ASTM and Caltrans Methods to Determine MR

This study compared ASTM C78-10 and CT 524 (2013) for determining the mixes' modulus of rupture (MR). This comparison is expected to help Caltrans decide if its current method should be replaced by ASTM C78-10. On the second construction day, two sets of three beams were therefore prepared for each mix type. One set was cured and tested according to ASTM C78-10 and the other set according to CT 524 (2013). These two standards mainly differ in their approaches to initial curing of the beams, which is important because curing temperature significantly impacts the early-age strength of the mixes. ASTM C78 requires that beams shall be prepared and cured according to ASTM C31, the standard practice for making and curing concrete test specimens in the field. ASTM C31 requires that immediately after molding and finishing, the specimens shall be stored for a period up

to 48 hours in a temperature range from 16 to 27°C (60 and 80°F), in an environment where moisture loss is prevented. In this study this was achieved by housing the specimens in insulated boxes placed near the BCOA sections. CT 524 states the beams shall be sprayed with the curing compound as it is applied on the pavement, and then placed on top of the slabs as soon as the concrete is set. This was accomplished by placing the beams on top of the intermediate slabs between the test sections to ensure that the beams' presence would not interfere with the curing of the concrete in the test sections. The beams were protected with an insulating blanket to hold the heat and moisture while curing, as stated in CT 524. In summary, the beams tested at opening time were cured either inside isolation boxes (ASTM), or on top of the BCOA slabs and protected with an insulating blanket (CT).

The differences between the approaches, in terms of internal temperature of the beams, can be seen in Figure 5.10 to Figure 5.13. For the P2 and P3 mixes, the CT beams reached higher temperatures than the ASTM beams, up until the opening time. For the internally cured concrete, the opposite happened. Unfortunately, a reliable temperature record could not be registered for the CSA ASTM beam. Based on these results, which were highly dependent on the specific weather conditions during Day 2 construction, no clear difference in terms of temperature between the curing methods can be seen. A greater difference between the two methods would be expected in more extreme weather conditions, with lower or high temperatures, because of the impact they have on the CT beams; that is weather conditions have a larger influence on the beams cured according to CT 524 than on the beams cured according to ASTM C31. Consequently, this weather-dependence will also introduce more variability into the CT 524 results. This dependence limits the use of CT 524 as a standard for evaluating the compliance of a concrete mixture to the mix design where specimens are cured under standard laboratory conditions, 23.0±2.0°C (73.5±3.5°F).
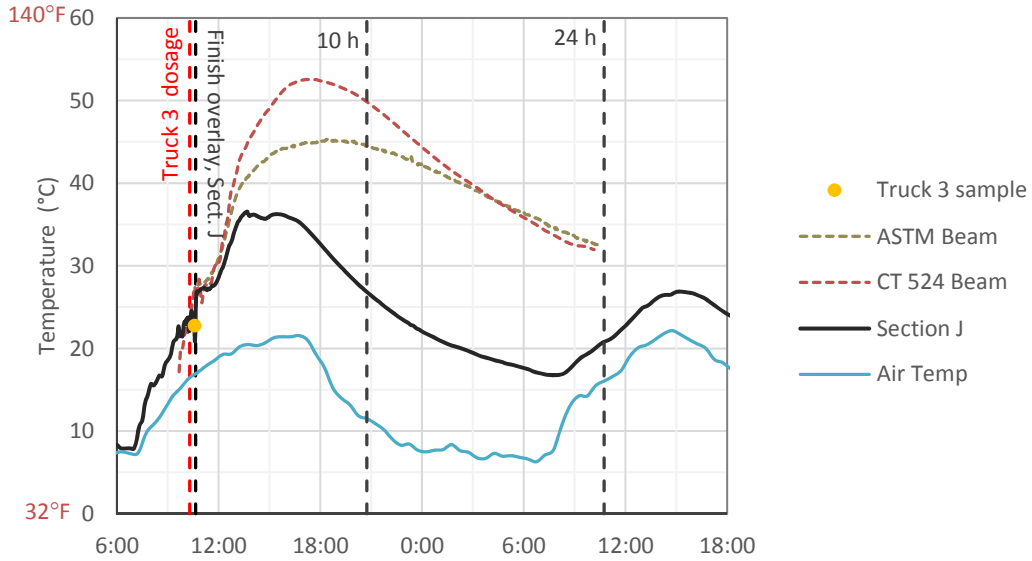
Note: Truck 3 was sampled to cast ASTM and CT P2 beams. It was also used to build Section J.

Figure 5.10: Temperature tracking of the P2 mix, Day 2.
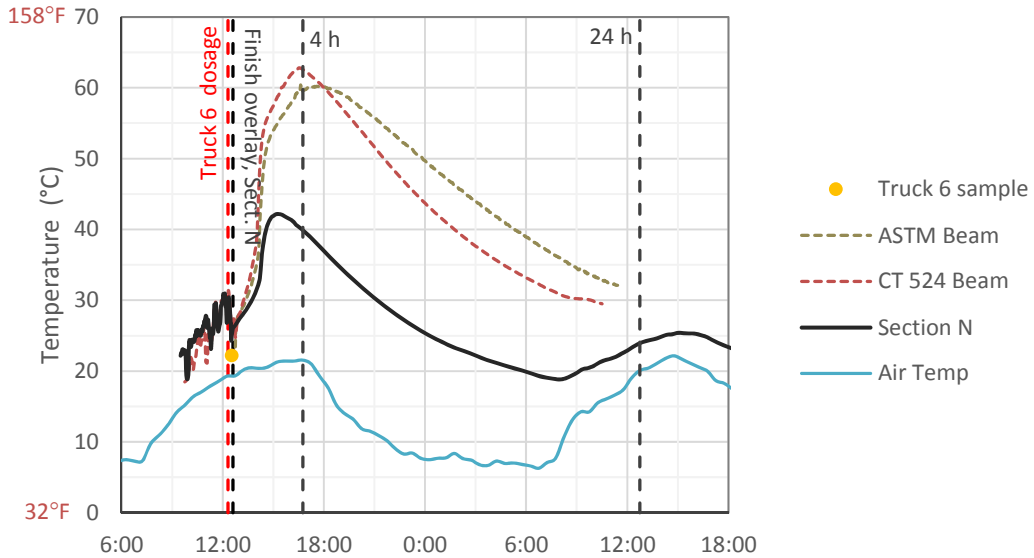
Note: Truck 6 was sampled to cast ASTM and CT P3 beams. It was also used to build Section N.

Figure 5.11: Temperature tracking of the P3 mix, Day 2.

Notes: Truck 7 (volumetric mixer) was sampled to cast ASTM and CT CSA beams. It was also used to build Section O. Unfortunately, the thermocouple measuring temperature inside one of the ASTM beams did not work properly, so the corresponding temperature data are not shown in this figure.

Figure 5.12: Temperature tracking of the CSA mix, Day 2.
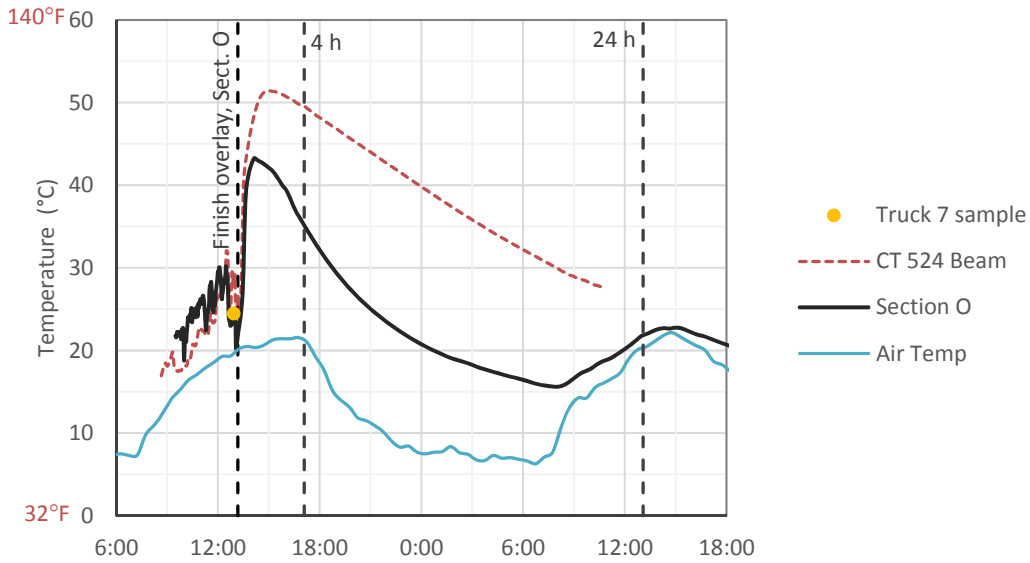

Note: Truck 5 was sampled to cast ASTM and CT ICC beams. It was also used to build Section K.

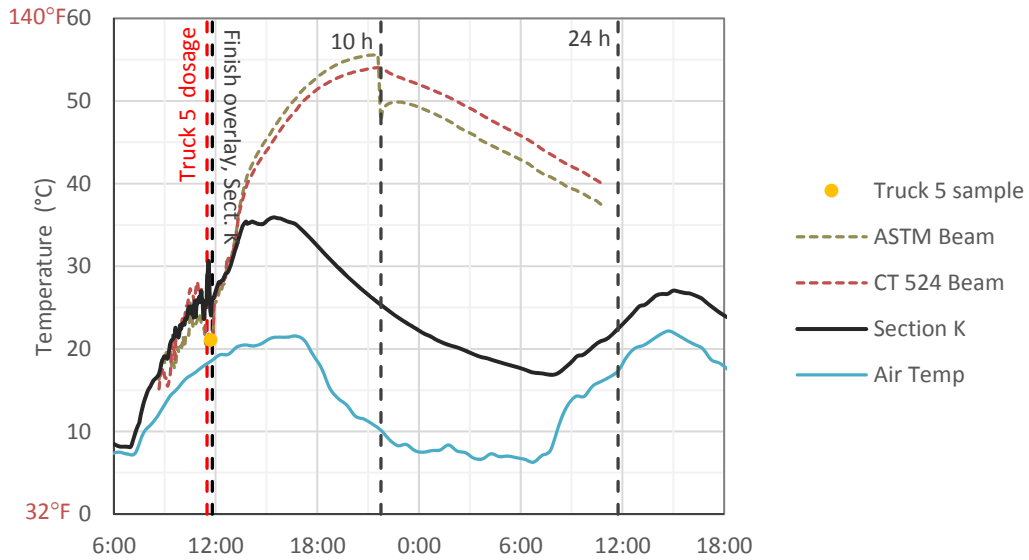**Figure 5.13: Temperature tracking of the P2-ICC mix, Day 2.**

Figure 5.14 shows the flexural strength (MR) results according to ASTM C78 and CT 524 for each mix. As can be seen, the resulting MR values for all the mixes were higher with the CT standard than with the ASTM standard. On average, the CT MR results were 12 percent higher than ASTM results. An ANOVA indicated that the differences were statistically significant, with p-value=0.01. One reason for the observed difference is that CT 524 and ASTM C78 use slightly different formulas to calculate flexural strength. Specifically, CT 524 applies a factor of 1.05 to the formulas that result from classical beam theory, which are used in ASTM C78. This factor was introduced into the CT 524 standard, which is based on third-point loading, to make the results comparable to center-point loading tests. When the same formula was used for the two sets of beams, the resulting CT 524 strength values were on average 6 percent higher than the ASTM results and the differences were not statistically significant (p-value=0.13). This indicates that the differences between the CT and ASTM results were not related to the curing process of the beams, but to the formula used for the calculations.

An attempt was made to connect the differences between both methods to the maturity of the specimens. *Maturity* is the term used in ASTM C1074-11 for "the extent of the development of a property of a cementitious mixture." Maturity can be quantified by using a *maturity index* that takes into account the temperature history of the mix during the curing period. The basic hypothesis of the maturity approach is that there is a unique relationship between the maturity index and the development of strength, or any other mechanical property under consideration. The maturity was computed for ASTM and CT beams at an age of opening time. In this particular case, the maturity indexes were determined using the temperature-time factor, as specified in ASTM C1074-11, assuming a datum temperature of 0°C. Next, the ratios of the maturity of the CT and ASTM beams (maturity of CT beams divided by maturity of ASTM beams) were plotted versus their flexural strength ratios (CT MR divided by ASTM MR), as shown in Figure 5.15. (Note: to prepare this figure, the ASTM formulas were used to calculate the flexural strengths of both ASTM and CT beams.) As the figure shows, there is a very low correlation between the two ratios. This seems to indicate that the temperature differences did not have a significant effect on the flexural strength differences between the two methods. However, this outcome cannot be extrapolated to other mixes, testing times, or environmental conditions.

It should be noted that evaluating the flexural strength of the field mix contributes to accomplishing two different goals. One of these goals is to verify the compliance of the concrete mixture to the mix design, which requires beam-curing that does not significantly differ from standard laboratory conditions, upon which the mix design is based. The second supported goal is the determination of the opening time. The compliance of CT 524 and ASTM C78 with this second goal is evaluated below.
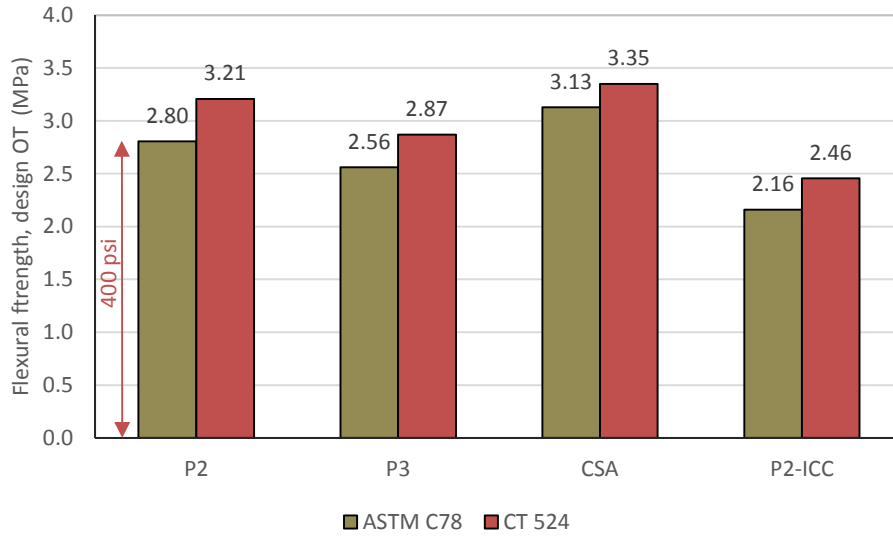
Note: each value in the figure is the average of three tests.

Figure 5.14: Comparison of ASTM and CT methods for flexural strength (MR) after opening time.
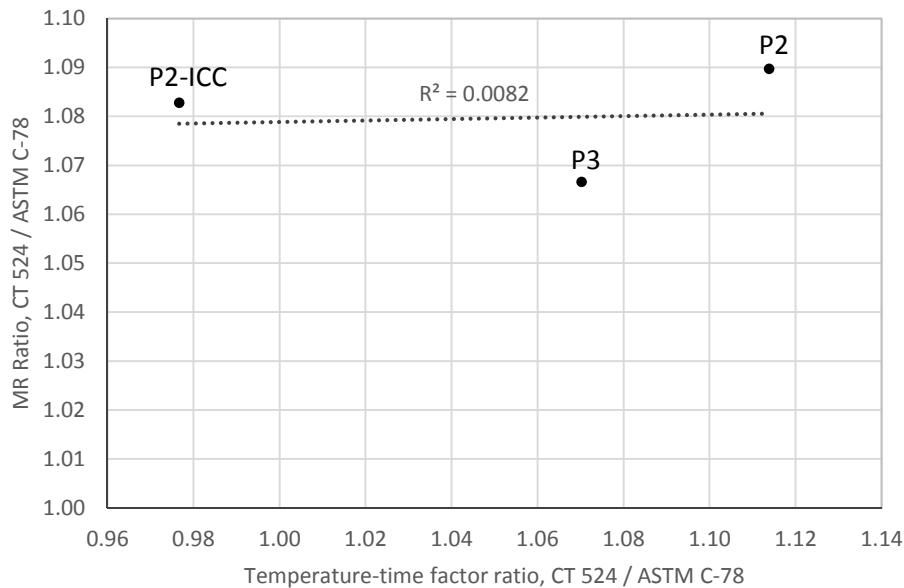
Notes: The same formula was used for the CT and ASTM beams to calculate flexural strengths used for this graph.

The CSA mix is not included in this plot since the temperature record inside the corresponding ASTM beam was unavailable.

Figure 5.15: Effects of maturity on flexural strength (MR).

The preceding figures include the temperature recorded in the concrete overlays during and after concrete placement. For each specific mix, the beam and section mix came from the same truck, and that is the reason why both temperature records are very similar to each other during the first minutes. However, after this initial period, the temperature of the concrete in the overlays was clearly lower than the temperature in the beams, regardless of whether they were cured according to the CT or ASTM method. This result was expected because of the overlays' high surface to volume ratio, which facilitates heat dissipation. This result was also related to the air temperature, wind speed, and radiation from the sun on the second construction day. Based on these temperature records, the temperature-time factors computed for the CT beams at the design opening times were between 25 percent and 45 percent higher than the indexes computed for the corresponding slabs. For P2 and P2-ICC, the concrete in the overlay would have required roughly 16 hours to reach the level of maturity that the CT beams achieved in 10 hours. For P3 and CSA, the overlay concrete would have required approximately 5 hours to reach the maturity indexes that the CT beams reached after 4 hours. Similar results were obtained for ASTM-cured beams. As expected, the maturity differences between beams and overlays were smaller for the four hour OT mixes than for the ten-hour OT mixes. This is because temperature of the concrete after placement is strongly influenced by cement hydration, which means the initial temperature evolution is very similar in slabs and beams. This fact is apparent in Figure 5.10 to Figure 5.13.

As noted above, the maturity levels of the concrete in the CT and ASTM beams were much higher than in the overlay. This outcome has important implications for closure times because the flexural strength results for these beams would have led to overestimates of the actual strength of concrete in the overlay. It should be noted that Caltrans Standard Special Provisions for constructing jointed plain concrete pavements with rapid strength concrete specifies that the beams fabricated for early-age testing should be cured "such that the monitored temperatures in the beams and the slab are always within 5 degrees F" (2.8°C). This specification refers to the trial slabs that must be produced before the mix is approved for construction. This temperature requirement might be very difficult to achieve for rapid strength mixes like those used in this BCOA construction. An alternative approach would be to link the strength of the beams and slabs on the basis of concrete maturity. In most overnight closures, the pavement must be opened to traffic at the start of the commute, regardless of its strength. However, when working with longer closures and 10-hour opening time mixes, the weather forecast for temperatures and a mix-specific calibrated maturity relationship can be used to estimate the appropriate number of hours before opening time to stop paving to have the correct opening time strength in the last slab placed.

5.4.2   *Comparison of Concrete Flexural Strength to Compressive Strength*

Figure 5.16 is a plot of flexural strength (MR) versus compressive strength (fc), and it shows relatively high variability in the resulting data, which makes sense given the large number of variables that influence both types of strength. Nonetheless, the P2-ICC mix had the lowest MR/fc ratios of all the mixes.
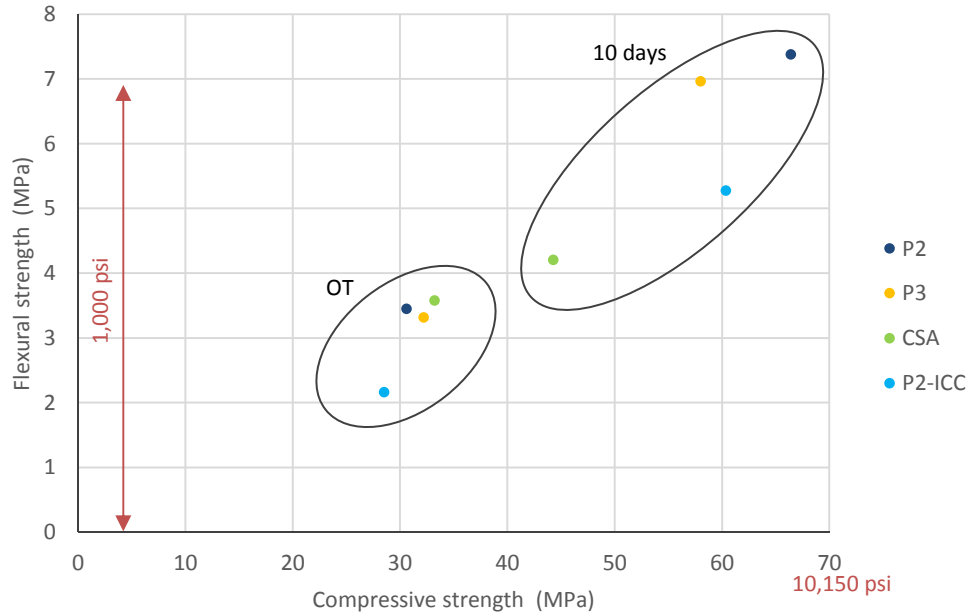
Note: Each point in the figure corresponds to the average of three cylinders (compressive strength) and three beams (flexural strength).

Figure 5.16: Relationship between average flexural and average compressive strength for the field mixes.

It is widely known that the MR-fc relationship is unique to each mix. That is why a QC/QA approach for estimating flexural strength consists of calibrating the MR-fc equation for a specific mix. This equation can then be used to predict the flexural strength of that specific mix, with the compressive strength results as the basis. This approach is expected to improve the accuracy of MR predictions versus using generic relationships like the ACI or CEB-FIB (Comité Euro-International du Béton-Fédération Internationale de la Précontrainte). The soundness of the approach was evaluated by conducting the following steps:

1. For each of the four mixes, an equation MR-fc was calibrated using the results of MR and fc testing conducted on the mixes prepared in the laboratory. Testing ages were OT, 4×OT, and 45 days. These tests were part of the laboratory testing conducted for this research project. The calibrated functions (one for each of the four mixes) are shown in Figure 5.17. In that figure, the flexural strength of each tested beam is plotted versus the average compressive strength of the mix at the same age.
2. The compressive strength and the flexural strength of the field mixes were measured after OT and 10 days. For each of the mixes, three cylinders were tested in compressive strength at each testing age and, similarly, three beams were tested in flexural strength at each testing age. In Figure 5.17, the

flexural strength of each of the beams is plotted versus the average compressive strength of the mix the corresponding age. As shown in that figure, the agreement between field-mix data and the laboratory-calibrated equation varied from mix to mix.

3. For each field-mix and age, the flexural strength was estimated using the laboratory-calibrated equation with the average compressive strength measured for the field-mix at the corresponding age.

4. The prediction error (e) was determined for each tested beam as the difference between the flexural strength measured in the beam and the predicted flexural strength. The root mean square (RMS) of the prediction error ranged from 0.25 MPa (37 psi) in mix CSA to 1.33 MPa (193 psi) in mix P3. RMS is defined as the square root of the mean square: $RMS = \sum(e_i)^2/N$

It should be noted that lab-mix and field-mix data were very similar to each other for the CSA and P2-ICC mixes. For these two mixes, the laboratory-calibrated MR-fc equation accurately predicted the flexural strength of the field mix, with the compressive strength results as the basis. For the P2 and P3 mixes, the lab-mix and field-mix data were relatively close to each other for the design OT but disagreed considerably at an age of 10 days. No definitive explanation was found for this disagreement. The pooled (four mixes) RMS of the prediction error was 0.97 MPa (140 psi), which seems relatively high for an approach to be used for QC/QA. Nonetheless, the pooled error was reduced to 0.55 MPa (80 psi) when the 10-day data for the P2 and P3 mixes were discarded.
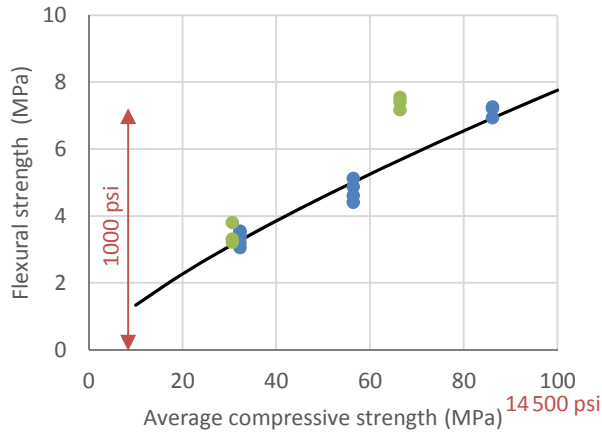
P2 (10-h OT with Type II/V cement)
MSE = 1.24 MPa (180 psi)
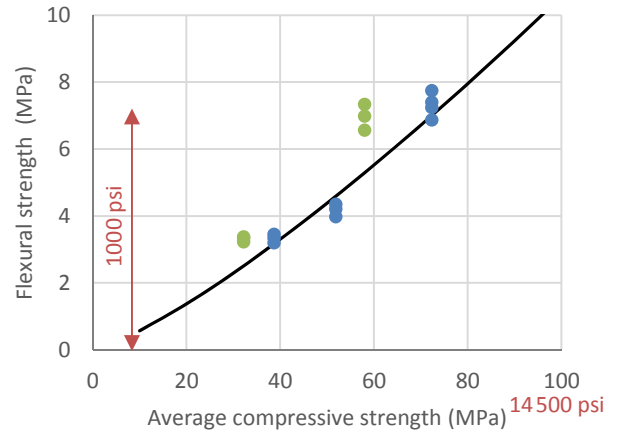
P3 (4-h OT with Type III cement)
MSE = 1.33 MPa (193 psi)
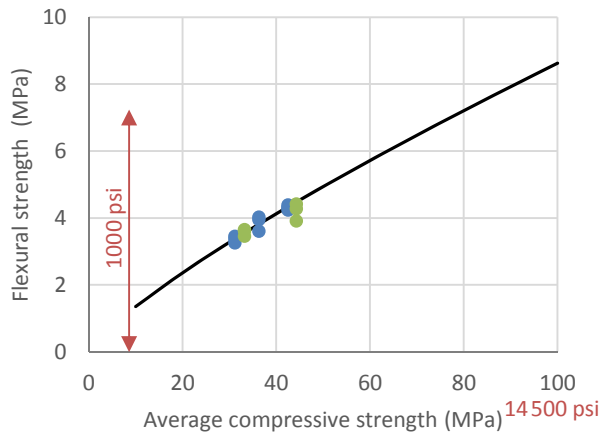
CSA (4-h OT with CSA cement)
MSE = 0.25 MPa (37 psi)
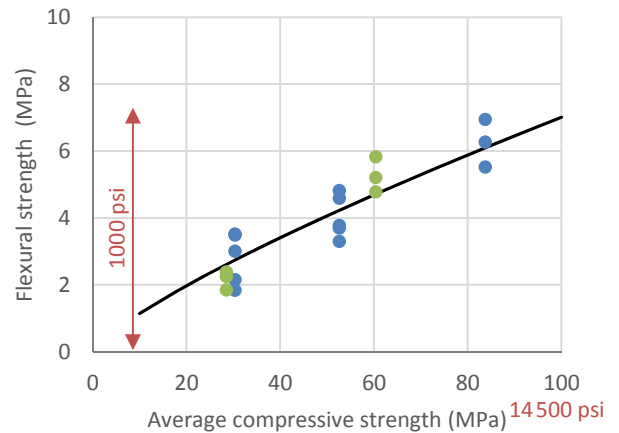
P2-ICC (ICC based on P2 mix)
MSE = 0.62 MPa (89 psi)

Note: The positive curvature (upwards) of the lab-calibrated MR-fc function for mix P3 was not expected. A definitive explanation was not found for that outcome.

Figure 5.17: Flexural strength prediction based on compressive strength.

(This page intentionally blank)

6   DATA COLLECTED FROM ENVIRONMENTAL SECTIONS

As noted in Chapter 1, the 245 sensors embedded in the *environmental sections* (ENV sections) began collecting data the day before the overlay construction, which occurred between February 23 and 25, 2016. A representative collection of the data recorded from those dates up until August 4, 2016, is presented below, along with a first evaluation of the engineering reasonableness of the data. This evaluation allowed the detection of any sensors that were producing invalid or questionable data.

6.1   Data Registered by Thermocouples

To collect temperature data, each of the six environmental sections was instrumented with fifteen thermocouples that were installed in one slab of each section, in three different locations, and stacked at five different depths. Their positions within the slab were at the center, at an interior corner, and at an exterior corner (adjacent to the shoulder). They were at depths of 5 mm (0.2 in.), 20 mm (0.8 in.), 50 mm (2.0 in.), at the slab bottom, and in the asphalt base (30 mm, 1.2 in., below asphalt surface). Details of the thermocouple layout can be found in Section 3.2.2 of this report.

Most of the thermocouples provided reasonable temperature data starting immediately after construction of the overlay. An example of their readings is presented in Figure 6.1. As expected, diurnal temperature variation (maximum-minimum for each day) decreased with increased depth.

Several problems related to thermocouples records did occur during this initial period.

- Five of out the 90 thermocouples installed produced invalid or questionable data and have been excluded from future analyses. They are listed below:
    - Therm.L.S14=C.145
    - Therm.M.S14-L.005
    - Therm.O.S14-L.005
    - Therm.O.S14-L.145
    - Therm.O.S14-R.005

    Note: the instrument-naming convention is described in Section 3.3 of this report.

- Most of the thermocouples produced noisy data or none during rainfalls. Those data were discarded from future analyses (the temperature data gaps in Figure 6.1 in the first half of March 2016, are due to that problem). This problem was caused by short-circuits in the LVDT sensors that were recording joint displacements, and was attributed to improper sealing of the LVDT's cable connections. The problem disappeared after the cables connections were properly sealed.
- One of the modules registering data from the thermocouples became disconnected and did not register data between May 22 and June 1. This failure affected Sections J, K, and L, whose thermocouples were connected to this module.
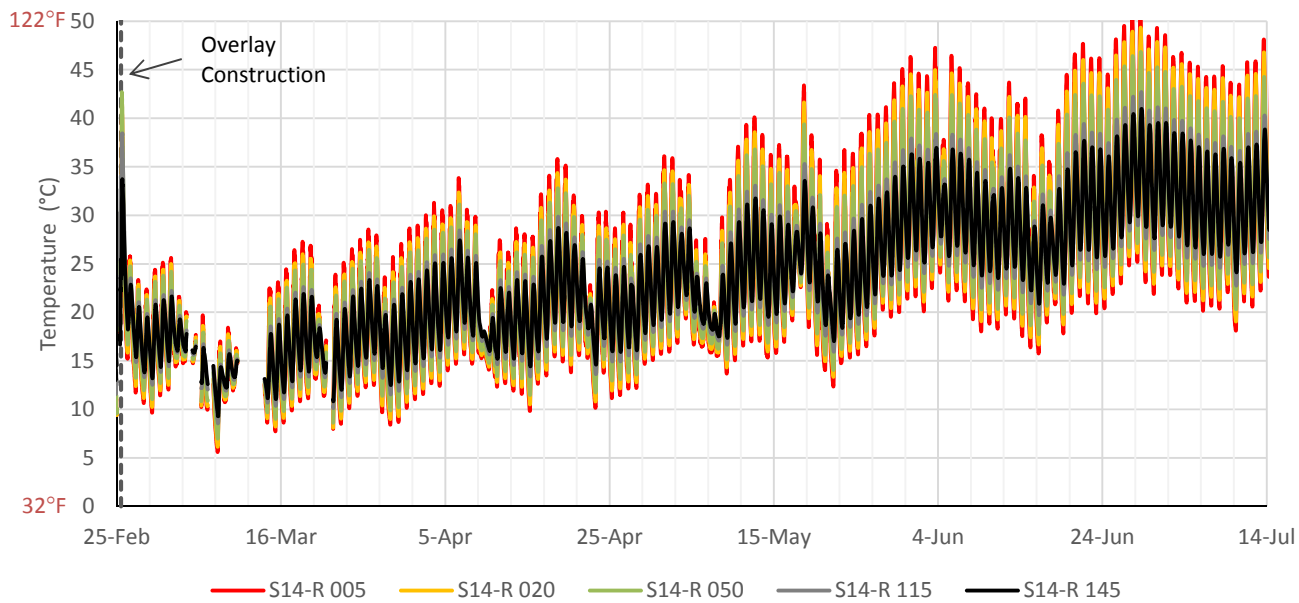
Note: the three-digit number at the end a sensor ID indicates the depth of the sensor in mm.

Figure 6.1: Example of temperature readings from thermocouples (Section N).

6.2 Data Registered by Relative Humidity Sensors

A set of relative humidity (RH) sensors was placed in each of five of the environmental sections. The goal was to measure this variable for each type of concrete and curing procedure: P2 (Section L), P2 cured with SRA (Section M), P3 (Section N), CSA (Section O), and P2-ICC (Section K). One slab per section was instrumented with RH sensors, except for Section L, where two slabs were instrumented. Section L was instrumented with twice as many of these sensors because P2 concrete is used in most HVS sections. As was discussed in Section 3.2.2, two types of RH sensors were used: the Campbell Scientific CS215-L and the Sensirion SHT75—and they are referred to as *RHC* and *RHS* respectively in this report. As was explained earlier, the sensing part of the CS215-L is also an SHT75 sensor. The main difference between the sensors is that the RHC incorporates signal conditioning while the RHS requires signal conditioning to be conducted by the data acquisition system. Another important difference is that the encapsulation of the SHT75 is already provided with the RHC sensors. For the RHS, it was necessary to manufacture a capsule in the laboratory, which was done using a plastic tube and a Gore-Tex® membrane following recommendations of the Univ. of Pittsburgh team.

Two RHC sensors were placed at the center of the instrumented slab, at 20 and 50 mm (0.8 and 2.0 in.) depth. The goal of this subset was to measure the effect of depth. Two RHS sensors were placed at 20 mm (0.8 in.) depth, one at the center of the instrumented slab and the other at a shoulder corner, 175 mm (7.0 in.) from the edge. The

goal of this subset was to measure differential drying due to the effect of the shoulder. More details of RH sensors layout can be found in Section 3.2.2 of this report.

One problem developed with one of the RHC sensors, RHC.M.S12=C.020 (CS215-L type, located in Section M at 20 mm [0.8 in.] depth), which started to measure unrealistically high diurnal RH variations on May 9, 2016. These variations were in line with clogging of the pores of the sensor capsule.

Examples of the readings collected by the RHC and RHS sensors in Section K are presented, respectively, in Figure 6.2 and Figure 6.3. Both types of sensors, when located at 20 mm (0.8 in.) depth, clearly show the drying that takes place during periods with no rainfall and the increased moisture after periods of rainfall. These RH data reflect also diurnal changes related to temperature fluctuations. It should be noted that although RH values exceeding 100 percent are shown for the RHS sensors in Figure 6.3, these values should actually be regarded as 100 percent. In fact, RHC sensors directly report 100 percent in these cases. For RHS sensors, it is possible to use the direct results based on actual sensor readings, which can result in more than 100 percent relative humidity. These values, even if unrealistic, still reflect the drying and wetting processes taking place in the concrete.
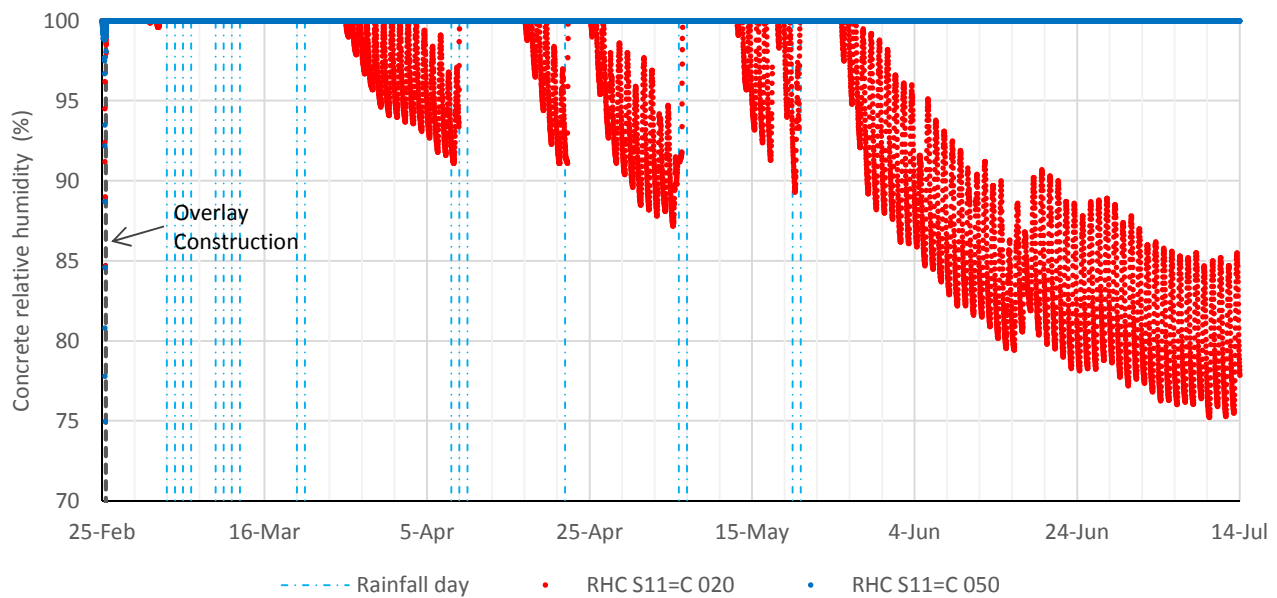
Notes: The series "Rainfall day" indicates days when any rainfall occurred.
          The three-digit number at the end a sensor ID indicates the depth of the sensor in mm.

Figure 6.2: Example of readings from RHC sensors (Section K).
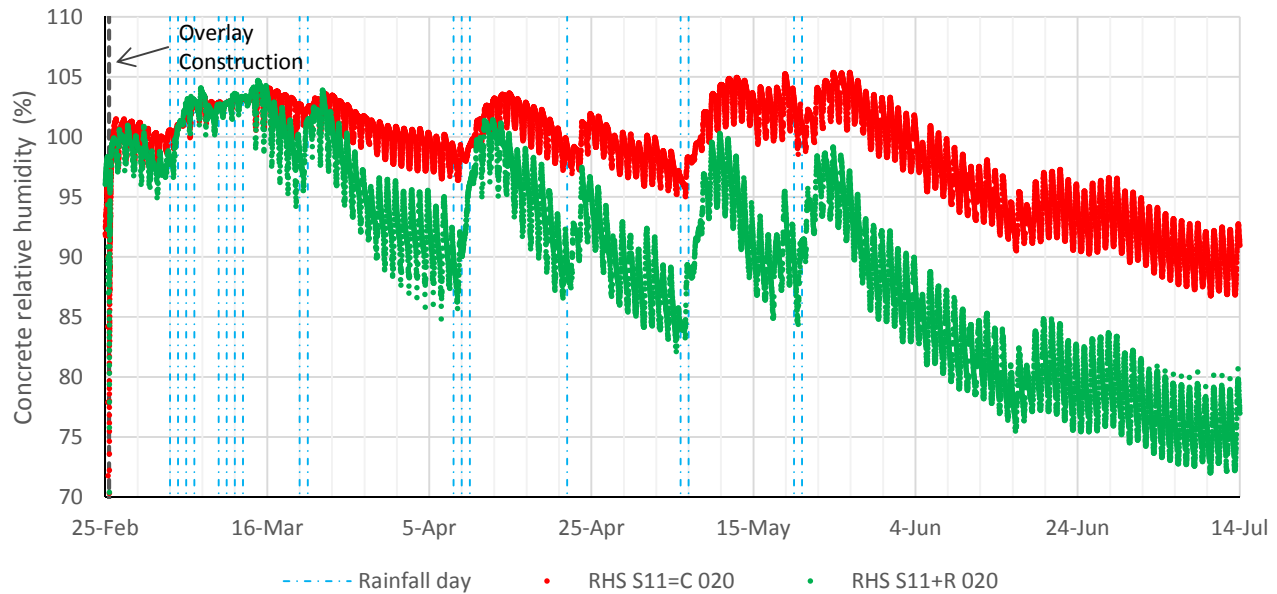
Notes: The series "Rainfall day" indicates days when any rainfall occurred.

The three-digit number at the end a sensor ID indicates the depth of the sensor in mm.

Figure 6.3: Example of readings from RHS sensors (Section K).

Daily mean values (i.e., the mean of all the readings for a day) were computed for all the sensors in order to conduct a preliminary analysis of the RH data, and the results for the RHC and RHS sensors are presented in Figure 6.4 and Figure 6.5, respectively. The RH values presented in the two figures are those measured at the center of the instrumented slab, at 20 mm (0.8 in.) depth. The two sensors, RHC and RHS, were only 100 mm (4 in.) apart, so they should have reported very similar values for each section. As the figures show, the two types of sensors do present a similar evolution pattern, including the tendency to dry during periods without rainfall and the rapid rewetting after rainfalls. Nonetheless, considerable differences exist between the two types of sensors. One possible source of the differences is an initial offset in the values measured by RHS sensors. Support for this hypothesis comes from the observation that even after the rainy periods some of these sensors did not reach 100 percent RH, despite how close they were to the surface. Since both the RHC and RHS used the SHT75 sensor unit the differences may be due to the type of encapsulation or from manipulation of the SHT75 unit to produce the RHS sensors in the laboratory. Overall, RHC values seem to change more uniformly than RHS values, but a definitive argument to use one sensor type over another has not been found.

One argument against using the RHC sensors is they do not show self-desiccation for any mixes, as reflected in Figure 6.6. This figure shows the relative humidity measured at 50 mm (2.0 in.) depth for the different mixes and

curing procedures. These data show no evidence of drying for any of the mixes, except for CSA at the end of the evaluation period. Nonetheless, internal desiccation due to the cement hydration process (self-desiccation) was expected for the P2 and P3 mixes due to the low water/cement ratio of these mixes, which was slightly over 0.30. Concrete self-desiccation was also expected in the P2-ICC, although less than in the P2 and P3 mixes. As Figure 6.6 shows, almost no self-desiccation was measured in any of these mixes. However, it is very likely that self-desiccation did take place, at least in the P2 and P3 mixes, but the RHC sensors were unable to capture it. No RHS sensor was located at 50 mm (2.0 in.) depth, so it is unknown whether or not these sensors would have been able to capture concrete self-desiccation.
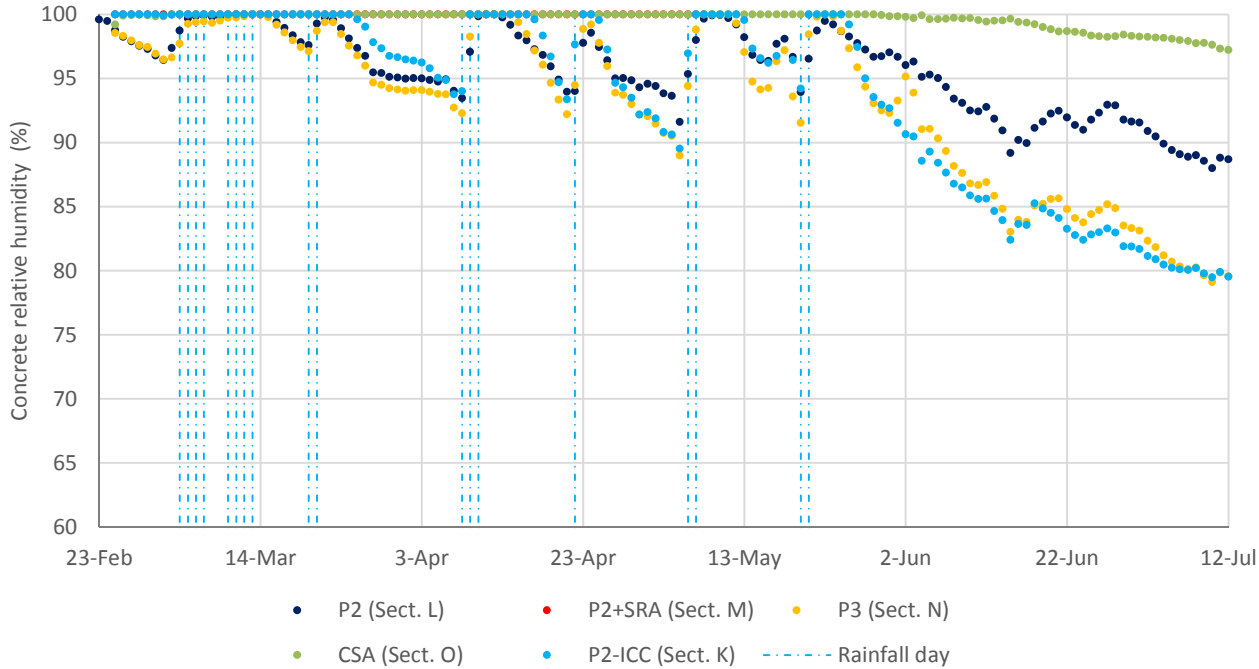
Notes: Each point in the graph is the average of RH values measured in one day.

The series "Rainfall day" indicates days when any rainfall occurred.

The sensor in Section M (P2 cured with SRA) clogged on May 9. This sensor was measuring 100 percent RH, at all times, up to May 9.

Figure 6.4: Relative humidity measured by RHC sensors (Campbell Scientific CS215-L) at 20 mm (0.8 in.) depth.
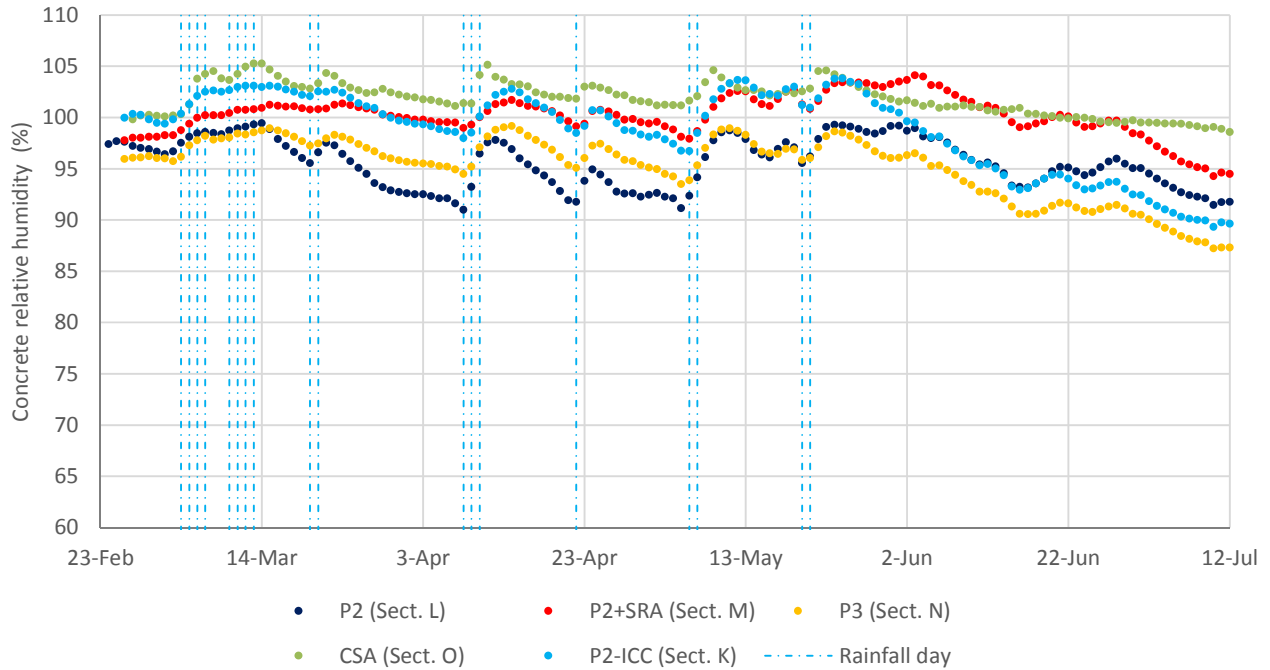
Notes: Each point in the graph is the average of RH values measured in one day.

The series "Rainfall day" indicates days when any rainfall occurred.

Figure 6.5: Relative humidity measured by RHS sensors (Sensirion SHT75) at 20 mm (0.8 in.) depth.
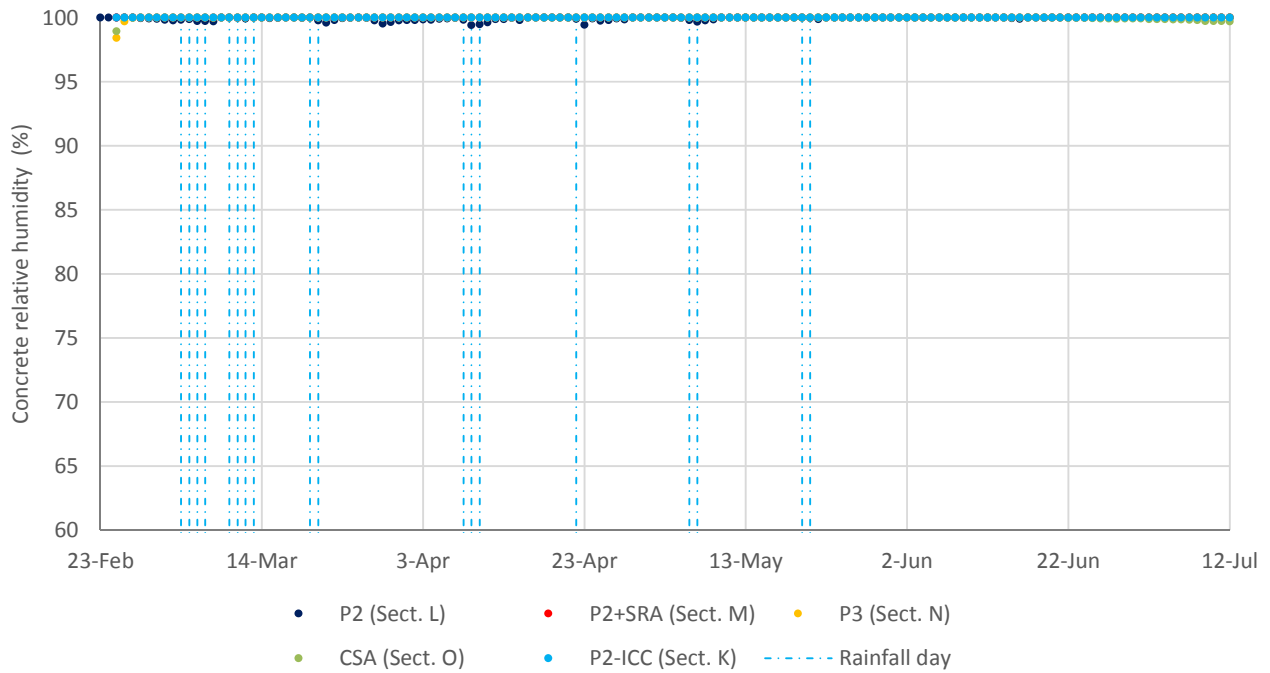
Notes: Each point in the graph is the average of RH values measured in one day.

The series "Rainfall day" indicates days when any rainfall occurred.

Figure 6.6: Relative humidity measured by RHC sensors at 50 mm (2.0 in.) depth.

6.3   Data Registered by Moisture Content Sensors

A set of moisture content (MC) sensors was placed in each of five of the environmental sections, with the goal of measuring this variable for each type of concrete and curing procedure: P2 (Section L), P2 cured with SRA (Section M), P3 (Section N), CSA (Section O), and P2-ICC (Section K). One slab per section was instrumented with MC sensors except for Section L, where two slabs were instrumented. This exception for Section L was made because the P2 concrete used in Section L was also used in most of the HVS sections. These sensors were installed at the center of one slab per section, at 20 and 50 mm (0.8 and 2.0 in.) depth. (Details of MC sensor layout appear in Section 3.2.2 of this report.)

Data from one MC sensor out of the sixteen installed was discarded. This sensor, MC.K.S11=C.020, resulted in unrealistically low and unstable MC values.

As described in Section 3.5, data collection for these sensors was conducted differently from the rest of the sensors. Instead of the Campbell Scientific DASs, two A3 NEMA data loggers by SMT Research were used to collect MC data. Data collected with these data loggers were periodically transferred to a server. Then, an online application by SMT Research was used to download the data from the server. Some problems were found with this data collection procedure and as a result there are frequent gaps in the collected data, as reflected in the example in Figure 6.7.

The data in Figure 6.7 constitute a representative example of the readings from the MC sensors. In this figure, drying during periods without rainfall can be seen for the sensors located at 20 mm (0.8 in.) depth. Increased moisture after periods of rainfall can also be seen in Figure 6.7. It appears that in both wet and dry periods, the environmental effects on moisture content were not as noticeable as they were on concrete relative humidity. The diurnal variations of MC are smaller for the sensor located at 50 mm (2.0 in.) depth than for the sensor located at 20 mm (0.8 in.) (see Figure 6.7). The same pattern was observed for the relative humidity sensors, as described above. Diurnal variations of the moisture content at 20 mm (0.8 in.) depth follow a trend similar to the diurnal variations of relative humidity, which means that the measured moisture content increases as temperature increases. It should be noted that these sensors do not measure the moisture content in the concrete itself, but in the wood they are embedded in, and consequently this variable is an indirect indication of the moisture content in the concrete.
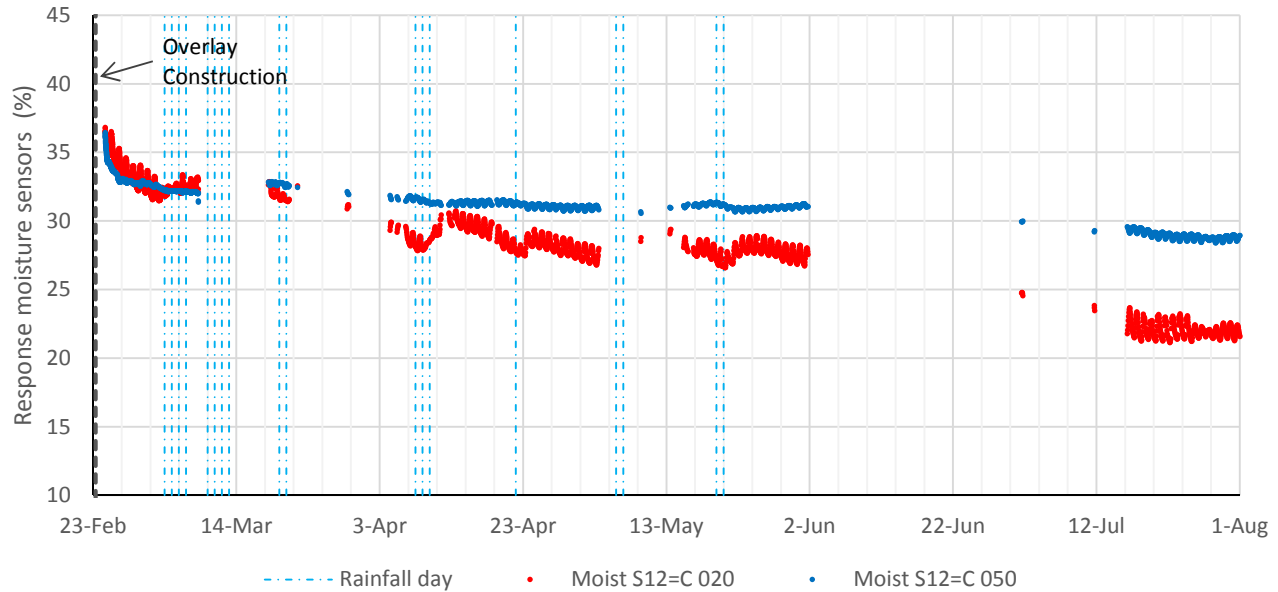
Note: The series "Rainfall day" indicates days when any rainfall occurred.

Figure 6.7: Example of moisture content readings (Section L).
(*Note:* sensors manufactured by SMT Research Ltd.)

6.4 Data Registered by Vibrating Wire Strain Gages

The six environmental sections were instrumented with vibrating wire strain gages (VWSG) in order to measure strain developed due to temperature and moisture-related actions. As explained above, four of these sections (L, M, N, and O) were built exclusively to monitor environmental response, while two of them (J and K) were also tested with the Heavy Vehicle Simulator (HVS). Environmental sensors in these sections started to collect data before the overlay construction, so that early-age response was also monitored.

One slab per section was instrumented with VWSG sensors except for Section L, where two slabs were instrumented. This section was instrumented with twice as many of these sensors because the P2 concrete used for it and its slab size (1.8×1.8 m² [approximately 6×6 ft²]) were also used in most of the HVS sections. The gages were placed at three locations in the slabs—at the slab center, at an exterior shoulder corner, and at an interior corner—and at two depths—20 mm (0.8 in.) and 95 mm (3.7 in.), the latter of which is 20 mm (0.8 in.) above the bottom of the slab. Each pair of strain gages, top and bottom, can be used to determine slab expansion-contraction as well as bending. (More information concerning the instrument layout can be found in Section 3.2.2 of this report.)

As noted earlier (Section 4.2, Figure 4.14), eight beams 500×150×40 mm³ (18×6×x1.6 in³) were also instrumented with VWSG sensors. These beams represent the four mixes (P2, P3, CSA, and P2-ICC) and the two curing procedures (curing compound and SRA plus curing compound) used for the construction of the BCOA sections. These beams were used to measure the unrestrained expansion-contraction of the different concrete mixes due to temperature and moisture changes. The beams were free to expand and contract because they were not bonded to any support.

This report uses the following conventions for referring to strain: a positive sign indicates an expansion and a negative sign indicates a contraction. A baseline for strain was determined after concrete field setting time (FST), i.e., strain was assumed to be zero at the FST. *Field setting time* is defined here as the time at which the concrete in the field is first able to develop stress when it is subjected to imposed deformations. The FST was determined for each of the environmental sections based on visual examination of strain and temperature evolution after concrete placement, following the methodology described in Reference *(21)*.

One VWSG sensor out of the 64 installed was discarded. This sensor, StSGT.K.S12=C.020, was broken during the construction of the overlay. Other than this, the only problem with VWSG sensors were the shadows by the Heavy Vehicle Simulator (HVS) that occasionally affected the response of the environmental sections. Because of the large volume of the HVS units, the shadows they projected affected not only the specific section they were testing but the adjacent sections as well. Occasionally there was even other machinery being used to evaluate the sections, such as a falling weight deflectometer, that projected shadows onto the environmental sections. These situations were tracked when the shadow (coming from the HVS or other objects) continuously affected an environmental section for more than a half hour and the part of the environmental response data collected during these periods has been disregarded.

An example of VWSG records is presented in Figure 6.8. This figure shows strain and temperature measured with the two gages located close to Joint 2 in Section M. These two gages showed similar strain values after overlay construction, before Joint 2 deployed. (Note that the three digits at the end of the sensor code indicate sensor depth in mm, measured from the surface of the slab). Negative strain indicates shrinkage, both moisture-related and thermal. After Joint 2 deployed, the top strain gage registered larger values of strain (in absolute value) than the bottom strain gage. This *differential shrinkage* (top compared to bottom) is mainly due to the concrete first drying at the top of the overlay and proceeding downward (top-down). Differential shrinkage is also caused by the temperature gradients that exist when the concrete sets (locked temperature gradients). An important observation from Figure 6.8 is the large differential shrinkage values that were registered in this section, around 250 $\mu\varepsilon$ at the end of the evaluation period shown in the figure. This differential shrinkage indicates very high levels of drying

shrinkage. This section, where P2 mix was cured with SRA, was one of the sections with the best drying shrinkage performance. Larger differential shrinkage values were registered in other sections.
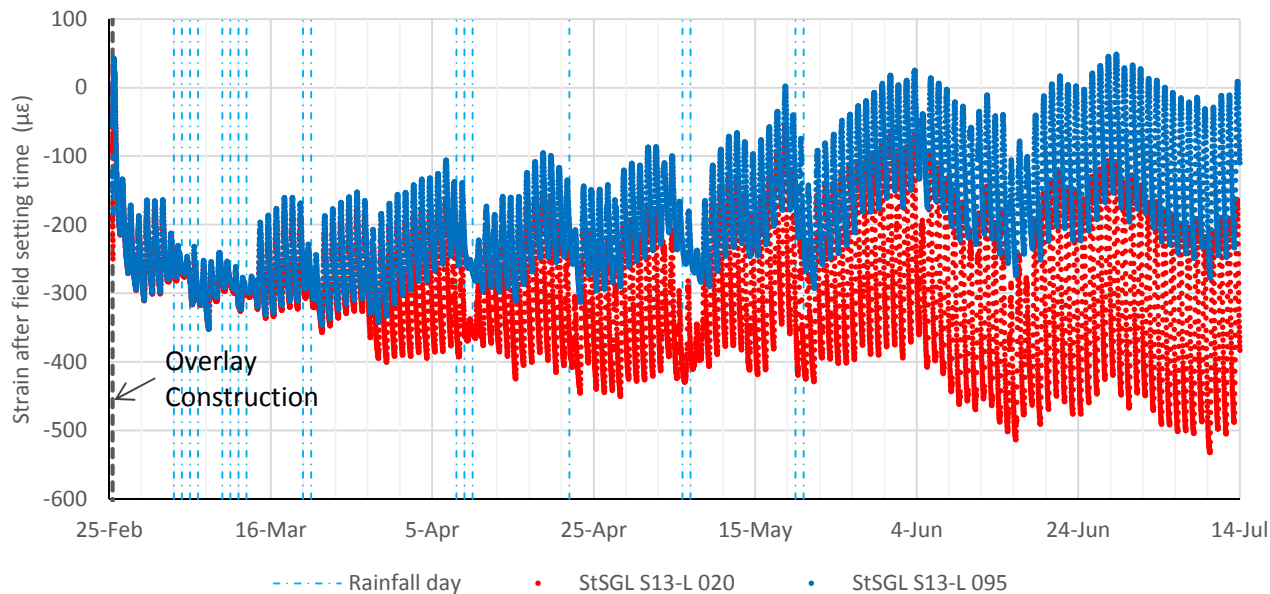
Figure 6.8: Example of readings from VWSG sensors (Section M).

6.5 Data Registered by LVDT Sensors

A set of linear variable displacement transducer (LVDT) devices—nine joint displacement measuring devices (JDMDs) and two interface opening measuring devices (IOMDs)—was placed in each of five of the environmental sections in order to measure slab displacements due to temperature and moisture-related actions. The five instrumented sections are Section L (P2), Section M (P2 cured with SRA), Section N (P3), Section O (CSA), and Section K (P2-ICC). This means that one section for each material and curing procedure was instrumented with JDMDs and IOMDs. As explained above, the JDMDs measure vertical displacement at slab corners and edges and the opening and closing of transverse joints. The IOMDs measure the opening of the concrete-asphalt interface. (Details of the JDMD and IOMD sensor layouts appear in Section 3.2.2.)

This report uses the following conventions for referring to displacements: a positive sign indicates upward vertical movement and a negative sign indicates a downward vertical movement. This applies to JDMDs that measure vertical displacements of slabs corners and edges. For JDMDs that measure joint opening and closing and for

IOMDs, positive sign indicates expansion and a negative sign indicates contraction, the same conventions used for VWSG sensor data.

None of the 53 LVDT sensors has been discarded. For most of the sensors, the measured displacements presented mid- and long-term evolutions, as well as diurnal variations, that were compatible with the temperature and moisture-related changes the slabs were experiencing. In a few cases the displacements were not what was initially expected, although further analysis revealed the reason was that not all joints were deployed and, consequently, the slabs were not actually working as independent slabs. The main problem encountered with JDMDs and IOMDs was the electrical noise mixed in with the data during rain periods; this was due to improper sealing of the LVDT cable connections. The short circuits coming from the LVDTs also affected thermocouple readings. This problem disappeared after the cable connections were properly sealed. Other problems related to the JDMD records are listed below.

- A sudden displacement of a few millimeters was measured for two JDMD sensors in Section O. This was attributed to a displacement of the core of the LVDTs, which were not spring-loaded in these two particular JDMDs. It should be mentioned that some loose-core LVDTs were used for this project. In these cases, a manually-mounted spring pushed the LVDT core against the target. This installation allowed the use of a number of loose-core LVDTs, but the resulting system was not as reliable as a spring-loaded LVDT.
- Two of the vertical JDMDs in Section K went out of range for several hours on some days at the end of April. This can be seen in Figure 6.9 for JDMDs S11+R and S12-R. Measuring range of JDMD sensors was ±5 mm.

These movements were computed after the JDMDs and IOMDs were installed, which was after the field setting time of the concrete, because the installation of these sensors is relatively time-consuming and cannot be conducted before saw-cutting operations. The JDMD and IOMD sensors were installed on Section L, which is in Lane 1, the same day the overlay was built, but for the rest of the environmental sections, all of which were in Lane 2, these sensors were installed the day after the overlay was built.

As examples, the vertical and horizontal JDMD displacements measured in Section K are shown, respectively, in Figure 6.9 and Figure 6.10. Both the vertical and horizontal JDMDs reflect the mid- and long-term evolution due to temperature and moisture-related changes as well as diurnal variations. As expected, the slab corners (sensors with a label ending in "+R" or "–R" in Figure 6.9) move upward and the joints (Figure 6.10) tend to open in the mid- and long-term due to moisture-related shrinkage. Diurnal variations reflect mainly temperature changes. Consequently, downward corner movements and joint closings are mainly experienced during daytime, and the opposite during nighttime. The same pattern is present in the rest of the sections, although the displacements were smaller than in Section K. That section presented higher displacements than the other sections for one main reason:

its slab size. The slab size in Section K is 3.6×3.6 m² (12×12 ft²) but the slabs of the other environmental sections instrumented with JDMDs are 1.8×1.8 m² (6×6 ft²). An example of JDMD readings for the latter slab size is included in Figure 6.11, which shows the vertical displacements measured in Section M.

Figure 6.12 shows the readings from the two IOMD sensors in Section K. The LVDT body of these sensors is attached to the concrete slabs, and the tip of the LVDT core rests on a metal bar that is anchored in the asphalt base (Figure 3.4). These sensors measure opening of the concrete-asphalt interface. Figure 6.12 shows that the Section K IOMDs registered very small readings, below 0.5 mm (0.02 in.), which indicates full bonding of the concrete and asphalt. It should be noted that the slab corners had moved roughly 6 mm upwards by the end of April (Figure 6.9). The IOMD readings indicate that the asphalt base followed the concrete slabs in this large upward movement. The same pattern was observed in all the environmental sections instrumented with IOMDs.
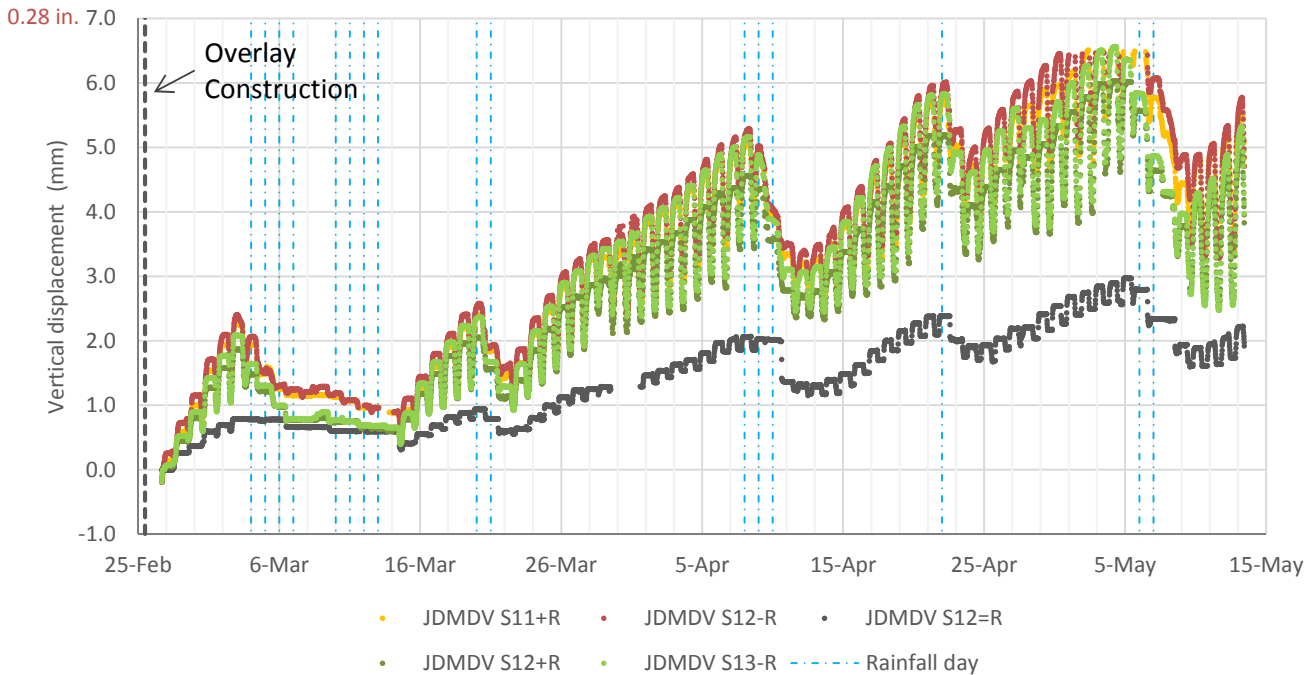
Notes: The series "Rainfall day" indicates days when any rainfall took place.

The sensors with labels ending in "+R" or "–R" are located at a shoulder corner of the slab. The sensor JDMDV S12=R is located at midslab at the shoulder edge. The sensor-naming convention is included in Section 3.2.

Figure 6.9: Example of records from vertical JDMDs (Section K).
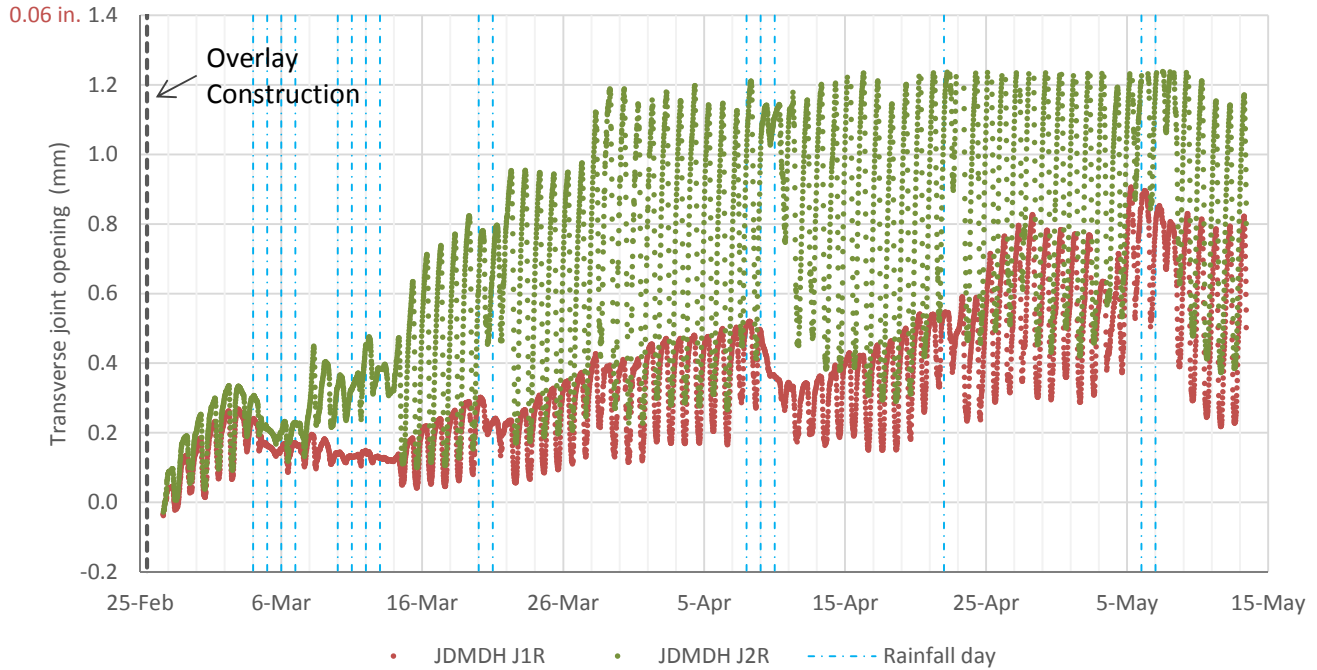
Note: The series "Rainfall day" indicates days where any rainfall took place.

Figure 6.10: Example of records from horizontal JDMDs (Section K).
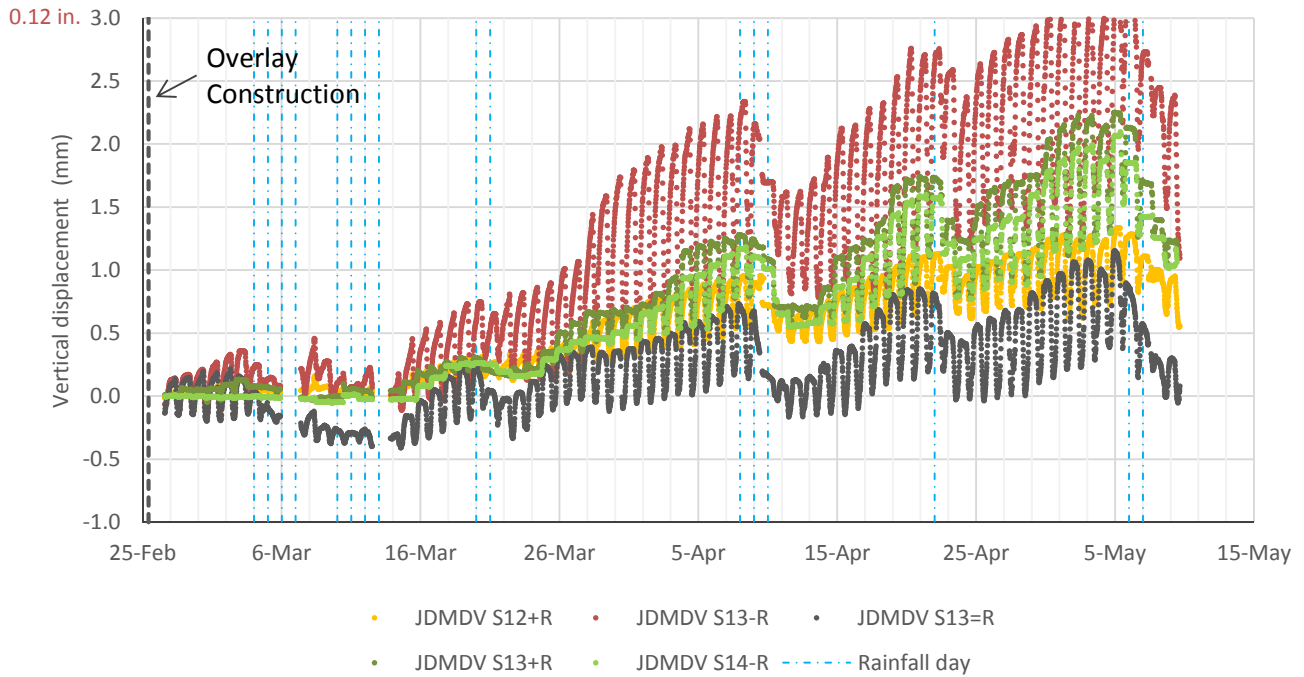
Notes: The series "Rainfall day" indicates days where any rainfall took place.
The sensors with labels ending in "+R" or "–R" are located at a shoulder corner of the slab. The sensor JDMDV S13=R is located at midslab at the shoulder edge. The sensor-naming convention is included in Section 3.2.

Figure 6.11: Example of records from vertical JDMDs (Section M).
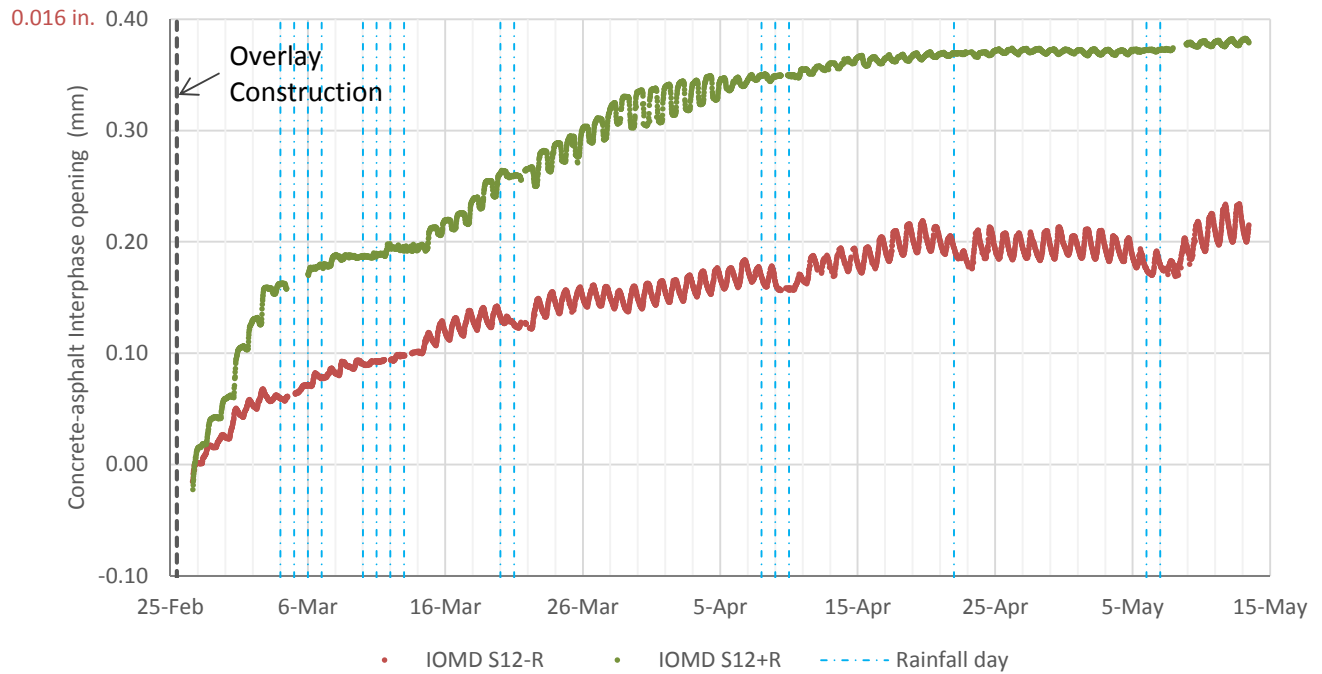
Notes: The IOMD sensors were located at the shoulder corners of the slab (Section 3.2.2.)

The series "Rainfall day" indicates days when any rainfall occurred.

Figure 6.12: Example of records from IOMDs (Section K).

7   SUMMARY, CONCLUSIONS, AND RECOMMENDATIONS

7.1   Summary

The design, construction, and initial monitoring of fifteen full-scale bonded concrete overlay of asphalt (BCOA) pavement sections is described in this report. Eleven of these sections were designed for HVS testing, while four of them were built to exclusively monitor the response of the slabs to environmental agents and cement hydration (environmental sections). The range of the different design factors included in the sections is presented below:

- Concrete types
    - Type II/V portland cement with a 10-hour design opening time (OT)
    - Internally cured concrete based on previous mix (Type II/V cement with a 10-hour design OT)
    - Type III portland cement with a 4-hour design OT
    - Calcium sulfoaluminate cement (CSA) with a 4-hour design OT

    Note: the Caltrans flexural strength requirement for opening time is 2.8 MPa (400 psi).

- Slab dimensions: half-lane width (1.8×1.8 m² [approximately 6×6 ft²] slabs]), widened lane (2.4×2.4 m² [approximately 8x8 ft², slabs]), and full-lane width (3.6×3.6 m² [approximately 12×12 ft²] slabs)
- Asphalt base type: conventional hot mix asphalt (old, existing mix) and rubberized asphalt (new placement)
- Asphalt base thicknesses: 50 to 120 mm (2 to 4.7 in.)
- Asphalt surface preparation techniques: sweeping (no texturing), micromilling, and milling
- Concrete curing procedures: curing compound and shrinkage-reducing admixture (topical use)

Construction of the concrete overlays took place on February 23 and 25, 2016. Weather conditions during construction were relatively mild, and no major incidents happened during construction.

In addition to the construction QC/QA, additional testing was conducted in order to compare ASTM C78-10 and California Test 524 (2013) for determining the mixes' modulus of rupture (MR). These two standards mainly differ in their approaches to initial curing of the beams.

Testing was also conducted with the goal of evaluating the use of concrete compressive strength (fc) to predict the modulus of rupture of the field mixes used in this BCOA construction. A specific equation MR-fc was calibrated for each of the mixes using the results of MR and fc testing conducted on the mixes prepared in the laboratory. Then, the compressive strength of each of the field mixes was used to predict the field modulus of rupture.

A total of 560 sensors were placed in the BCOA sections. The characteristics of these sensors, and their layout and installation, are described in this report. Of the total number of sensors, 315 were focused on the HVS testing and 245 constituted the instrumentation of the environmental sections.

The environmental sensors started to collect data the day before the overlay construction. Several of these sensors were discarded, based on the data they collected up until August 4, 2016. The discarded sensors included five thermocouples, one moisture content sensor, and one vibrating wire strain gage. Other than these sensors, the environmental sensors provided data that were compatible with the thermal, moisture-related, and structural responses that can be expected of the BCOA sections due to environmental actions and cement hydration process.

7.2   Conclusions

The main conclusions from the construction QC/QA testing of the rapid strength concrete (RSC) mixes are presented below:

- Overall, all the concrete mixes met the Caltrans requirements included in Section 40 of the Standard Specifications and in the Standard Special Provisions 40-5 applicable to jointed plain concrete pavements built with rapid strength concrete.

- The minimum flexural strength requirement of 2.8 MPa (400 psi) was fulfilled by all the rapid strength concrete mixes at the design opening time, with the exception of the Type III cement concrete placed the second construction day. The actual opening time of this mix was slightly over the design opening time of 4 hours.

- All the portland cement–based mixes far exceeded the Caltrans 10-day flexural strength requirement of 4.5 MPa (650 psi). The flexural strength of these mixes increased more than 100 percent from the opening age to 10 days.

- The increase in flexural strength from design opening age to 10 days was much smaller in the CSA-based concrete than in the mixes with portland cement. The 10 day flexural strength of the CSA-based concrete placed the first construction day was slightly below 4.5 MPa (650 psi), the Caltrans minimum requirement.

- The replacement of 50 percent of the sand of the Type II/V cement mix with pre-wetted lightweight aggregates carried a decrease in flexural strength of 30 percent after 10 hours (design opening time of the original mix) and of 25 percent after 10 days. This decrease was much higher than the expected result based on preliminary laboratory testing and results from similar experiments.

- Some section-to-section differences were observed for the P2 mix. The concrete used for the construction of Sections B and J was very fluid, and the Section B concrete presented some visual indications of segregation.

The main conclusions of the comparison of ASTM C78-10 and CT 524 (2013) are:

- Modulus of rupture differences between both standards were related to the formula used to determine the modulus of rupture. Differences between both standards results were not statistically significant when the same formula was used in the calculations.

- No clear difference was found between both curing approaches based on the temperatures recorded inside the beams.

- The temperatures measured inside the beams for both curing approaches were considerably higher than the temperatures measured in the pavement slabs. Consequently, both curing approaches would have considerably overestimated the maturity of the concrete in the slabs at the design opening time.

It must be emphasized that these outcomes were highly dependent on the specific weather conditions during construction. In extremes of weather, with either lower or higher temperatures, differences between ASTM C78-10 and CT 524 would be expected, since weather conditions are expected to affect the CT 524 beams much more than they are expected to affect the beams cured following the ASTM procedures.

The conclusion from the prediction of flexural strength from compressive strength values is:

- The root mean square (RMS) of the prediction error ranged from 0.25 MPa (37 psi) in the mix with CSA cement to 1.33 MPa (193 psi) in the mix with Type III cement. For two of the mixes, the prediction error also depended on age of the concrete. The pooled (four mixes) RMS of the prediction error was 0.97 MPa (140 psi), which seems relatively high for the approach to be used for QC/QA.

7.3   Recommendations

There are no recommendations presented in this report. Recommendations regarding implementation of BCOA will be included in the final report of this project.

REFERENCES

1. Rasmussen, R. O., and D.K. Rozycki. "Thin and Ultra-Thin Whitetopping," NCHRP Synthesis of Highway Practice 338, National Cooperative Highway Research Program, National Research Council, Washington, DC, 2004.

2. Han, C. "Synthesis of Current Minnesota Practices Of Thin and Ultra-Thin Whitetopping," Minnesota Department of Transportation, St. Paul, 2005.

3. Harrington, D., and G. Fick. "Guide to Concrete Overlays: Sustainable Solutions for Resurfacing and Rehabilitating Existing Pavements", 3rd Edition, National Concrete Pavement Technology Center, 2014.

4. Mateos, A., J. Harvey, J. Paniagua, and F. Paniagua. 2015. Development of Improved Guidelines and Designs for Thin Whitetopping: Literature Review. University of California Pavement Research Center Technical Memorandum UCPRC-TM-2015-01.

5. Jones, D., R. Wu, and S. Louw. 2014. Full-Depth Recycling Study: Test Track Construction and First Level Analysis of Phase 1 HVS and Laboratory Testing Research Report UCPRC-RR-2014-03

6. Jones, D., R. Wu, B. Tsai, and J. Harvey, 2011. Warm-Mix Asphalt Study: Test Track Construction and First-Level Analysis of Phase 3a HVS and Laboratory Testing (Rubberized Asphalt, Mix Design #1). University of California Pavement Research Center Research Report UCPRC-RR-2011-02.

7. American Concrete Institute. 2013. ACI CT-13 ACI Concrete Terminology.

8. Bentz, D.P., and W.J. Weiss. 2011. Internal Curing: A 2010 State-of-the-art Review. U.S. Department of Commerce, National Institute of Standards and Technology.

9. Bentz, D.P., E.J. Garboczi, and K.A. Snyder. 1999. A Hard Core/Soft Shell Microstructural Model for Studying Percolation and Transport in Three-Dimensional Composite Media, NISTIR 6265, U.S. Department of Commerce.

10. Shah, S.P., W.J. Weiss, and W. Yang. 1998. Shrinkage Cracking—Can It Be Prevented? *Concrete International-Design and Construction* 20(4), 51-55.

11. Bentz, D. 2005. Curing with Shrinkage-Reducing Admixtures: Beyond Drying Shrinkage Reduction. *Concrete International* 27 (10): 55-60.

12. Villani, C., C. Lucero, D. Bentz, D. Hussey, D.L. Jacobson, and W.J. Weiss. 2014. Neutron Radiography Evaluation of Drying in Mortars with and without Shrinkage Reducing Admixtures. American Concrete Institute Fall Meeting, Washington, DC (Vol. 26).

13. Nmai, C., R. Tomita, F. Hondo, and J. Buffenbarger. 1998. Shrinkage-Reducing Admixtures. *Concrete International* 20(4), 31-37.

14. Dang, Y., J. Qian, Y. Qu, L. Zhang, Z. Wang, D. Qiao, and X. Jia. 2013. Curing Cement Concrete by Using Shrinkage Reducing Admixture and Curing Compound. *Construction and Building Materials* 48, 992-997.

15. Li, Z., and J.M. Vandenbossche. 2013. Redefining the Failure Mode for Thin and Ultra-Thin Whitetopping with 1.8-m by 1.8-m (6×6-ft) Joint Spacing, *Transportation Research Record: Journal of Transportation Research Board,* Transportation Research Board of the National Academics, Washington, DC.

16. Li, Z., N. Dufalla, F. Mu, and J.M. Vandenbossche. 2013. "Bonded Concrete Overlay of Asphalt Pavements Mechanistic-Empirical Design Guide (BCOA-ME)," Theory Manual, *FHWA TFP Study* 5(165).

17. National Cooperative Highway Research Program. 2004. "AASHTO Mechanistic- Empirical Design Guide," NCHRP Project 1-37a, Transportation Research Board, Washington, DC.

18. Heath, A.C., and J.R. Roesler. 1999. Shrinkage and Thermal cracking of Fast-Setting Hydraulic Cement Concrete Pavements in Palmdale, California. University of California Pavement Research Center, Institute of Transportation Studies. Draft Research Report UCPRC-RR-1999-07.

19. du Plessis, Louw, and J.T. Harvey. 2003. Environmental Influences on the Curling of Concrete Slabs at the Palmdale HVS Test Site. University of California Pavement Research Center, Institute of Transportation Studies, University of California, Berkeley. Draft Research Report UCPRC-RR-2003-05.

20. Wu, R., J.D. Lea, and D. Jones. 2012. "A Modular Data Acquisition System for Heavy Vehicle Simulator Tests," in Advances in Pavement Design through Full-scale Accelerated Pavement Testing, D. Jones, J. Harvey, A. Mateos, I. Al-Qadi, eds. CRC Press: Davis, California. p. 147-152.

21. Mateos, A., J. Harvey, R. Wu, F. Paniagua, and J. Paniagua. 2019. Development of Improved Guidelines and Designs for Thin Whitetopping: Environmental Response of Full-Scale BCOA Sections. University of California Pavement Research Center Research Report: UCPRC-RR-2017-03. *(In process)*

APPENDIX: PHOTOGRAPHIC REPORT OF TEST TRACK CONSTRUCTION

Asphalt Paving

Figure A.1: Full-depth reclamation (FDR) surface cleaning and preparation prior to placement of new HMA.

Figure A.2: Application of prime coat on top of FDR layer.

Figure A.3: Hot mix asphalt (HMA) paving.

Figure A.4: HMA being dumped into the asphalt paver.

Figure A.5: Roller compaction of the edge of the HMA layer.

Figure A.6: Temperature tracking inside the HMA.

Figure A.7: Patch on distressed area of the test track.

Figure A.8: Compaction of patch on distressed area of the test track.

Figure A.9: Milling machine with micromilling teeth spacing.

Figure A.10: Disposal of milled material.

Figure A.11: Old asphalt surface after milling (note debonding between the two asphalt lifts).

Figure A.12: Micromilled old HMA surface.

Instrumentation Lane 1

Figure A.13: Lane 1 with form work and instruments ready to be paved on new RHMA-G.

Figure A.14: Layout of instruments in an HVS section.

UCPRC-RR-2017-02

Figure A.15: Lane 1 ready to be paved.

Figure A.16: Close-up of dynamic strain gages.

Figure A.17: Close-up of thermocouple rods and rod of IOMD protected by red straw.

Figure A.18: Close-up of the anchoring rods for the JDMD targets and rod of IOMD protected by yellow straw.

Figure A.19: Environmental Section L layout.

Figure A.20: Close-up of thermocouples attached to a fiberglass rod.

Figure A.21: Close-up of longitudinal and transverse static strain gages.

Figure A.22: Campbell Scientific Data acquisition systems.

Figure A.23: Protective pipes for instrumentation wiring.

Instrumentation Lane 2

Figure A.24: From left to right: static strain gages, IOMD rod, anchoring rods for the JDMD targets, and thermocouples attached to a fiberglass rod.

Figure A.25: Longitudinal (left) and transverse (right) static strain gages.

Figure A.26: Pipes running instrument wires across the pavement structure.

Figure A.27: Close-up of transverse dynamic strain gages.

Figure A.28: Close-up of two sets of thermocouples.

Figure A.29: From left to right: two moisture content sensors, thermocouples attached to a fiberglass rod, two RHC relative humidity sensors, and one RHS relative humidity sensor.

Paving Lane 1

Figure A.30: Roller screed on Section A prior to arrival of concrete.

Figure A.31: First concrete ready-mix truck arriving at the construction site.

Figure A.32: Truck with admixtures.

Figure A.33: Dosing accelerator into the ready-mix truck.

Figure A.34: Pouring concrete at the beginning of the section.

Figure A.35: Sampling of concrete for QC/QA.

Figure A.36: Hand-rolling screed for concrete consolidation.

Figure A.37: Protecting the dynamic strain gages.

Figure A.38: Consolidation of concrete with hand-operated roller screed.

Figure A.39: Bull-float finishing of the concrete surface.

Figure A.40: The difference in PCC layer thickness between Section A (left, 150 mm [6 in.]) and Section B (right, 115 mm [4.5 in.]).

Figure A.41: Concrete truck leaving test track.

Figure A.42: Metal rake tining of the concrete surface.

Figure A.43: Metal rake tining of the concrete surface.

Figure A.44: Protective system for the instrument pipes.

Figure A.45: Cylinder and beam molds for QC/QA specimen preparation.

Figure A.46: Concrete beams inside insulated curing boxes.

Figure A.47: Temperature tracking inside beams and cylinders.

Figure A.48: Filling the gap between asphalt and form work with foam.

Figure A.49: Protecting the instrumentation before concrete pouring.

Figure A.50: Section with curing compound already applied.

Figure A.51: Manual application of curing compound.

Figure A.52: Disposal of leftover concrete.

Figure A.53: Volumetric mixer ready to mix and pour the CSA concrete.

Figure A.54: Volumetric mixer and CSA concrete consolidation with hand-operated roller screed.

Figure A.55: CSA section after concrete consolidation.

Figure A.56: Pouring concrete around instruments.

Figure A.57: Protecting instrumentation while pouring concrete.

Figure A.58: P2 (Type II/V cement) concrete consolidation.

Figure A.59: Edge finishing.

Figure A.60: Flexural beam preparation.
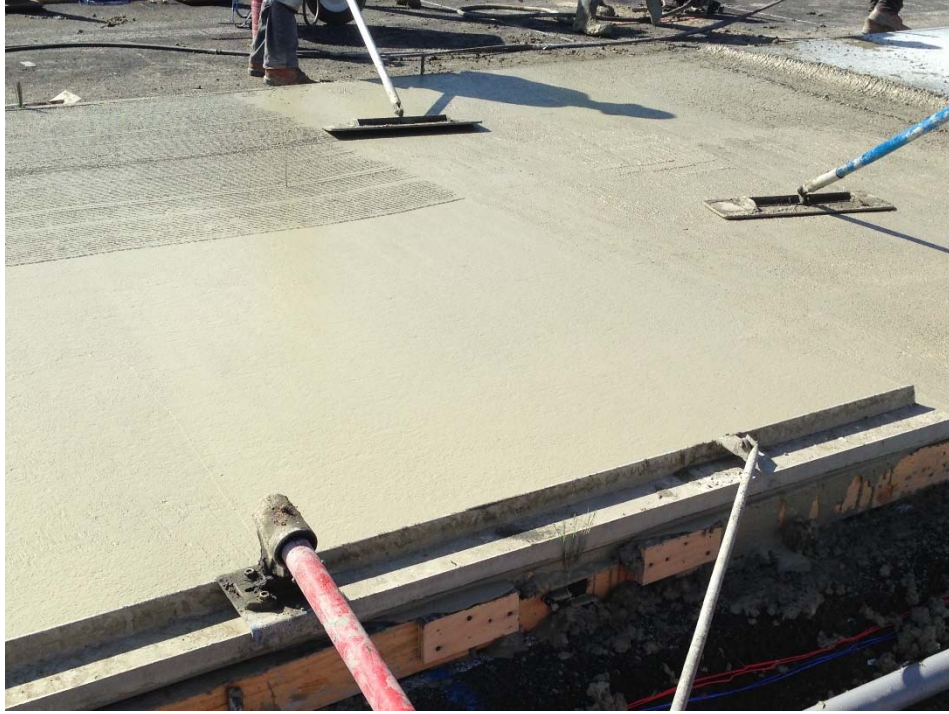
Figure A.61: Slump test.

Figure A.62: Slump test measurement.

Figure A.63: Curing compound application.

Figure A.64: Pads to measure the curing compound application rate.

Figure A.65: Bull-float finishing of the concrete surface.

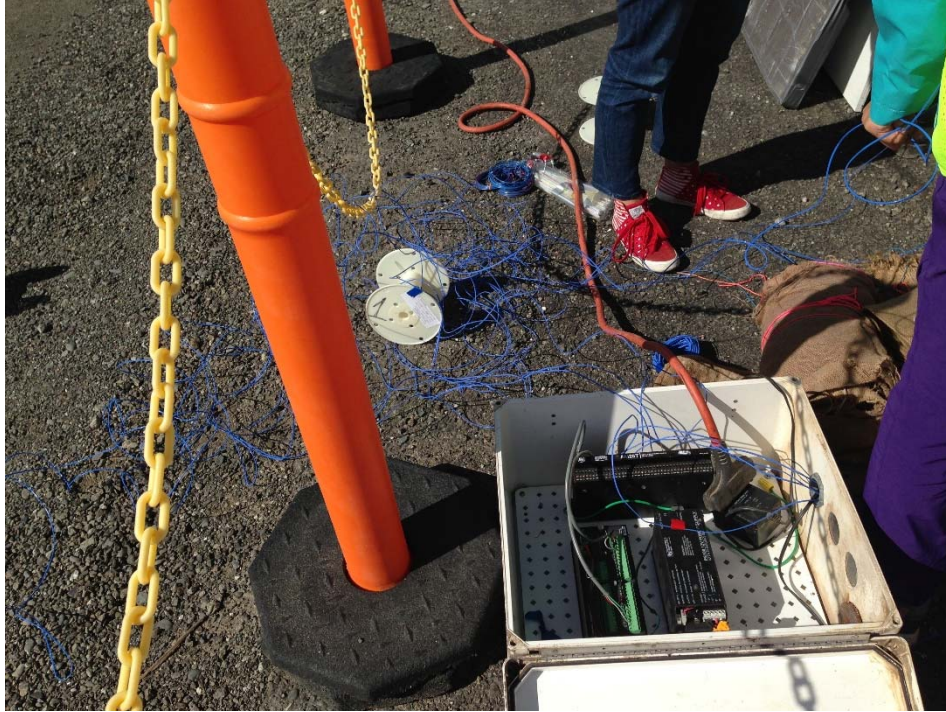**Figure A.66: Section edge finishing.**

Figure A.67: Section K after tining and application of curing compound.

Figure A.68: Concrete cylinders and beams for QC/QA.

Figure A.69: The data acquisition system for tracking temperature inside concrete specimens.

Figure A.70: A thermocouple inside a concrete beam.

Figure A.71: Tracking the surface temperature on the CSA section.

Figure A.72: Manual application of curing compound.

Figure A.73: Grid for concrete saw-cutting.

Figure A.74: Saw-cutting.

Figure A.75: Vacuum cleaning after saw-cutting.

Figure A.76: Saw-cutting transverse joints.
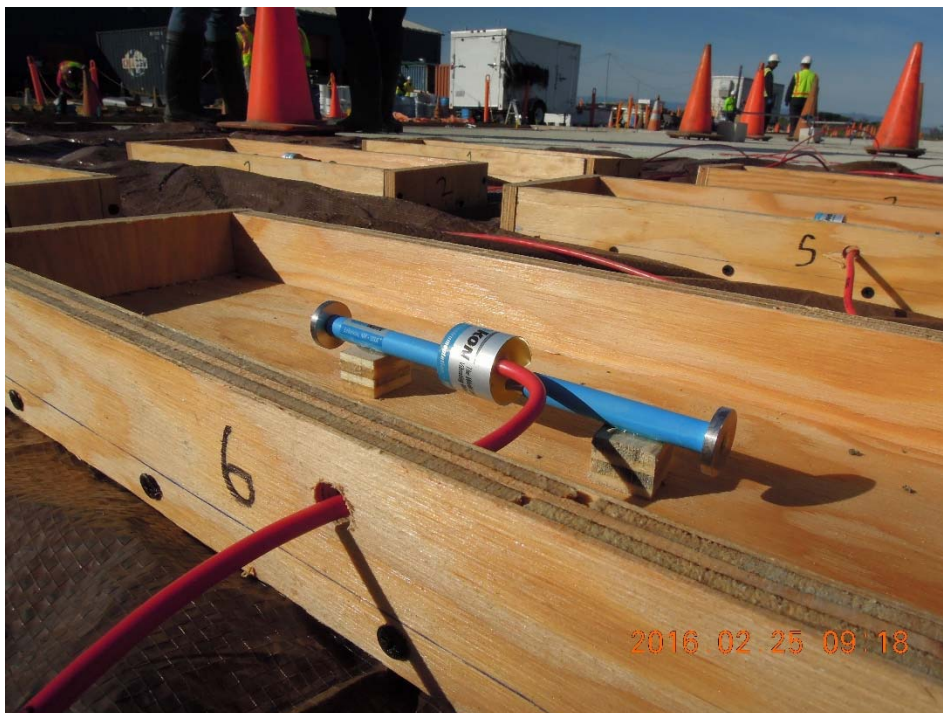
Figure A.77: Targets and holders for JDMDs.

Paving Lane 2

Figure A.78: Lane 1 (first plane) and Lane 2 (beyond Lane 1) ready to be paved.

Figure A.79: Sieve for preparing the unrestrained shrinkage beams.

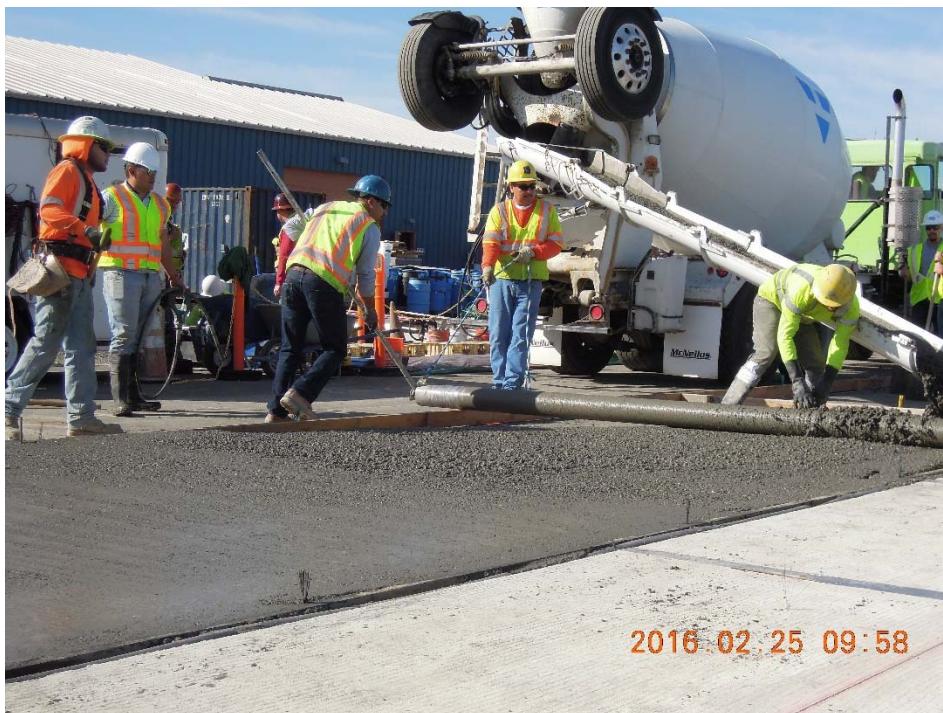**Figure A.80: Unrestrained shrinkage beam mold with strain gage inside.**

Figure A.81: Flexural beam molds.

Figure A.82: Wet sieving of concrete for preparing the unrestrained shrinkage beams.

Figure A.83: Vibrating concrete for wet sieving.

Figure A.84: P2 (Type II/V cement) concrete pouring and consolidation.

Figure A.85: Metal rake tining.

Figure A.86: Pouring concrete around instrumentation.

Figure A.87: Flexural beam preparation.

Figure A.88: Saw-cutting and vacuum cleaning.

Figure A.89: Unrestrained shrinkage beams.

Figure A.90: Unrestrained shrinkage beams after application of curing compound.

Figure A.91: Manual application of curing compound.

Figure A.92: Concrete beams ready to be cured on top of pavement slab (California Test 524).

Figure A.93: Beams on top of pavement slab, under insulation blanket (California Test 524).

Figure A.94: Concrete sampling for preparation of specimens.

Figure A.95: Concrete cylinders for compressive strength, modulus of elasticity, and CTE testing.

Figure A.96: Accelerator dosing into the ready-mix truck.

Figure A.97: Concrete pouring (discharge chute), consolidation (roller screed), and finishing (bull float).

Figure A.98: Bull-float finishing.

Figure A.99: Manual application of shrinkage-reducing admixture.

Figure A.100: Saw-cutting of transverse joints.

Post-Paving

Figure A.101: Longitudinal view of test sections after paving.

Figure A.102: Side view of Section H.

Figure A.103: Close-up of JDMD targets and holder.

Figure A.104: Side view of Section G.

Figure A.105: Saw cut to 1/3 of PCC depth.

Figure A.106: Wood form for separating sections.

Figure A.107: Full-depth cut for separating sections.

Figure A.108: IOMD (orange holder) and JDMDs (blue holders).

Figure A.109: Unrestrained shrinkage beams.

Figure A.110: Close up of environmental Section L.

Figure A.111: Longitudinal view of the east part of the test track.

Figure A.112: Longitudinal view of the west part of the test track.

Figure A.113: Longitudinal view of Lane 2.

Figure A.114: Close-up of the middle slab in an environmental section.

Figure A.115: Longitudinal view of environmental Section N.

Figure A.116: Longitudinal view of the test track.